Sequences of the reverse Krebs cycle are promoted by metals

Kamila B. Muchowska, Sreejith J. Varma, Elodie Chevallot-Beroux, Lucas Lethuillier-Karl, Guang Li and Joseph Moran*

Université de Strasbourg, CNRS, ISIS UMR 7006, F-67000 Strasbourg, France

moran@unistra.fr

Contents

General information

All reactions were carried out in 10 mL Pyrex glass culture tubes under inert atmosphere unless otherwise noted.

GCMS analysis was performed on a GC System 7820A (G4320) connected to a MSD block 5977E (G7036A), using Agilent High Resolution Gas Chromatography Column: PN 19091S – 433UI, HP – 5MS UI, 28 m×0.250 mm, 0.25 Micron, SN USD 489634H. All samples were prepared in ethyl acetate (200 μL sample volume). The analysis was carried out on a splitless 1 μL injection volume with an injection port temperature 250 °C. Column oven temperature program was as follows: 60 °C for 1 min, ramped at 30 °C min−1 to 310 °C with 3 min hold, with a total running time of 12.33 min. The mass spectrometer was turned on after 2 min and was operated at the electron ionization mode with quadrupole temperature of 150 °C. Data acquisition was performed in the full-scan mode (50-500). Hydrogen (99.999 % purity) was used as carrier gas at a constant flow rate of 1.5 mL min^{-1}.

^{1}H NMR spectra of starting material in $CDCl_3$ were recorded on a Bruker Avance400 (400 MHz) spectrometer at ambient temperature and are reported in ppm using residual $CHCl_3$ as the internal reference (7.26 ppm), unless otherwise noted. Coupling constants *J* are reported in Hz, as determined using the software (*MestReNova v6.0.2*). ^{13}C NMR spectra were recorded on a Bruker Avance400 (100 MHz) spectrometer and are reported in ppm using the residual solvent resonance as the internal standard ($CDCl_3$ at 77.0 ppm). ^{1}H NMR spectra of authentic TCA standards and crude reaction mixtures were recorded in water on a Bruker Avance300 (300 MHz) spectrometer at ambient temperature and are reported in ppm using sodium 3-(trimethylsilyl)-1-propanesulfonate (TMSPSA) as the internal reference (CH_3 resonance at 0 ppm). Solvent suppression of water in the ^{1}H NMR was achieved using the Bruker ZGESGP 1D sequence for water suppression using excitation sculpting with gradient.

Materials

Unless otherwise noted, all reagents and solvents were purchased from commercial suppliers and used without further purification. *Cis*-aconitic acid and triethyl oxalosuccinate were prepared using literature procedures,[1,2] as described in the Synthetic Procedures section.

Analytical methods

Derivatization procedure

Derivatization of carboxylic acids to esters was performed using a modified literature procedure.[3] For optimal gas chromatography resolution, the carboxylic acids were converted to ethyl esters using a mixture of ethanol/ethyl chloroformate (EtOH/ECF) or to methyl esters using a mixture of methanol/methyl chloroformate (MeOH/MCF).

A *ca.* 0.5-0.7 mL aliquot of the reaction mixture was basified using solid KOH and centrifuged (6000 rpm, 3 min). To 100 μL of the supernatant was added 1 M NaOH solution (150 μL), EtOH or MeOH (240 μL) and pyridine (30 μL), followed by ethyl chloroformate (ECF, 35 μL) or methyl chloroformate (MCF, 35 μL). This was vortexed for 30 s. A second 35 μL portion of ECF (or MCF) was added and the mixture was vortexed again for 30 s. Next, $CHCl_3$ (200 μL) was added, followed by vortexing (10 s). Finally, $NaHCO_3$ (400 μL) was added and the mixture was vortexed again for 10 s. The $CHCl_3$ layer was separated and dried over anhydrous Na_2SO_4. 50 μL of the dry $CHCl_3$ layer was used with 150 μL of ethyl acetate for the GC-MS analysis.

Product identification

Reaction products derivatized to methyl or ethyl esters of carboxylic acids were identified by comparing the mass spectra and retention times against analogously derivatized authentic samples (Fig. S1 – S15). ECF derivatization was preferred for small molecule substrates (pyruvate, lactate, malate, fumarate, succinate, α-ketoglutarate and α-hydroxyglutarate, alanine), while MCF derivatization gave clearer results (less elimination by-products and better resolution) for *cis*-aconitate, tricarballylate, isocitrate and citrate.

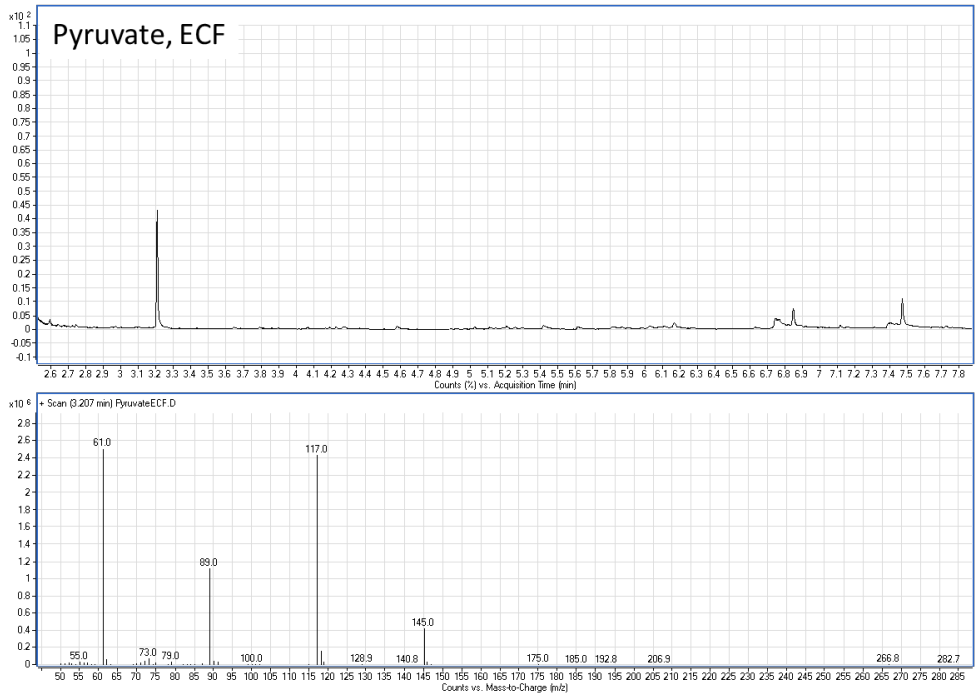

Figure S1 GC trace and mass spectrum of pyruvate characteristic peak (ECF derivatization).

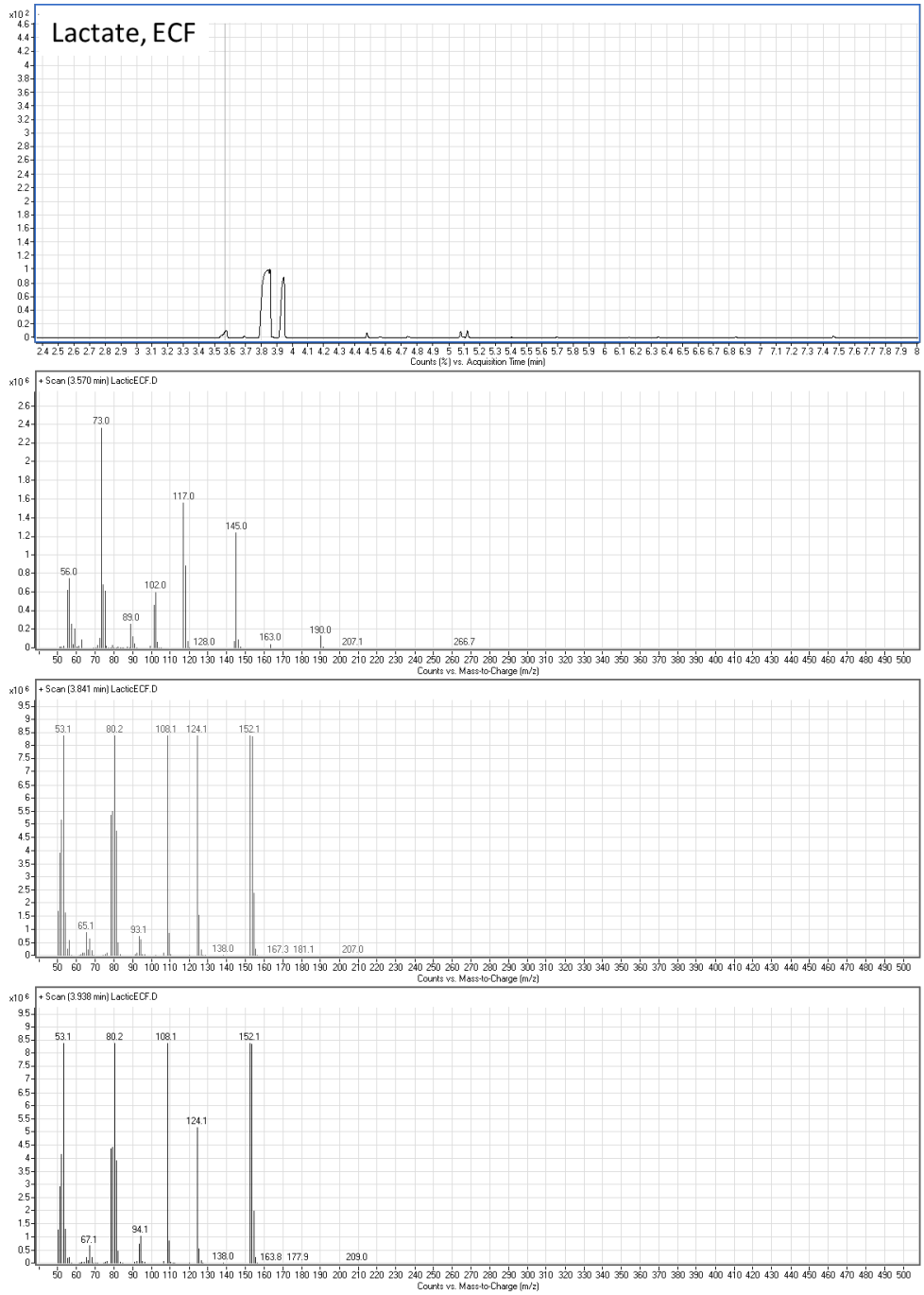

Figure S2 GC trace and mass spectra of lactate characteristic peaks (ECF derivatization).

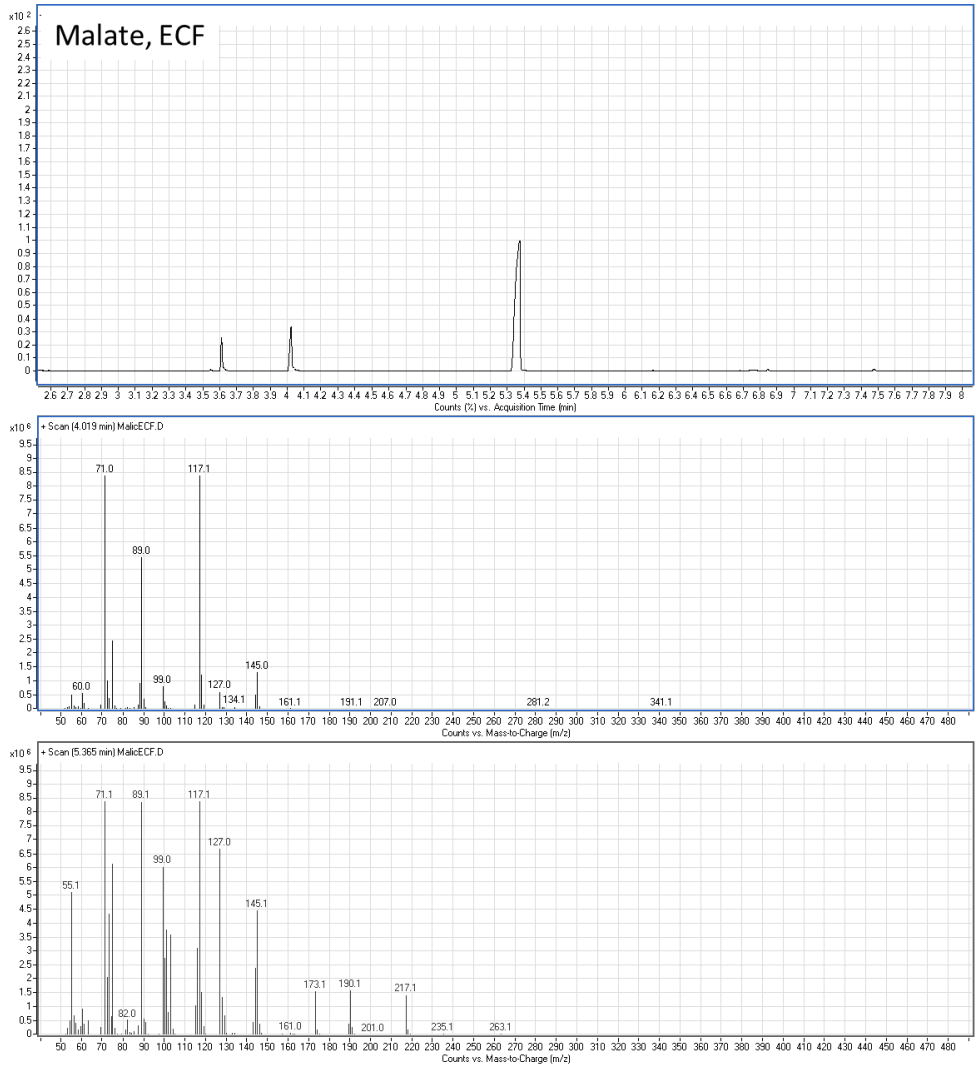

Figure S3 GC trace and mass spectra of malate characteristic peaks (ECF derivatization). The additional peak at ~3.6 min corresponds to trace fumarate (result of O-acylation of the hydroxyl group during derivatization and subsequent elimination, well below 5 % at malate concentrations ≤ 0.04 M).

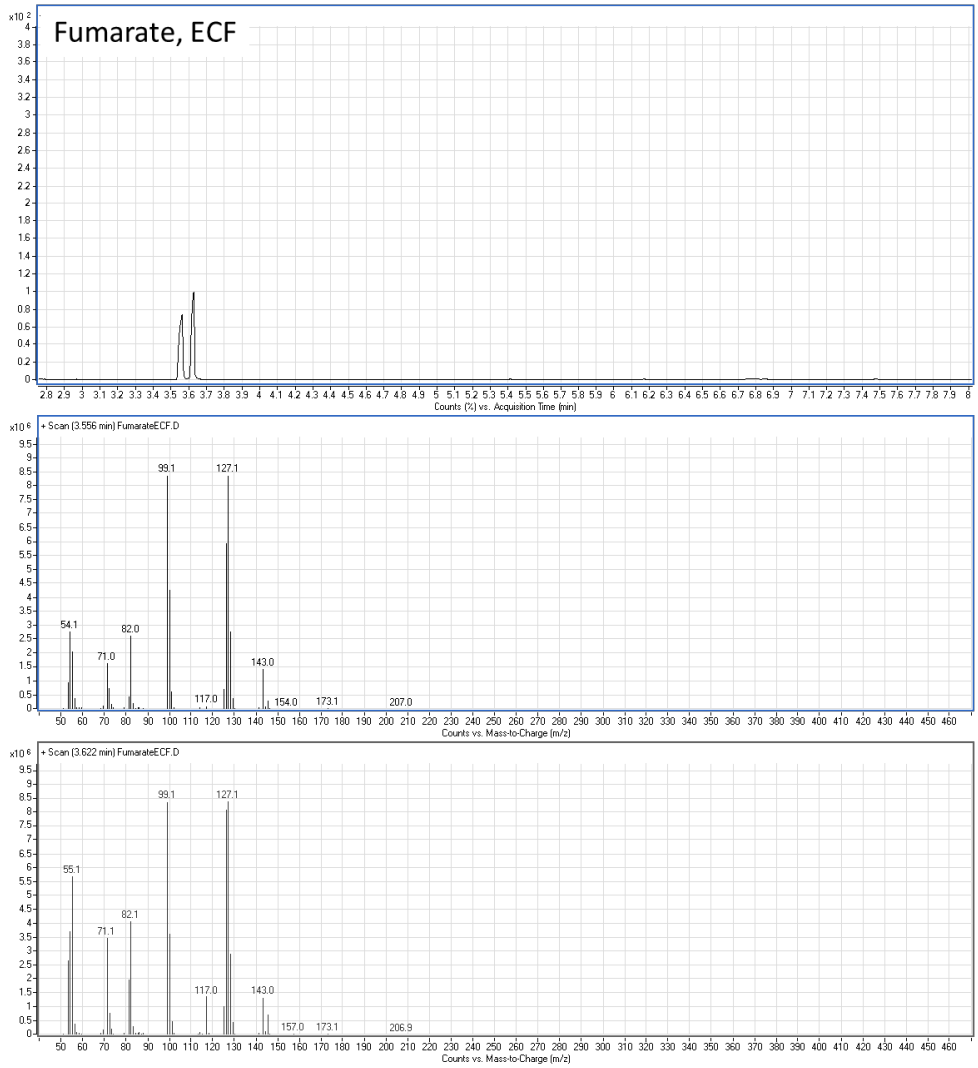

Figure S4 GC trace and mass spectra of fumarate characteristic peaks (ECF derivatization).

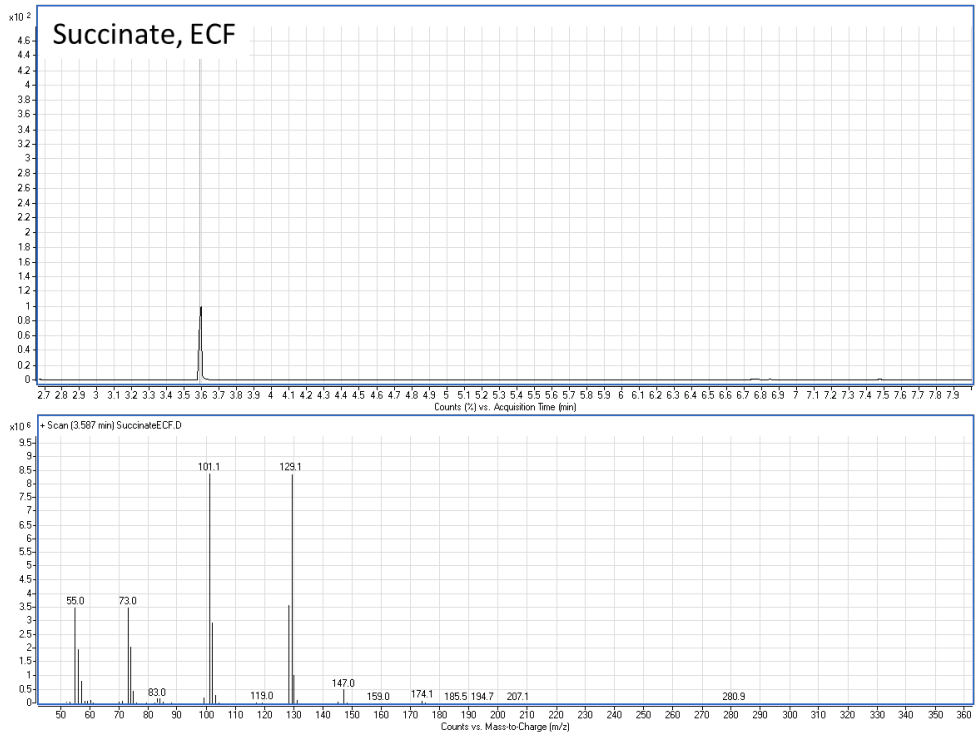

Figure S5 GC trace and mass spectrum of succinate characteristic peak (ECF derivatization).

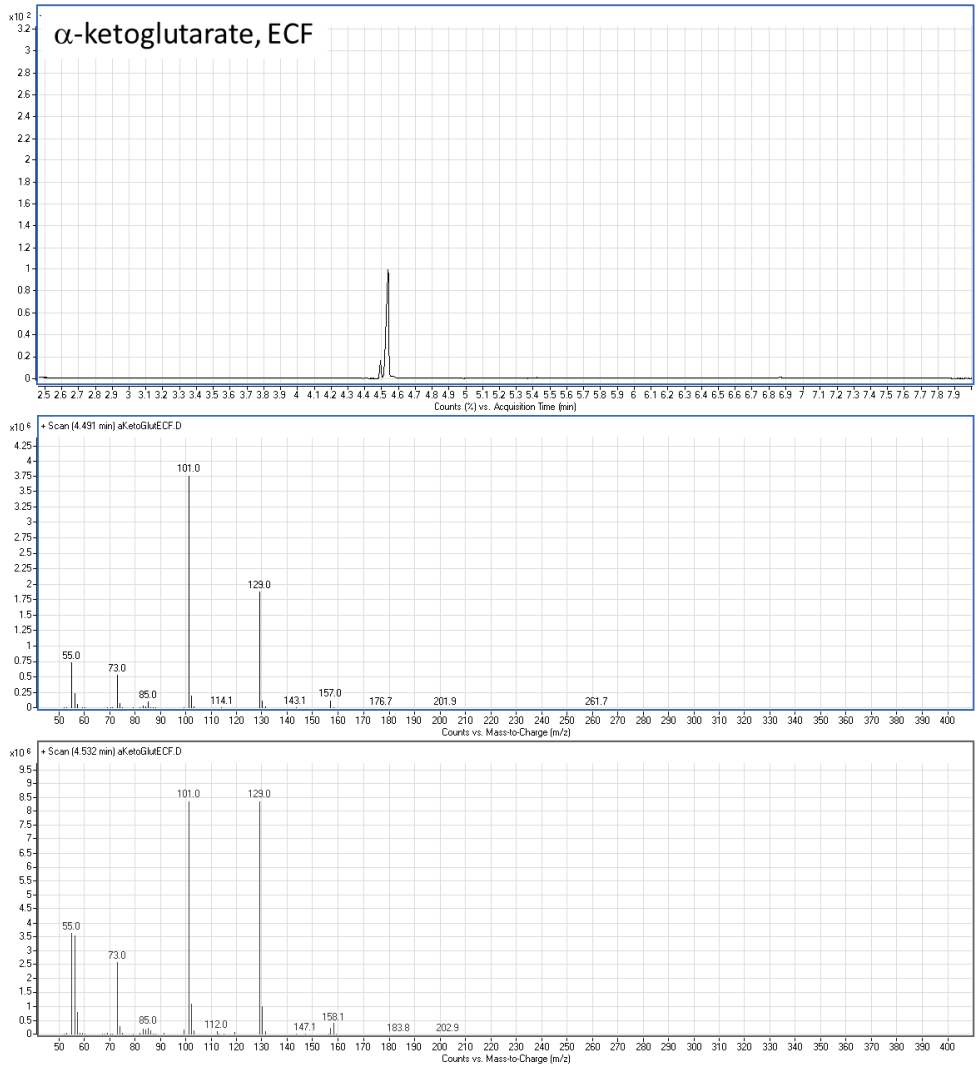

Figure S6 GC trace and mass spectra of α-ketoglutarate characteristic peaks (ECF derivatization).

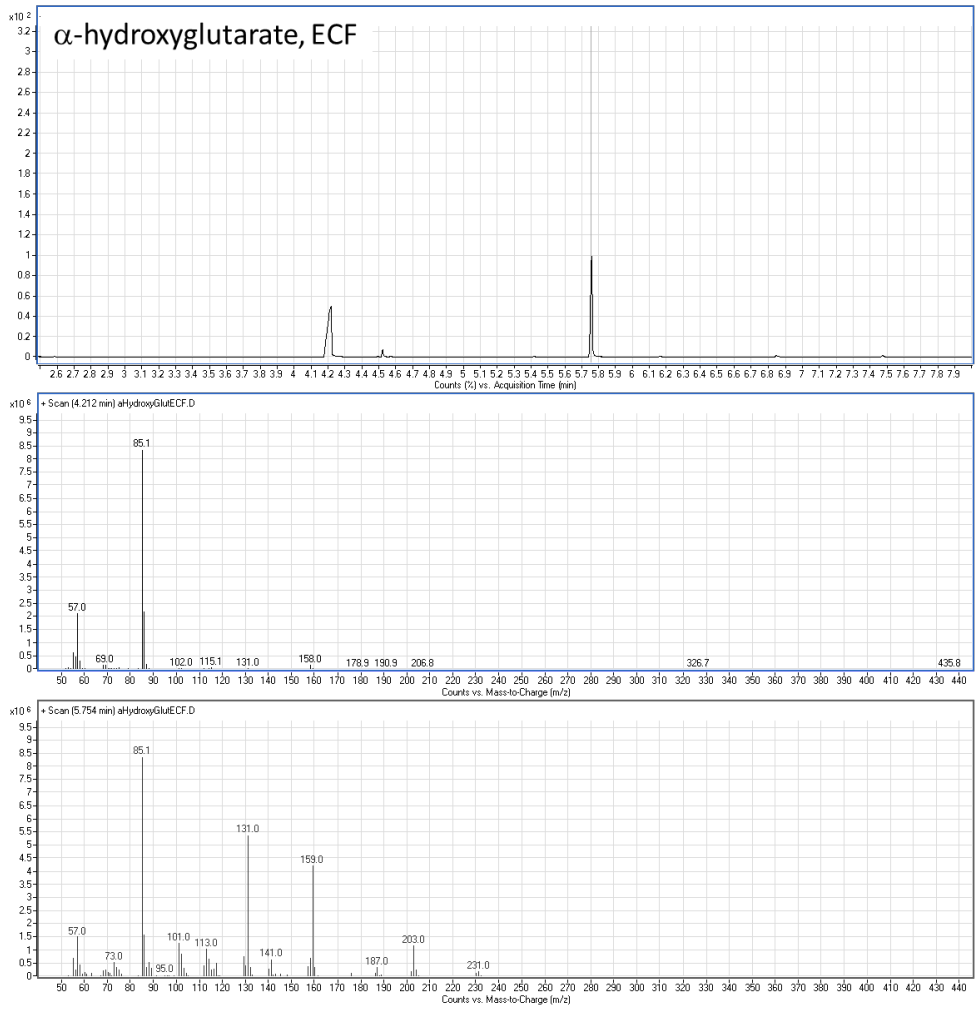

Figure S7 GC trace and mass spectra of α-hydroxyglutarate characteristic peaks (ECF derivatization).

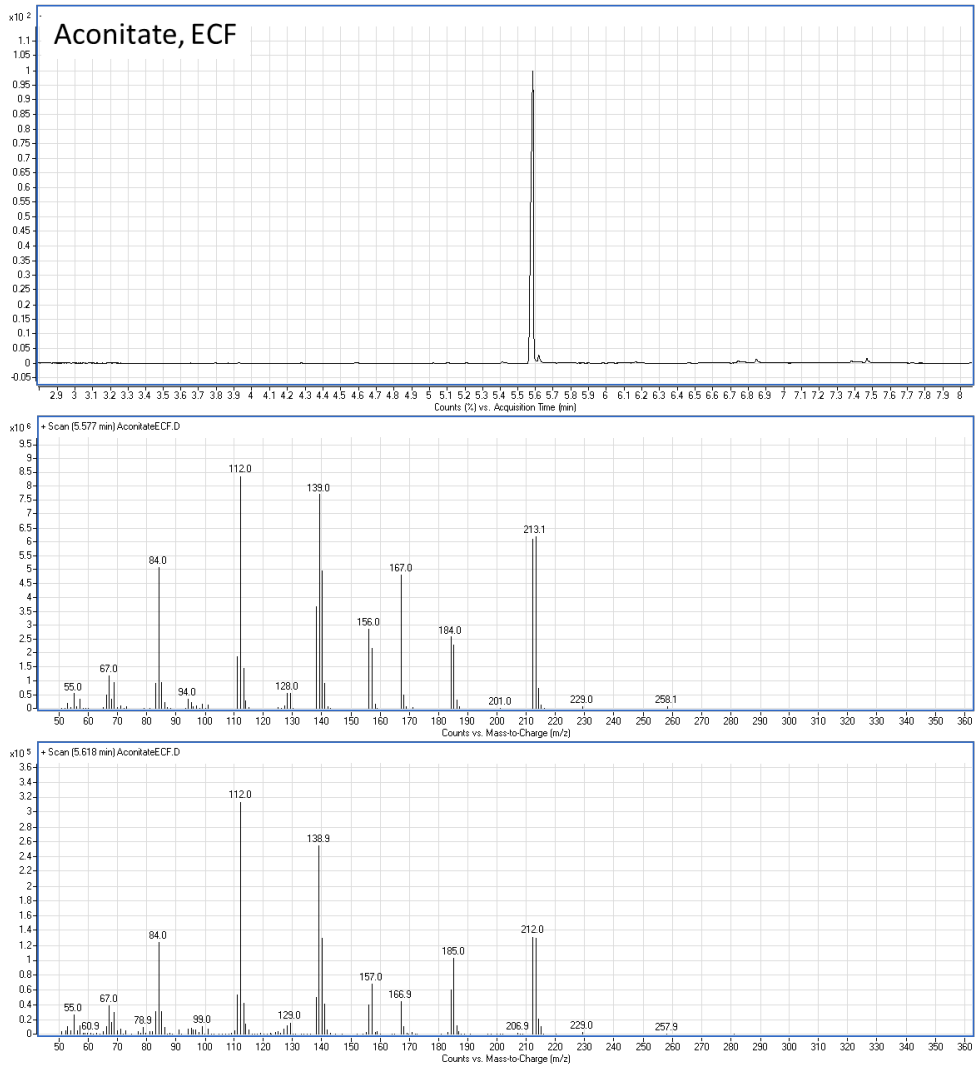

Figure S8 GC trace and mass spectra of *cis*-aconitate characteristic peaks (ECF derivatization).

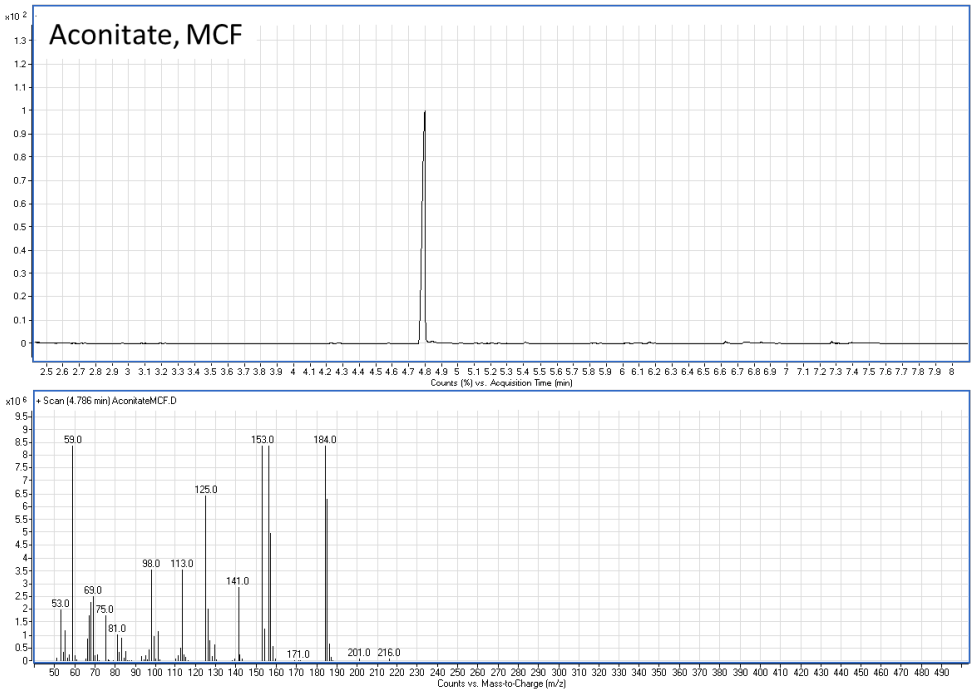

Figure S9 GC trace and mass spectrum of *cis*-aconitate characteristic peak (MCF derivatization).

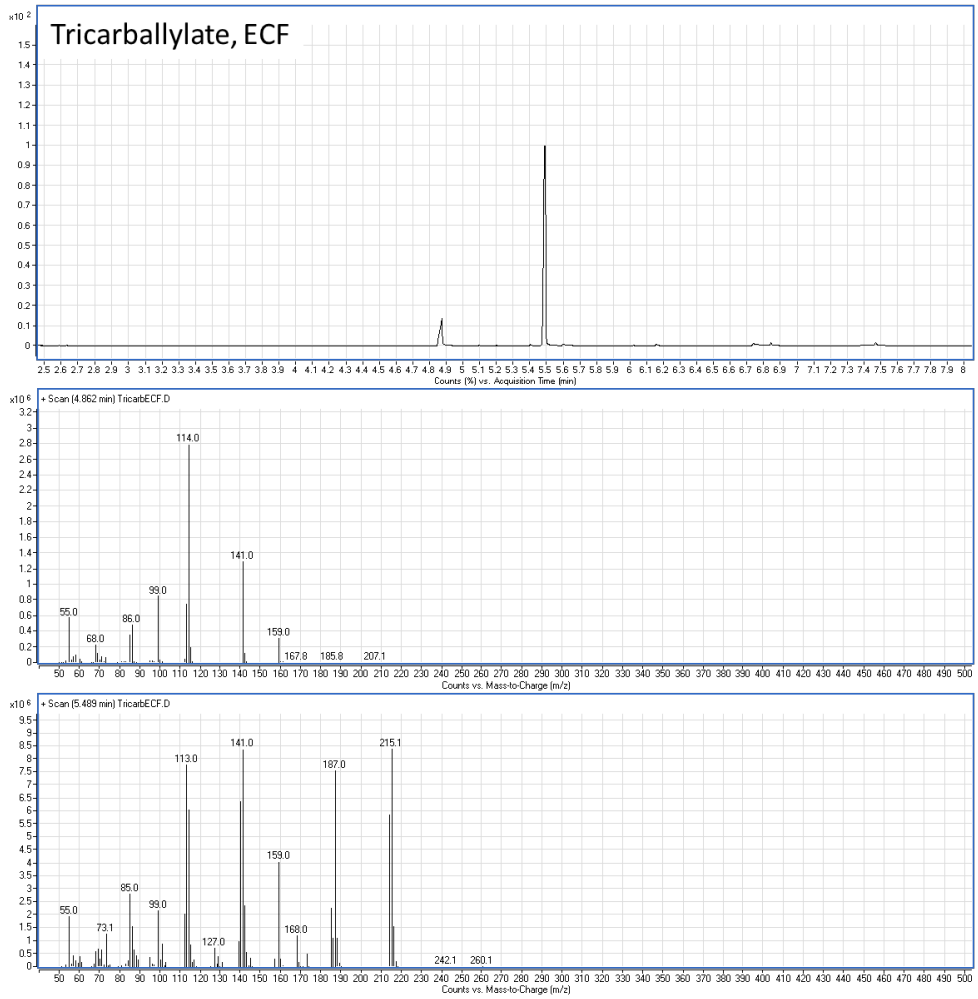

Figure S10 GC trace and mass spectra of tricarballylate characteristic peaks (ECF derivatization).

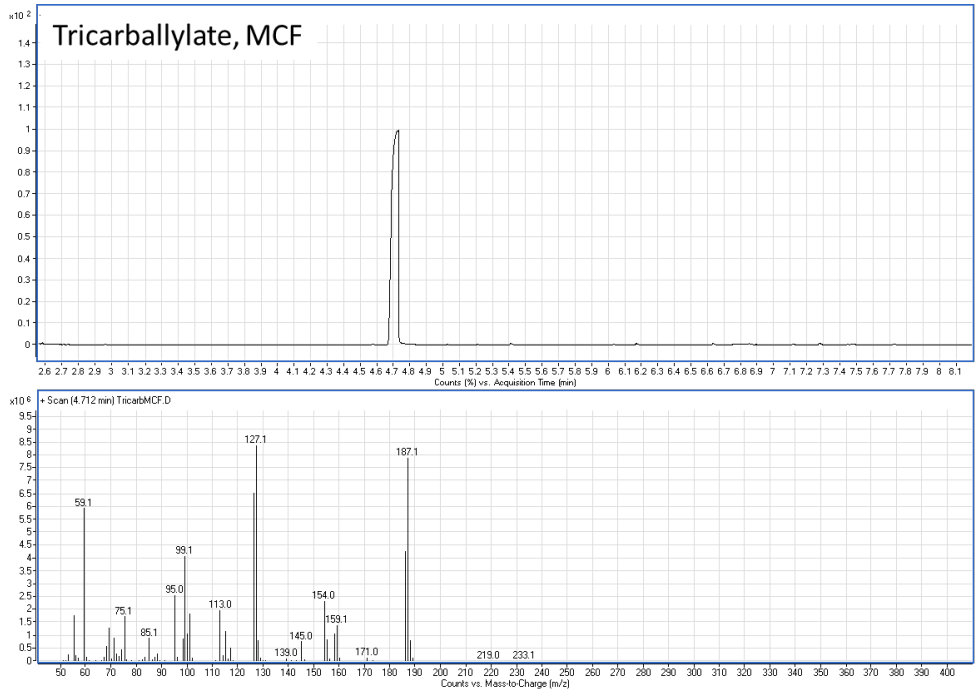

Figure S11 GC trace and mass spectrum of tricarballylate characteristic peak (MCF derivatization).

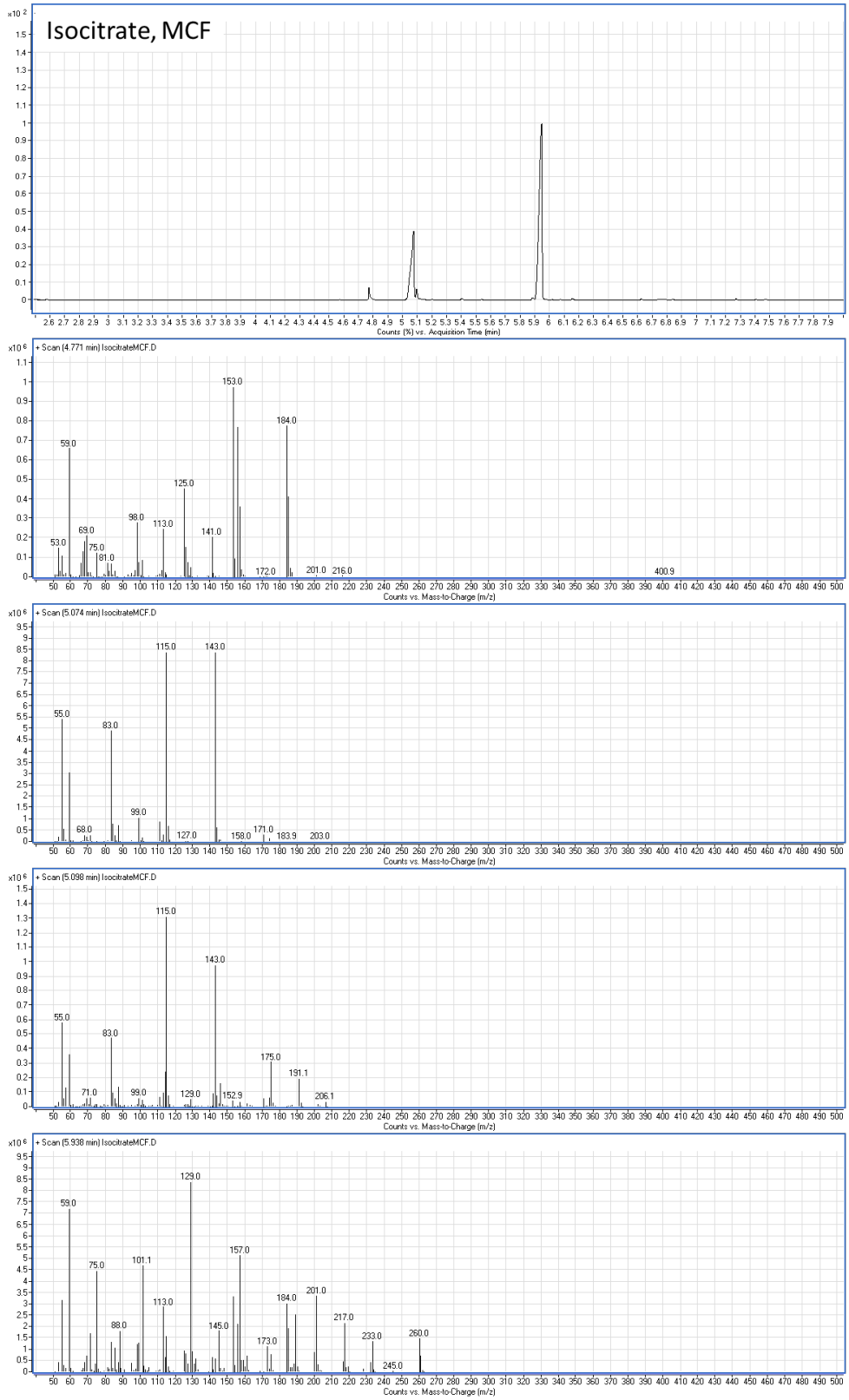

Figure S12 GC trace and mass spectra of isocitrate characteristic peaks (MCF derivatization). The additional peak at ~4.8 min corresponds to trace aconitate (result of O-acylation of the hydroxyl group during derivatization and subsequent elimination, < 5 % at isocitrate concentrations ≤ 0.04 M).

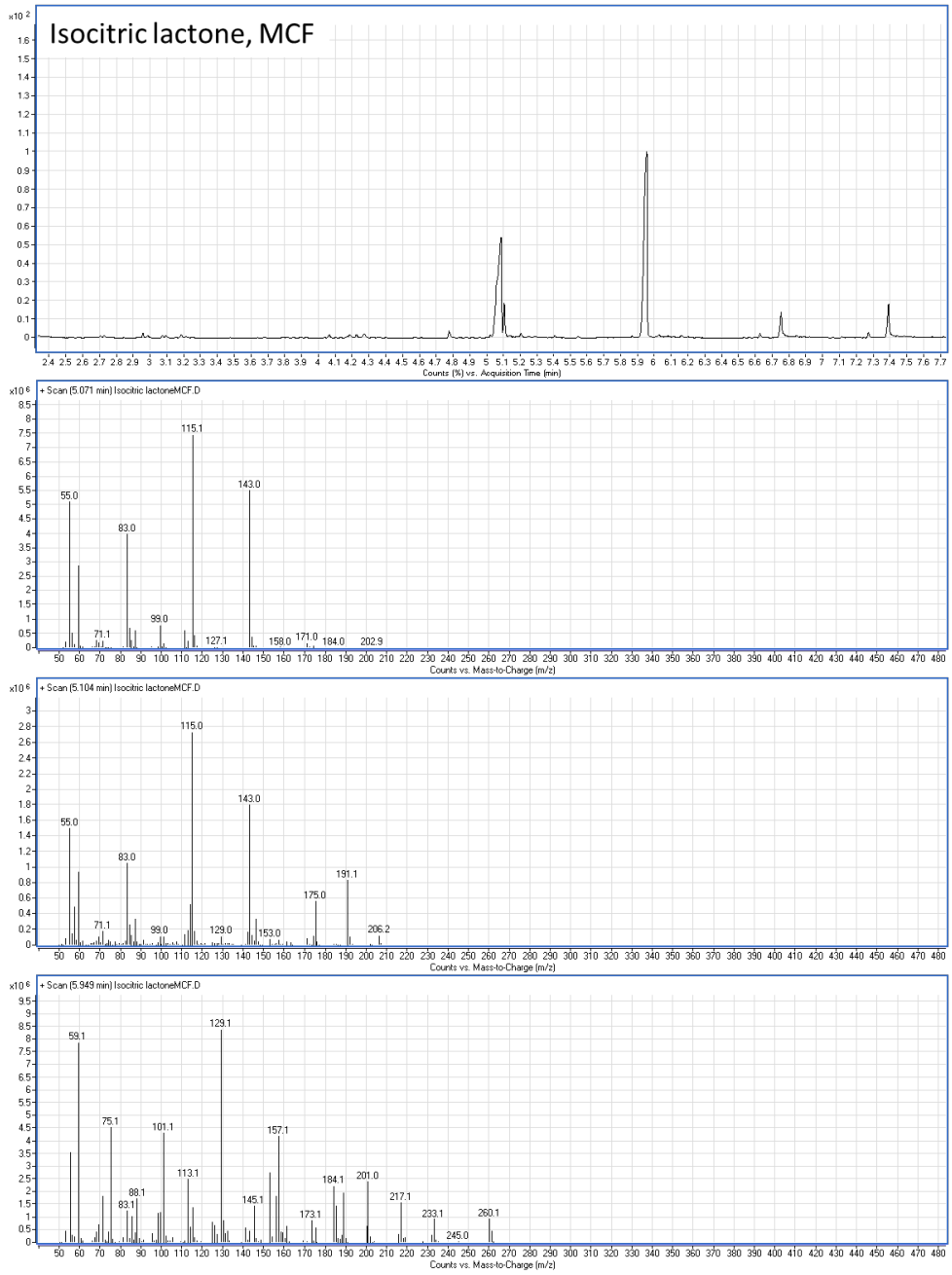

Figure S13 GC trace and mass spectra of isocitric lactone characteristic peaks (MCF derivatization).

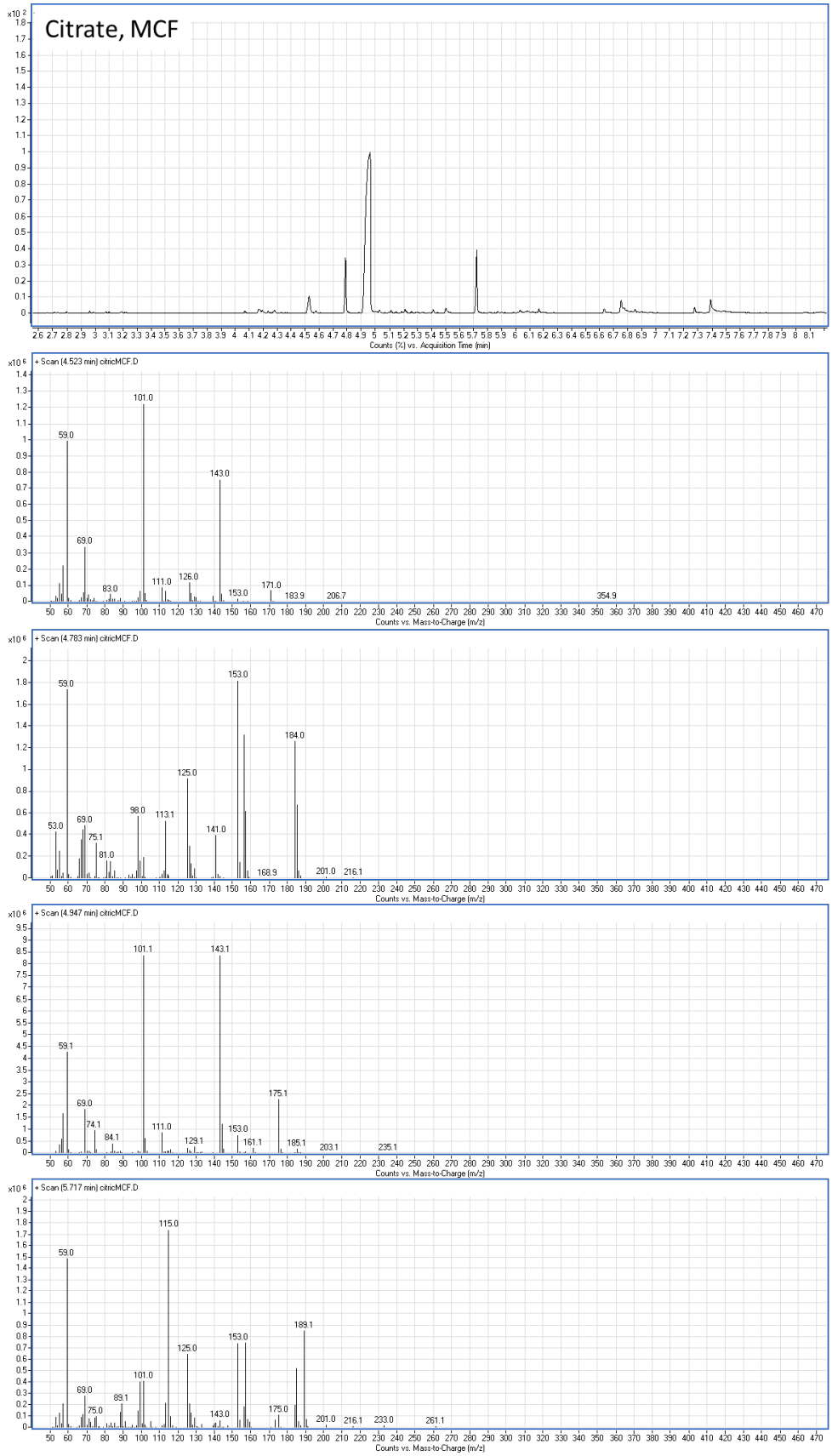

Figure S14 GC trace and mass spectra of citrate characteristic peaks (MCF derivatization). The additional peak at ~4.8 min corresponds to trace aconitate (result of O-acylation of the hydroxyl group during derivatization and subsequent elimination, < 5 % at citrate concentrations ≤ 0.04 M).

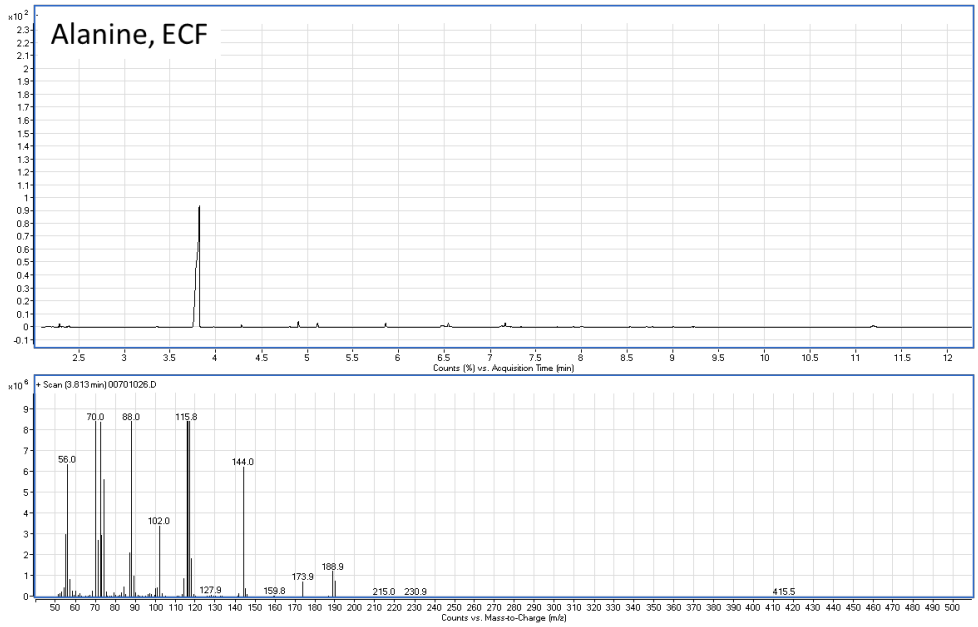

Figure S15 GC trace and mass spectra of alanine characteristic peak (ECF derivatization).

Experimental data

Table S1 Non-enzymatic reactions of the rTCA cycle (Fe^0 as reductant). Table S1 continues on the following page.

Entry	Substrate (0.1 mmol each)	Conditions[a]				Species present in the mixture post-reaction (%)											
						On-cycle								*Off-cycle*			
		Fe^0 (equiv.)	Zn^{2+} (equiv.)	Cr^{3+} (equiv.)	Micelles	**2**	**4**	**5**	**6**	**7**	**9**	**10**	**11**	**12**	**13**	**14**	**15**
Reduction																	
1	**3**	10	-	-	-		90±2	10±2									
2[b]	**5**	10	-	-	-		15±5	20±2	65±7								
3[b]	**8**	10	-	-	-				12±5		83±4	5±1					
Hydration/Dehydration																	
4[c]	**4**	-	10	-	-		86±1	14±1									
5[c]	**4**	10	10	-	-		94±1	4±1	2±1								
6[c]	**4**	10	10	-	yes		84±1	6±1	10±2								
7[d]	**4**	10	10	-	yes		82±1	7±2	11±3								
8[c,e]	**9**	-	1	-	-						51±12	49±12					
9[e]	**9**	-	1	-	-						93±1	7±1					
10[c,e]	**10**	-	1	-	-						12±9	88±9					
11[c]	**10**	-	1	-	-						8±0	92±0					
12[f]	**10**	-		6	-							67±0	33±0				
13[f]	**11**	-		6	-							23±5	77±5				
Three-step sequences																	
14[c,g]	**3**	20	-	-	-		90±2	8±1	2±1								
15[c,h]	**3**	10	15	4	-		83±1	6±3	4±1					7±3			
16	**3**	10	15	4	yes		55±7	4±0	23±6					19±5			
17[d]	**3**	10	15	4	-		98±0	2±0									
18[d]	**3**	10	15	4	yes		52±2	3±3	41±3					4±2			
19[c,g,i]	**8**	10	-	1	-				13±7		64±11	20±4	3±1				
20[j]	**8**	5	10	-	-				16±2	4±2	76±3	4±1					
21[j]	**8**	-	10	6	-	*Mixture of oxalosuccinate decomposition products, incl. succinate*											
22[j]	**8**	5	10	6	-						65±7	30±4	2±1		3±4		
23[j]	**8**	5	10	6	yes				5±4		72±5	21±0	2±1				

[a] Unless otherwise specified: 1 M HCl in H_2O, 16 h, 140 °C. [b] 3 h, 140 °C. [c] 48 h, 140 °C. [d] 20 °C, 24 h. [e] 1 M H_2SO_4 in H_2O, 16 h, 140 °C. [f] 1 h at 20 °C, 24 h at 140 °C. [g] pH adjusted with conc. HCl to <1 after 24 h. [h] Fe^0 and/or Zn^{2+} added in two portions. [i] Cr^{3+} added after 24 h. [j] Thermal cycling: 16 h at 140 °C, 10 h at 20 °C, 16 h 140 °C. [k] 3 h, 40 °C. [l] Malate-fumarate equilibrium. [m] Reaction with hydrazine hydrate (2 equiv.) [n] 0.1 mmol malic acid (**4**) added post-reaction and immediately derivatized (see Synthetic procedures for details). Reported yields are average values of at least two runs. Errors correspond to ±mean absolute deviation.

Continued from the previous page

Table S1 Non-enzymatic reactions of the rTCA cycle (Fe^0 as reductant)

Entry	Substrate (0.1 mmol each)	Conditions[a]				Species present in the mixture post-reaction (%)											
						On-cycle								*Off-cycle*			
		Fe^0 (equiv.)	Zn^{2+} (equiv.)	Cr^{3+} (equiv.)	Micelles	**2**	**4**	**5**	**6**	**7**	**9**	**10**	**11**	**12**	**13**	**14**	**15**
Competitive reduction																	
24[k]	**2+3+5+7+10**	10	15	6	yes	20±0	6[l]±2	18[l]±2	4±2	20±3		28±4		2±0	2±1	<1±0	
Reductive amination																	
25[m]	**2**	10	-	3	-									3±1			97±1
Micelle control experiment																	
26[n]	**-**	10	15	6	yes		99±0	1±0									

[a] Unless otherwise specified: 1 M HCl in H_2O, 16 h, 140 °C. [b] 3 h, 140 °C. [c] 48 h, 140 °C. [d] 20 °C, 24 h. [e] 1 M H_2SO_4 in H_2O, 16 h, 140 °C. [f] 1 h at 20 °C, 24 h at 140 °C. [g] pH adjusted with conc. HCl to <1 after 24 h. [h] Fe^0 and/or Zn^{2+} added in two portions. [i] Cr^{3+} added after 24 h. [j] Thermal cycling: 16 h at 140 °C, 10 h at 20 °C, 16 h 140 °C. [k] 3 h, 40 °C. [l] Malate-fumarate equilibrium. [m] Reaction with hydrazine hydrate (2 equiv.) [n] 0.1 mmol malic acid (**4**) added post-reaction and immediately derivatized (see Synthetic procedures for details). Reported yields are average values of at least two runs. Errors correspond to ±mean absolute deviation.

Table S2 Metal-promoted malate dehydration screen.[a]

Entry	Metal salt (10 equiv.)	Malate (**4**) (% of mixture)	Fumarate (**5**) (% of mixture)	Succinate (**6**) (% of mixture)
1	$Ni(acac)_2$	95	5	0
2	$NiCl_2\ 5H_2O$	88	12	<1
3	$FeSO_4\ 7H_2O$	94	6	0
4	$CuSO_4\ 5H_2O$	96	4	0
5	$MnSO_4\ H_2O$	94	6	0
6	$CoCl_2\ 6H_2O$	96	4	0
7	VCl_2	92	8	<1
8	$CrCl_2$	95	5	0
9	$Cr_2(SO_4)_3\ 12H_2O$	98	2	<1
10	$ZnCl_2$	94±1	4±1	2±1

[a] Unless otherwise specified: 0.08 mmol malic acid, Fe^0 powder (10 equiv.), 3 mL 1 M HCl in H_2O, 16 h, 140 °C. Where applicable, errors correspond to ±mean absolute deviation.

Table S3 Metal-promoted isocitrate dehydration screen.[a]

Entry	Metal salt (1 equiv.)	Temp. (°C)	Micelles	Isocitrate (**9**) (% of mixture)	Aconitate (**10**) (% of mixture)
1	$Ni(acac)_2$	140 °C	-	91	9
2	$FeSO_4\ 7H_2O$	140 °C	-	95	5
3	$CuSO_4\ 5H_2O$	140 °C	-	94	6
4	$MnSO_4\ H_2O$	140 °C	-	94	6
5	$CoCl_2\ 6H_2O$	140 °C	-	94	6
6	$Cd(OAc)\ 2H_2O$	140 °C	-	95	5
7	VCl_2	140 °C	-	95	5
8	Fe_2O_3	140 °C	-	95	5
9	Mn_2O_3	140 °C	-	97	3
10	Cr_2O_3	140 °C	-	95	5
11	As_2O_3	140 °C	-	49	51
12	$RuCl_3$	140 °C	-	58	42
13	$IrCl_3$	140 °C	-	51	49
14	$RhCl_3$	140 °C	-	54	46
15	$TiCl_3$	140 °C	-	100	0
16	$CrCl_3$	160 °C	-	100	0
17	$Pd(acac)_2$	140 °C	-	47	53
18[b]	$CrCl_2$	140 °C	-	62	38
19	$ZnCl_2$	140 °C	-	51±12	49±12
20[c]	$ZnCl_2$	140 °C	-	93±1	7±1
21[c]	$ZnCl_2$	140 °C	1% w/w	88±2	12±2
22[c]	$ZnCl_2$	25 °C	-	97	3
23[c]	$ZnCl_2$	25 °C	1% w/w	97	3
24[c]	-	140 °C	-	97	3
25[c]	-	140 °C	1% w/w	98	2
26[c]	-	25 °C	-	97	3

[a] Unless otherwise specified: 0.08 mmol isocitrate (as trisodium isocitrate hydrate),3 mL 1 M H_2SO_4 in H_2O, 48 h, 140 °C. [b] $TiCl_3$ as 20% *w/w* solution in 2N HCl [c] 1 M HCl in H_2O, 48 h. Where applicable, errors correspond to ±mean absolute deviation.

Table S4 Metal-promoted aconitate hydration screen.[a,‡]

Entry	Metal salt (1 equiv.)	Species present in the mixture post-reaction (%)			
		Isocitrate (**9**)	Aconitate (**10**)	Citrate (**11**)	Tricarballylate (**14**)
1	$FeCl_3$	-	99	1	-
2	$Cr_2(SO_4)_3$ $12H_2O$	-	67	33	-
3	$TiCl_3$[b]	-	82	10	9
4	$IrCl_3$	-	67	2	31
5	$RuCl_3$	-	97	3	-
6	$Co(OAc)_2$	-	98	2	-
7	$BiBr_3$	-	>99	<1	-
8	$TbCl_3$ $6H_2O$	8	92	<1	-
9	-	-	100	-	-

[a] Unless otherwise specified: 0.08 mmol aconitate, 3 mL 1 M H_2SO_4 in H_2O, 1 h at 20 °C, then 16 h at 140 °C. [b] $TiCl_3$ as 20% *w/w* solution in 2N HCl

[‡] In the aconitate hydration screen the following salts/oxides did not yield any citrate: CuI, $ZnSO_4$, $CuSO_4$ $5H_2O$, $NiSO_4$ $7H_2O$, $CoSO_4$ $7H_2O$, $FeSO_4$ $7H_2O$, $MnSO_4$ H_2O, $CrCl_2$, $Cd(OAc)_2$ $2H_2O$, $HgCl_2$, $Co(NH_3)_6Cl_3$, $Mn(OAc)_3$ $2H_2O$, MoO_2, MoO_3, WO_2, WO_3

Table S5 Reduction selectivity screen on five rTCA intermediates.[a]

Entry	Substrates	Reductant	Species present in the mixture post-reaction (%)								
			On-cycle						*Off-cycle*		
			2	**4**[b]	**5**[b]	**6**	**7**	**10**	**12**	**13**	**14**
1	**2+3+5+7+10**	Fe	13	13	3	19	1	25	1	23	1
2		Ni	32	3	5	11	25	22	0	1	1
3		Zn	0	20	30	4	0	1	2	35	8
4		Mn	19	7	14	4	11	25	1	14	4
5		$Na_2S_2O_4$	35	0	14	3	14	33	0	0	1
6		Mo	*No reaction (only starting materials present)*								
7		MoO2	*No reaction (only starting materials present)*								
8		TPGS-750-M[c]	*No reaction (only starting materials present)*								

[a] Reaction conditions: 0.1 mmol of each: sodium pyruvate, oxaloacetic acid, fumaric acid, α-ketoglutaric acid, *cis*-aconitic acid; 10 equiv. of reductant, 3 mL 1M HCl in H_2O, 3 h, 40°C. [b] Malate-fumarate equilibrium. [c] Control experiment to exclude reducing properties of micelles (1% *w/w* TPGS-750-M in 1M HCl in H_2O).

Table S6 Reductive amination at different temperatures, with Fe^0 or Ni^0 as reducing agents (0.1 mmol sodium pyruvate, 10 equiv. M^0, 3 mL 1M HCl in H_2O, 16 hrs).

Entry	Metal M^0	Temperature (°C)	Lactate (% of mixture)	Alanine (% of mixture)
1	Fe^0	140 °C	17±1	83±1
2		80 °C	13±0	87±0
3		25 °C	6±1	94±1
4	Ni^0	140°C	6±1	94±1
5		80 °C	*No reaction*	

Reported yields are average values of two runs. Errors correspond to ±mean absolute deviation.

Table S7 Non-enzymatic reactions of the rTCA cycle (Ni^0 as reductant).

Entry	Substrate (0.1 mmol each)	Conditions[a]				Species present in the mixture post-reaction (%)											
						On-cycle								*Off-cycle*			
		Ni^0 (equiv.)	Zn^{2+} (equiv.)	Cr^{3+} (equiv.)	Micelles	**2**	**4**	**5**	**6**	**7**	**9**	**10**	**11**	**12**	**13**	**14**	**15**
Reduction																	
1[b]	**3**	10	-	-	-		92±2	8±2									
2[b]	**5**	10	-	-	-			19±5	81±5								
3[b]	**8**	10	-	-	-				52±6		47±7	1±1					
Hydration/Dehydration																	
4	**4**	10	10	-	-		91±2	9±2	1±0								
5	**4**	10	10	-	yes	*No reaction (only starting material present)*											
Three-step sequences																	
6[c]	**3**	20	-	-	-		84±0	15±0	1±0								
7[c]	**3**	10	15	4	-		73±2	6±1						21±1			
8	**3**	10	15	4	-		66±2	9±1	2±0					24±1			
9	**8**	10	-	1	-				19±1		59±1	21±1	1±0				
10[d]	**8**	5	10	6	-				4±0		52±1	37±2	7±1				
11	**8**	5	10	6	yes	*Mixture of oxalosuccinate decomposition products, incl. succinate*											
Competitive reduction																	
12[b]	**2+3+5+7+10**	10	15	6	-	28±4	3[e]±0	5[e]±0	15±5	22±3		25±3			1±0	1±0	
Reductive amination																	
13	**2**	10	-	-	-									6±1			94±1

[a] Unless otherwise specified: 1 M HCl in H_2O, 16 h, 140 °C. [b] 3 h, 40 °C. [c] 16 h, 80 °C. [d] 48 h, 140 °C. [e] Malate-fumarate equilibrium. [f] Reaction with hydrazine hydrate (2 equiv.) Reported yields are average values of at least two runs Errors correspond to ±mean absolute deviation.

Gas chromatography traces

Sample chromatograms corresponding to entries 1 – 26 in Table S1 can be found below (Fig. S16 – S41).

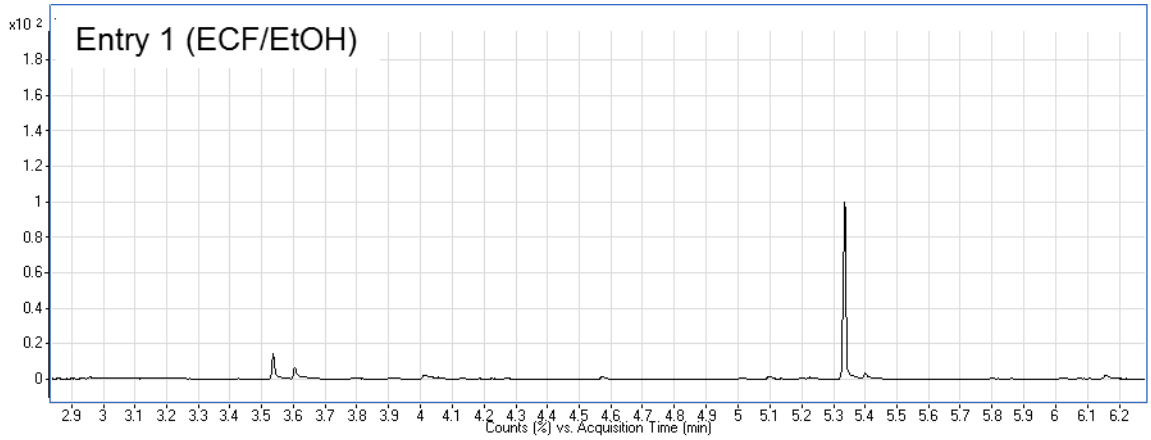

Figure S16 Chromatogram of the reaction mixture corresponding to entry 1, Table S1 (also: entry 1, Table 1).

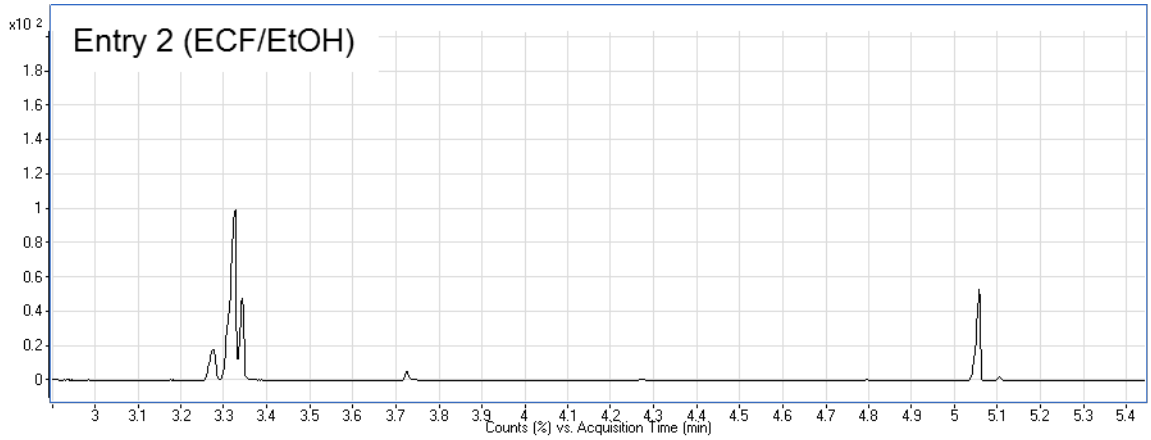

Figure S17 Chromatogram of the reaction mixture corresponding to entry 2, Table S1 (also: entry 2, Table 1).

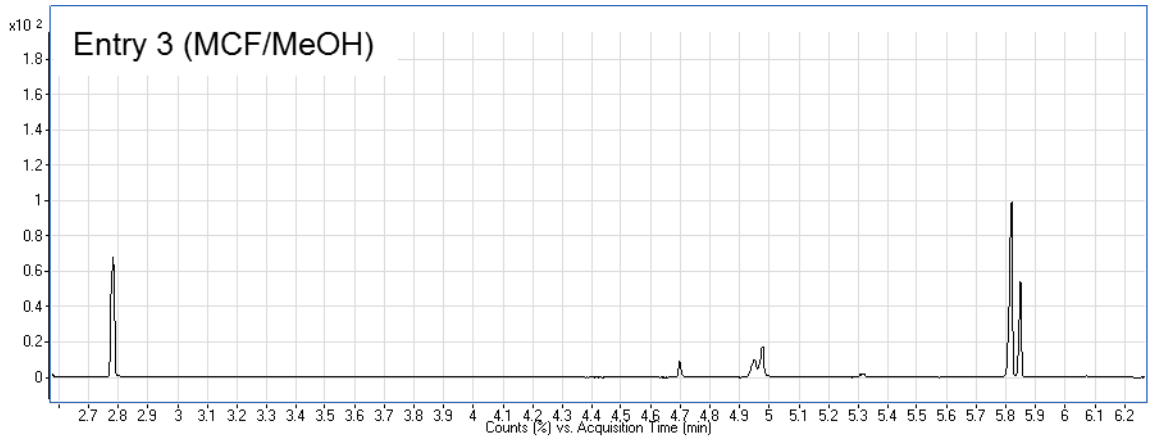

Figure S18 Chromatogram of the reaction mixture corresponding to entry 3 (Table S1).

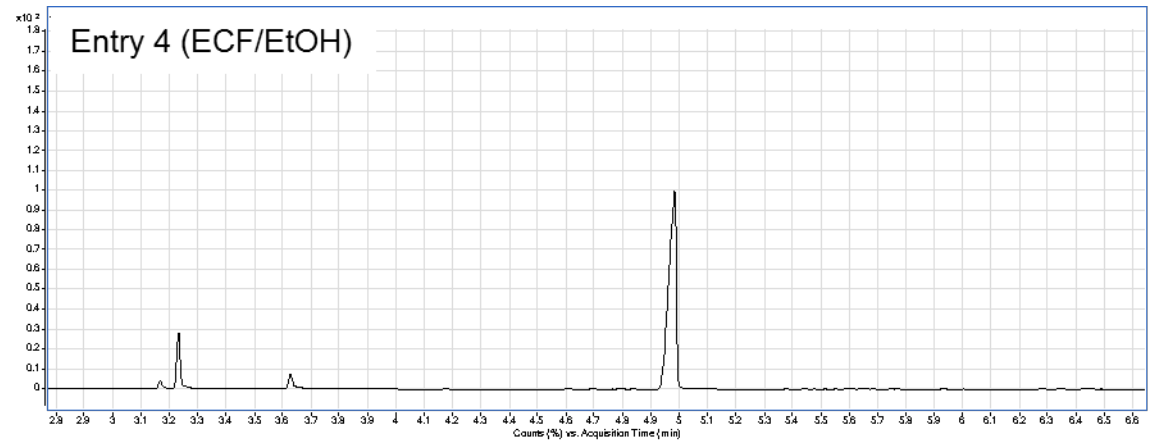

Figure S19 Chromatogram of the reaction mixture corresponding to entry 4 (Table S1).

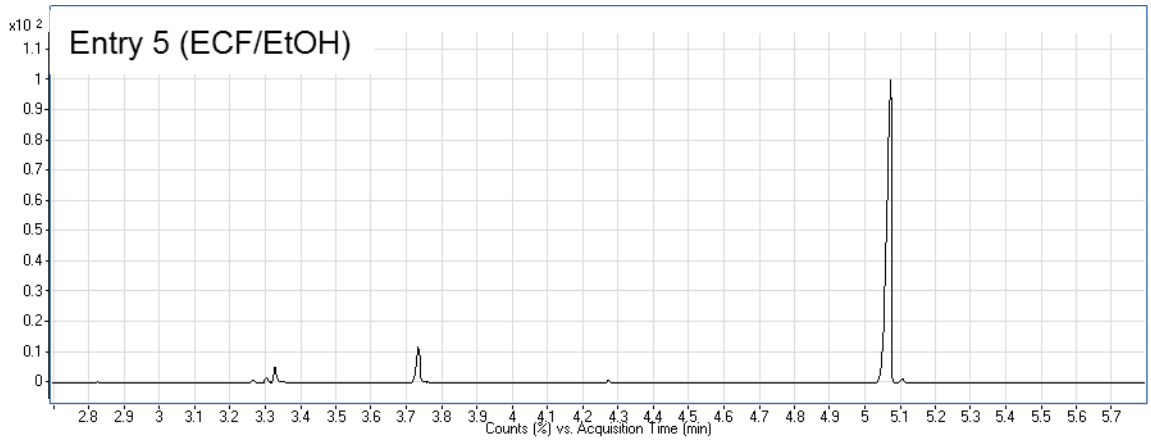

Figure S20 Chromatogram of the reaction mixture corresponding to entry 5, Table S1 (also: entry 5, Table 1).

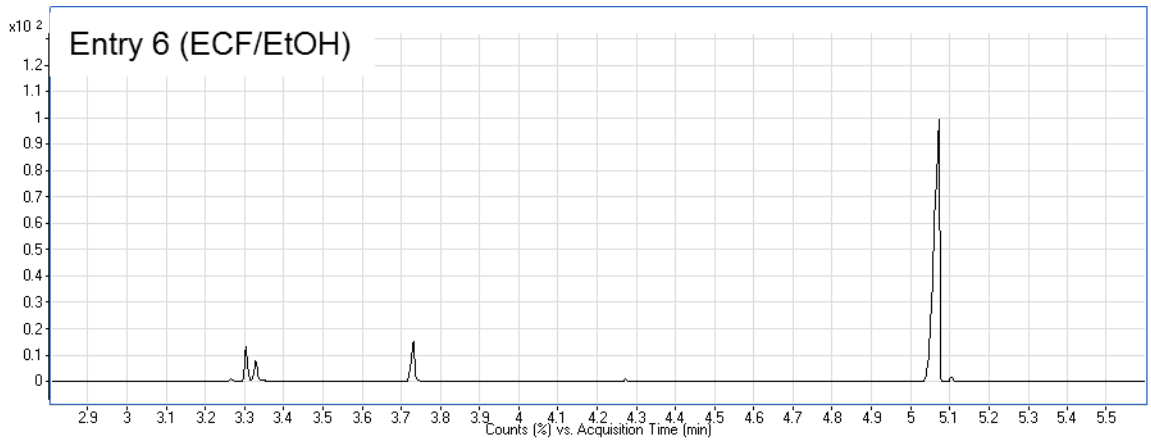

Figure S21 Chromatogram of the reaction mixture corresponding to entry 6 (Table S1).

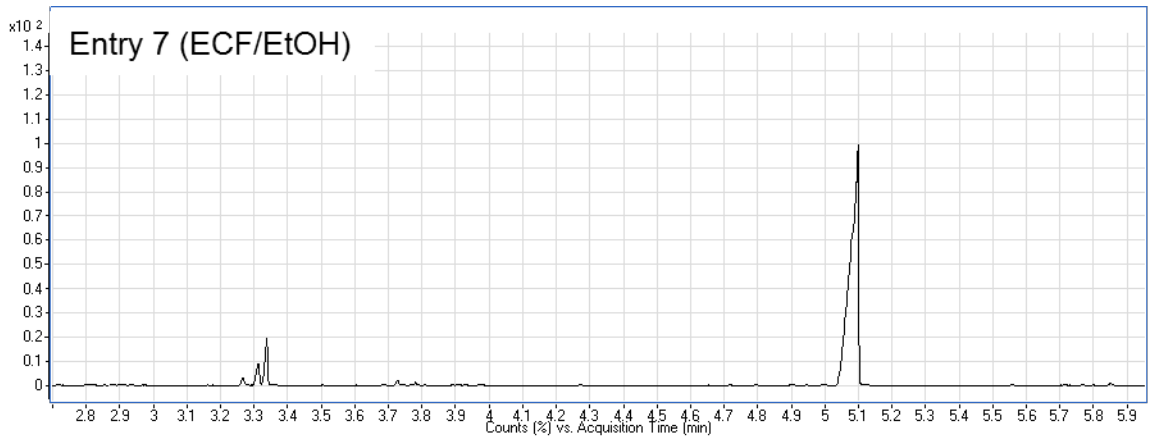

Figure S22 Chromatogram of the reaction mixture corresponding to entry, Table S1 (also: entry 6, Table 1).

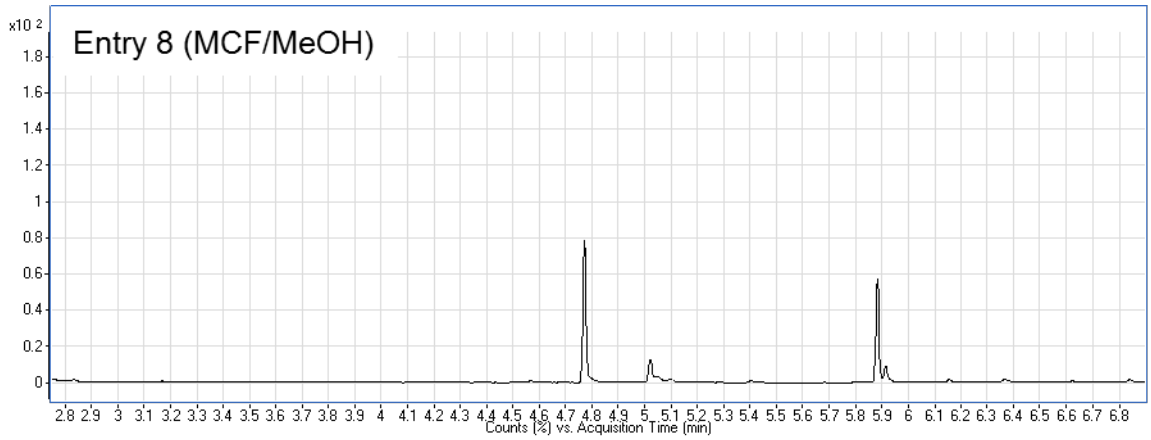

Figure S23 Chromatogram of the reaction mixture corresponding to entry 8, Table S1 (also: entry 7, Table 1).

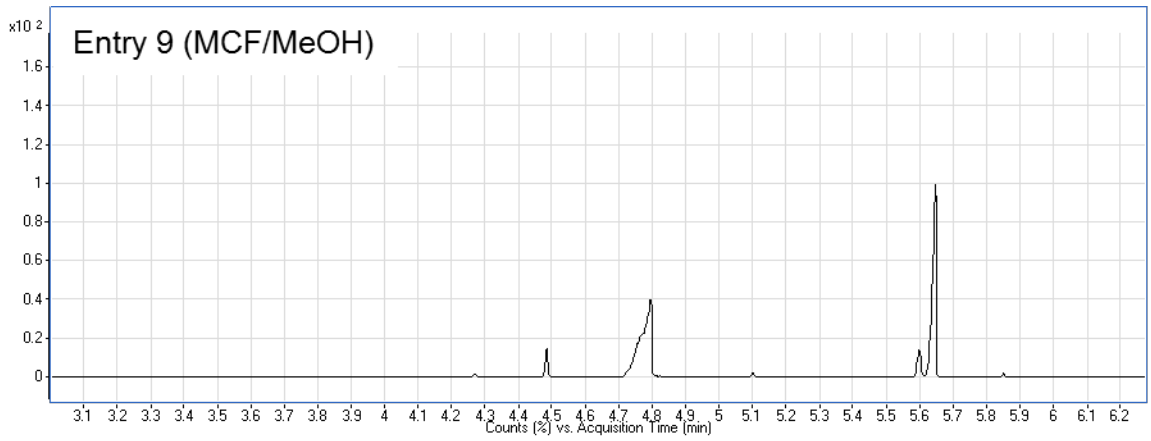

Figure S24 Chromatogram of the reaction mixture corresponding to entry 9 (Table S1).

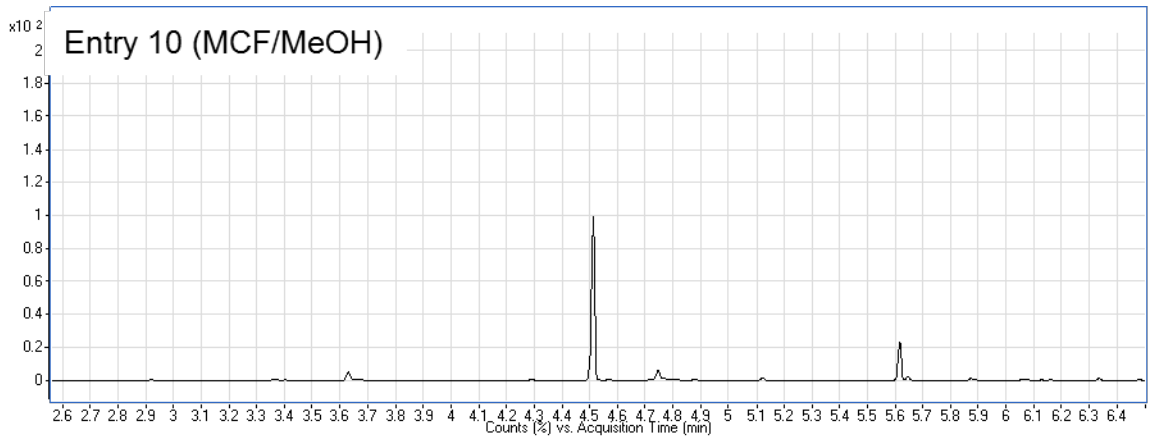

Figure S25 Chromatogram of the reaction mixture corresponding to entry 10, Table S1 (also: entry 8, Table 1).

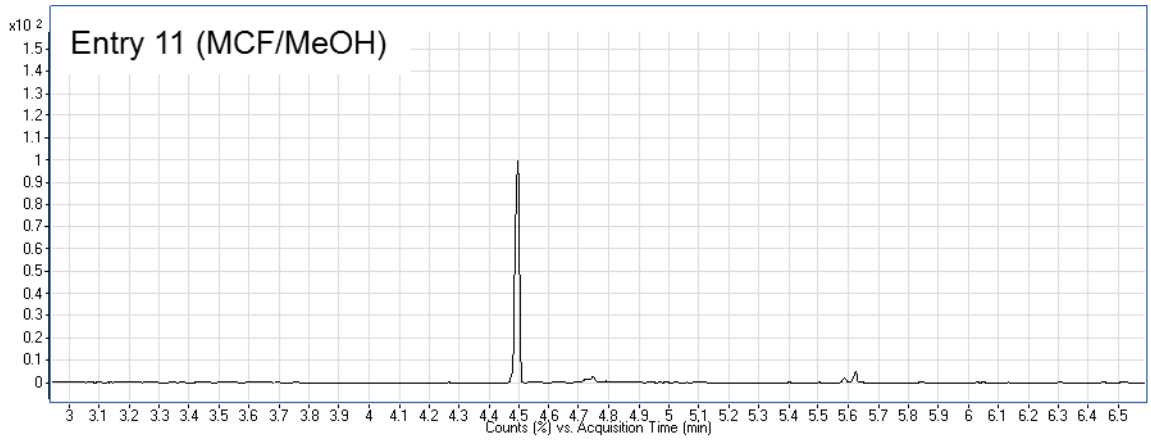

Figure S26 Chromatogram of the reaction mixture corresponding to entry 11 (Table S1).

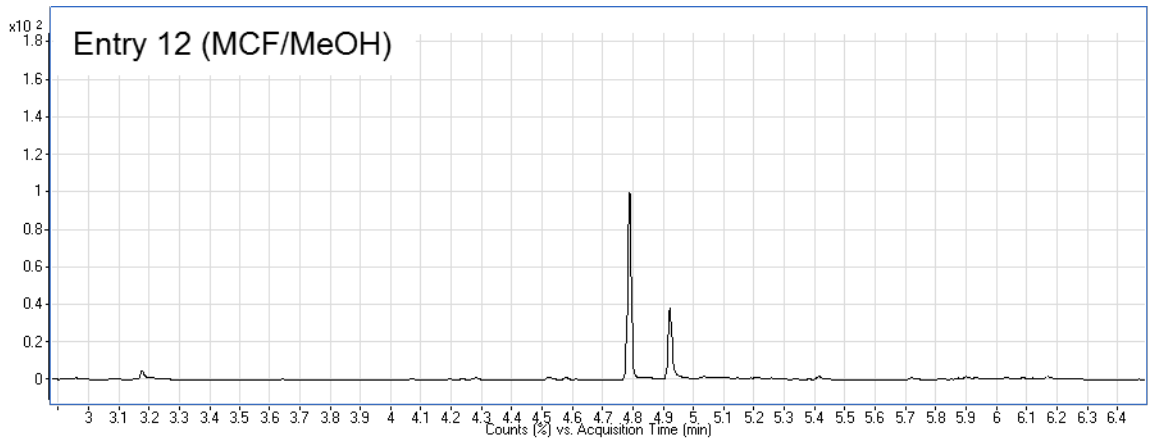

Figure S27 Chromatogram of the reaction mixture corresponding to entry 12, Table S1 (also: entry 9, Table 1).

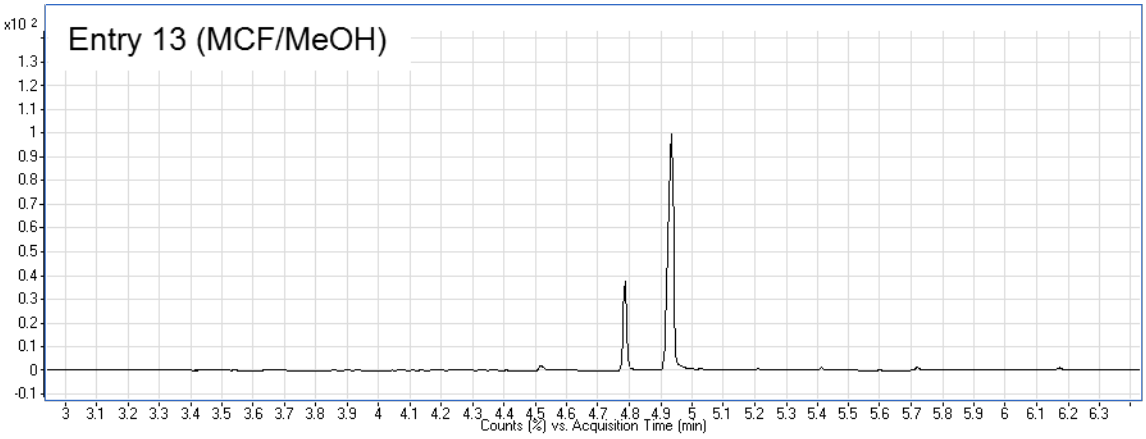

Figure S28 Chromatogram of the reaction mixture corresponding to entry 13, Table S1 (also: entry 10, Table 1).

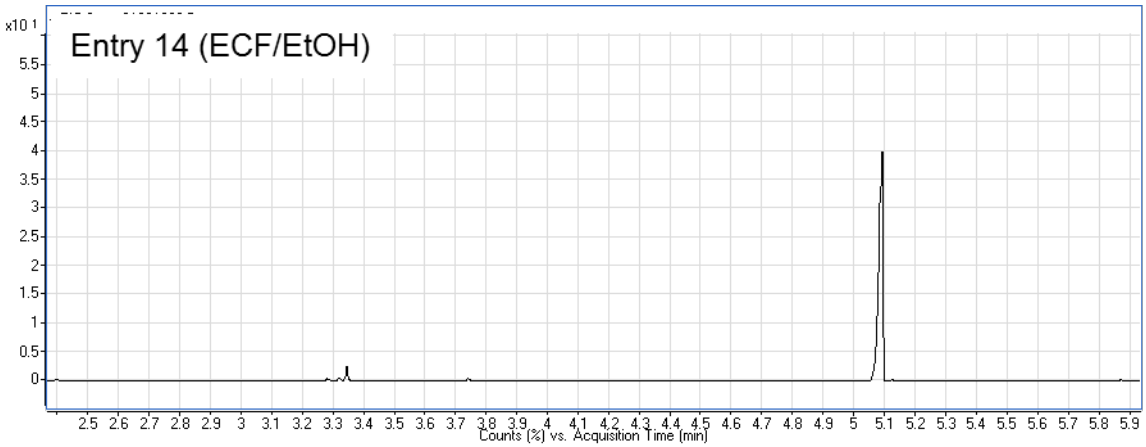

Figure S29 Chromatogram of the reaction mixture corresponding to entry 14 (Table S1).

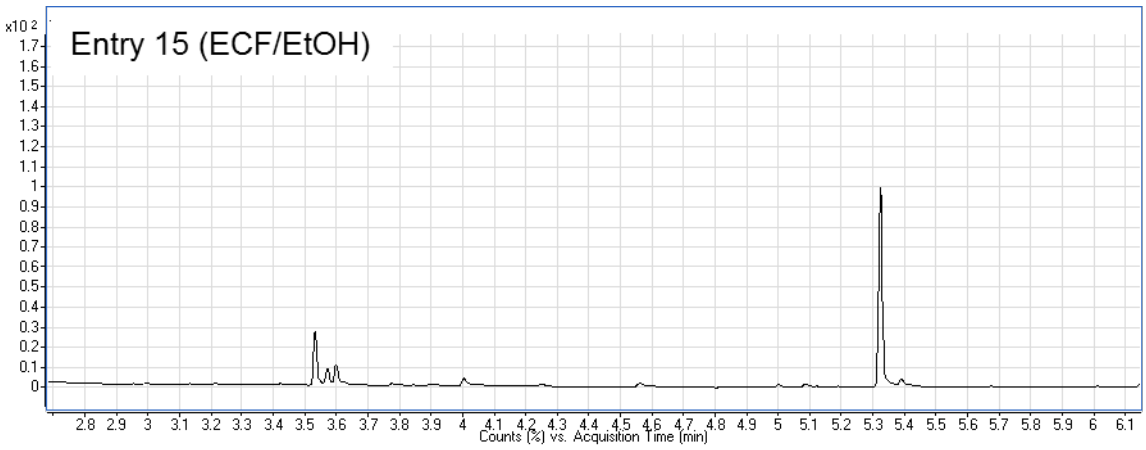

Figure S30 Chromatogram of the reaction mixture corresponding to entry 15 (Table S1).

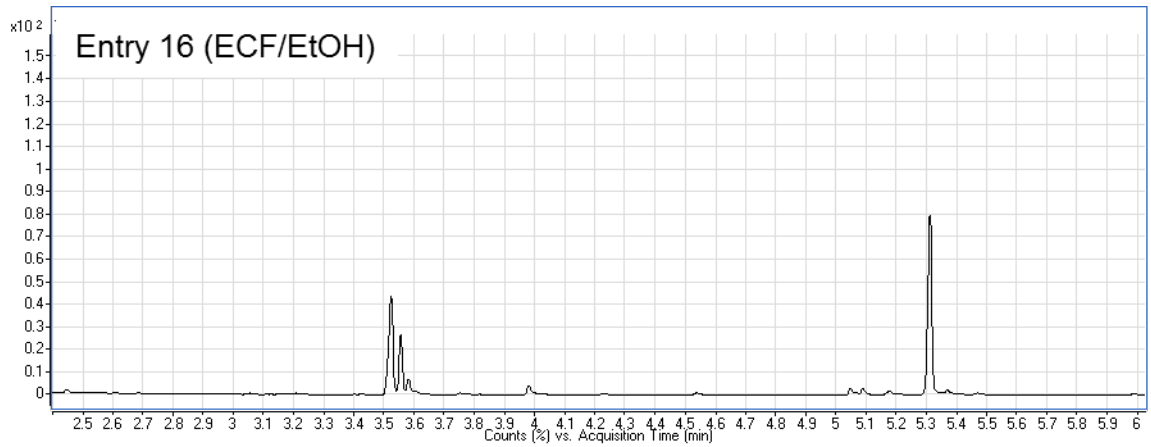

Figure S31 Chromatogram of the reaction mixture corresponding to entry 16 (Table S1).

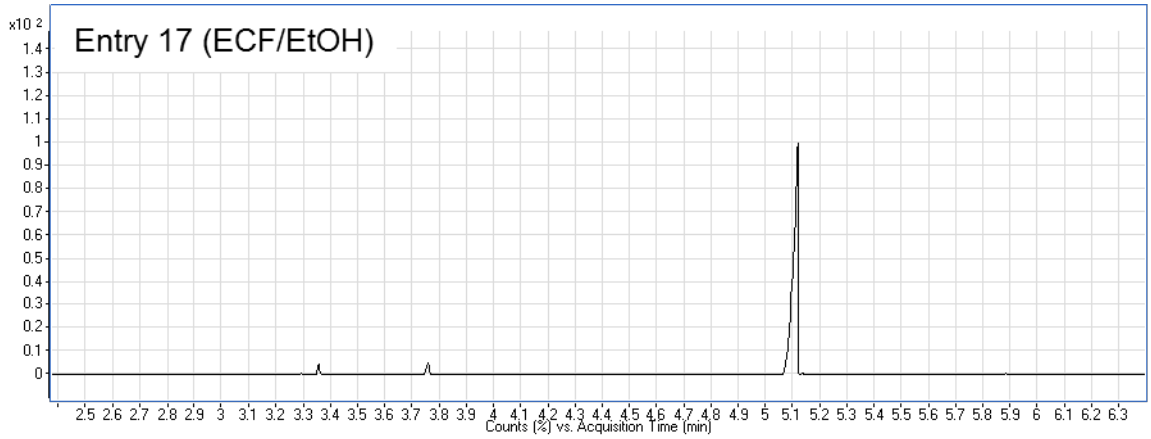

Figure S32 Chromatogram of the reaction mixture corresponding to entry 17 (Table S1).

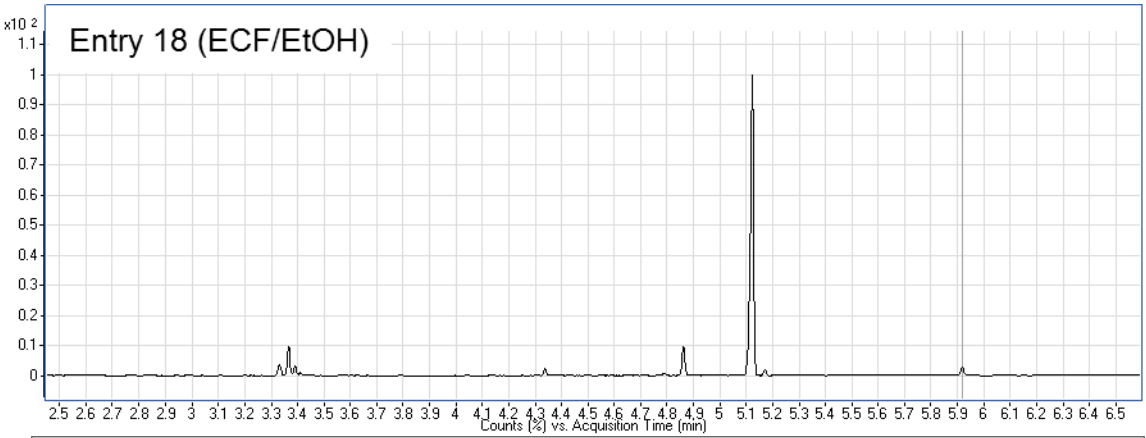
Entry 18 (ECF/EtOH)
x10 2
Counts (%) vs. Acquisition Time (min)

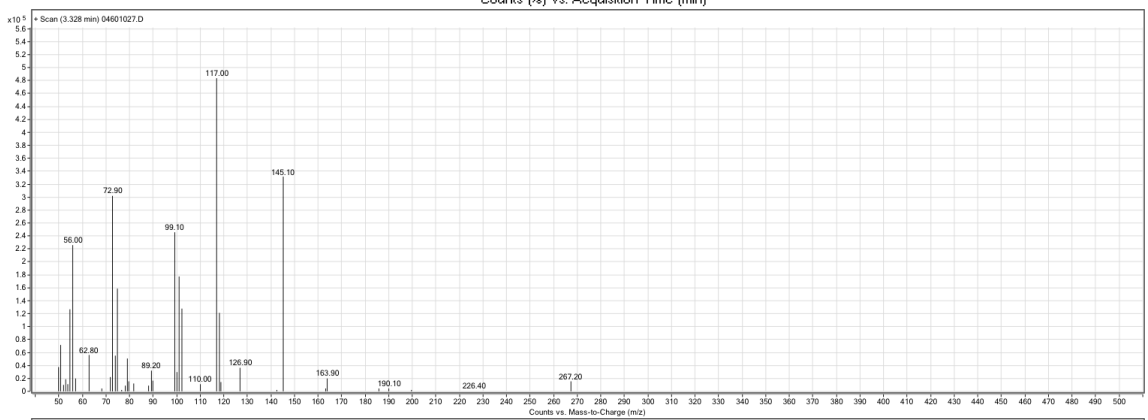
Scan (3.328 min) 04601027.D
117.00
145.10
72.90
99.10
56.00
62.80
89.20
126.90
110.00
163.90
190.10
226.40
267.20
Counts vs. Mass-to-Charge (m/z)

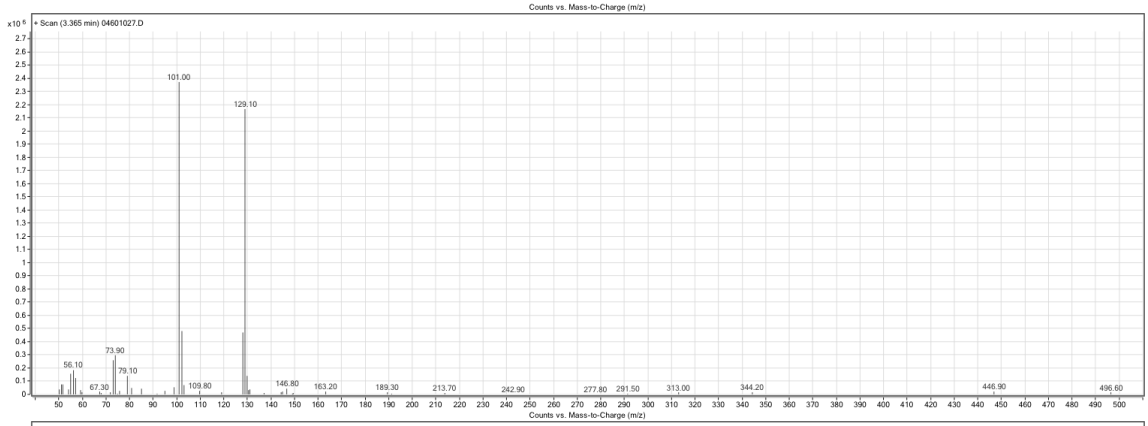
Scan (3.365 min) 04601027.D
101.00
129.10
73.90
56.10
79.10
67.30
109.80
146.80
163.20
189.30
213.70
242.90
277.80
291.50
313.00
344.20
446.90
496.60
Counts vs. Mass-to-Charge (m/z)

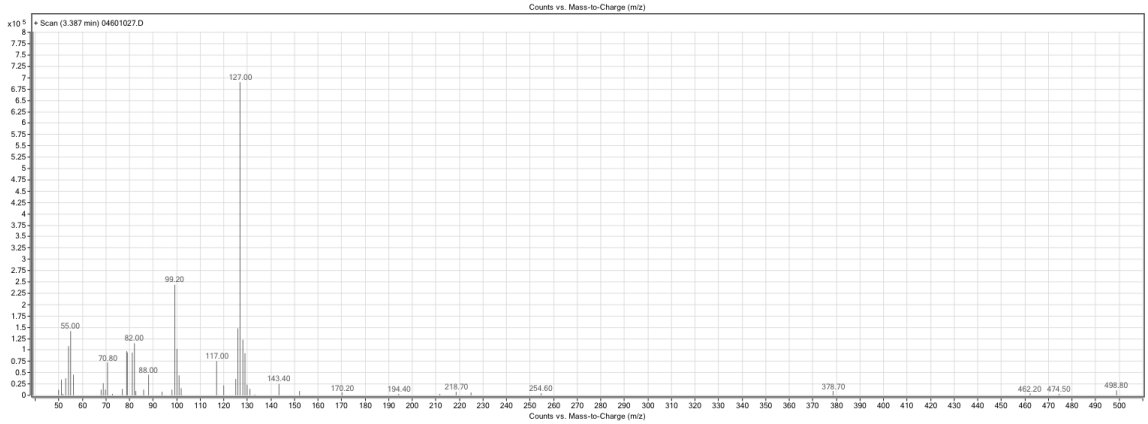
Scan (3.387 min) 04601027.D
127.00
99.20
55.00
82.00
70.80
88.00
117.00
143.40
170.20
194.40
218.70
254.60
378.70
462.20
474.50
498.80
Counts vs. Mass-to-Charge (m/z)

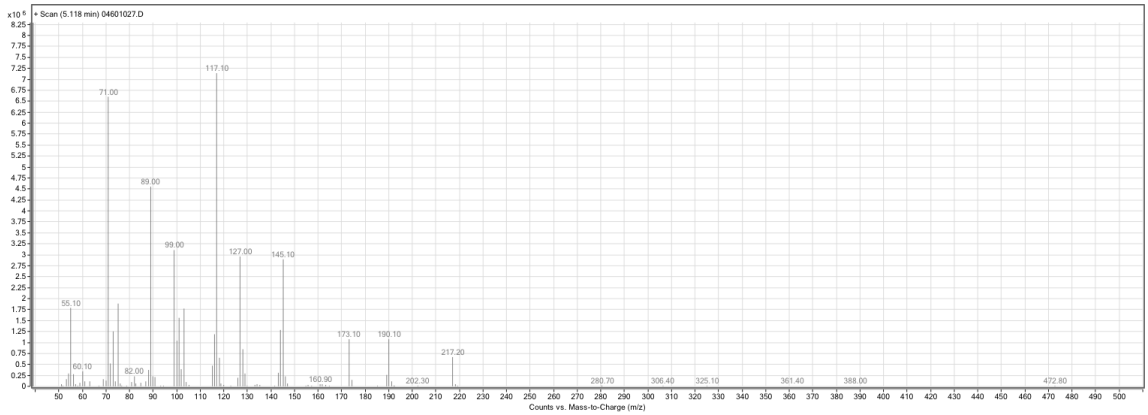

Figure S33 Chromatogram of the reaction mixture corresponding to entry 18, Table S1 (also: entry 11, Table 1), and MS spectra corresponding to analytical GC peaks.

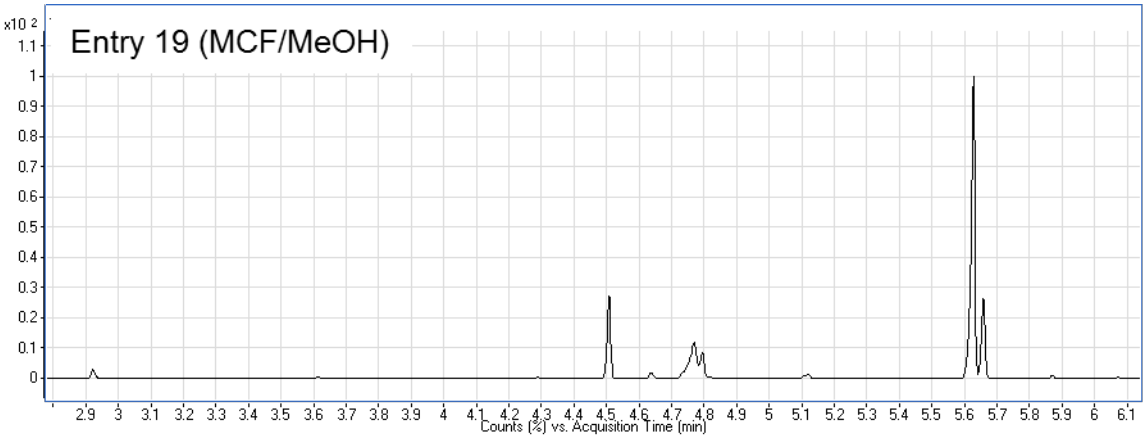

Figure S34 Chromatogram of the reaction mixture corresponding to entry 19 (Table S1).

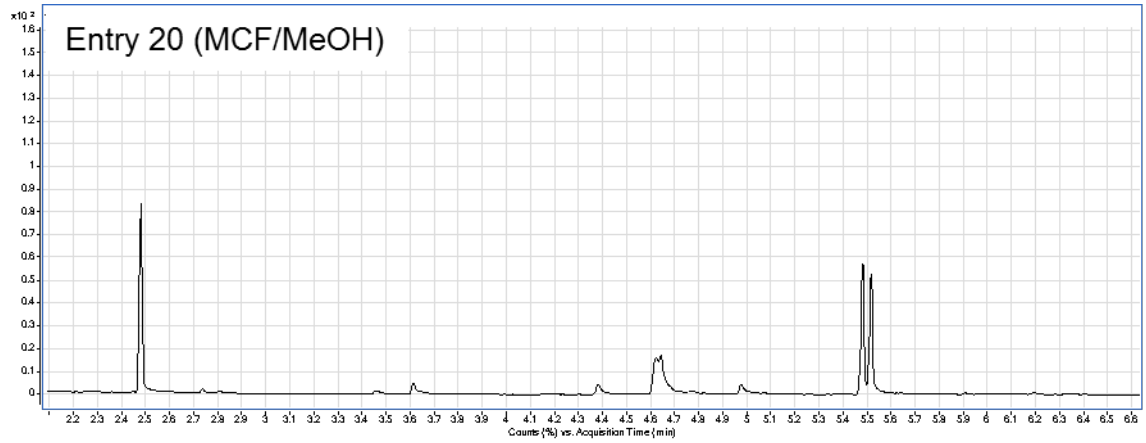

Figure S35 Chromatogram of the reaction mixture corresponding to entry 20 (Table S1).

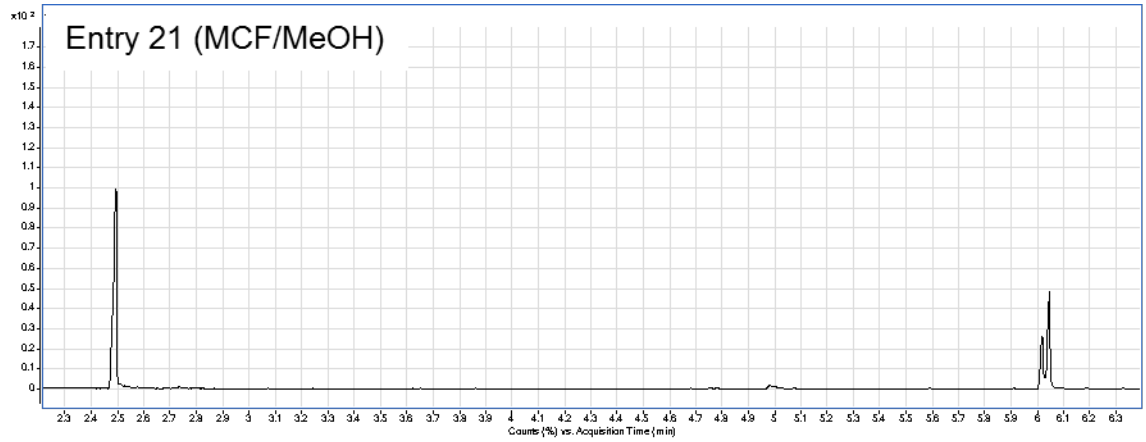

Figure S36 Chromatogram of the reaction mixture corresponding to entry 21 (Table S1).

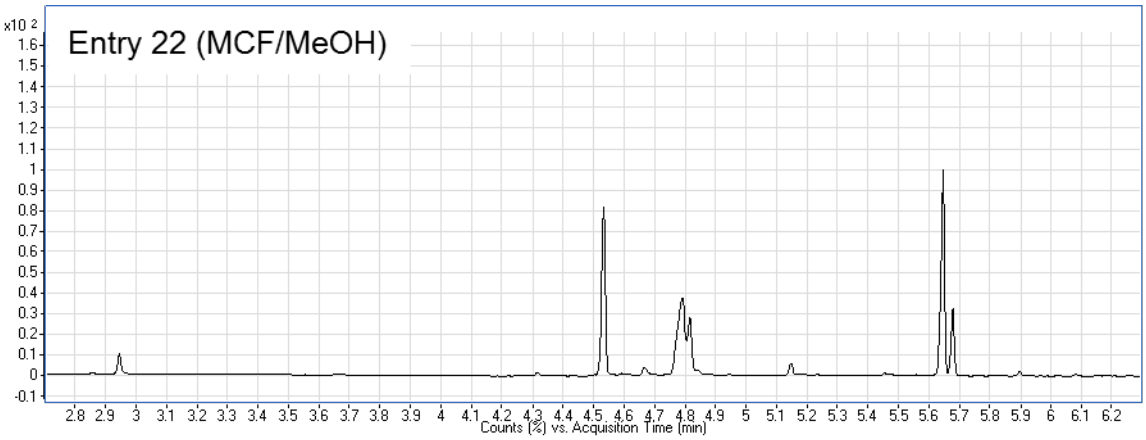

Figure S37 Chromatogram of the reaction mixture corresponding to entry 22, Table S1 (also: entry 12, Table 1).

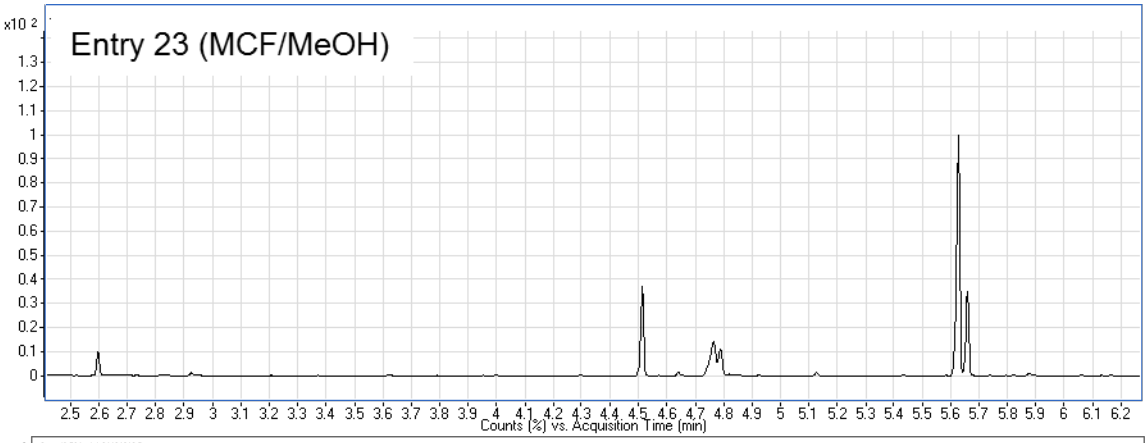
Entry 23 (MCF/MeOH)
x10 2
Counts (%) vs. Acquisition Time (min)

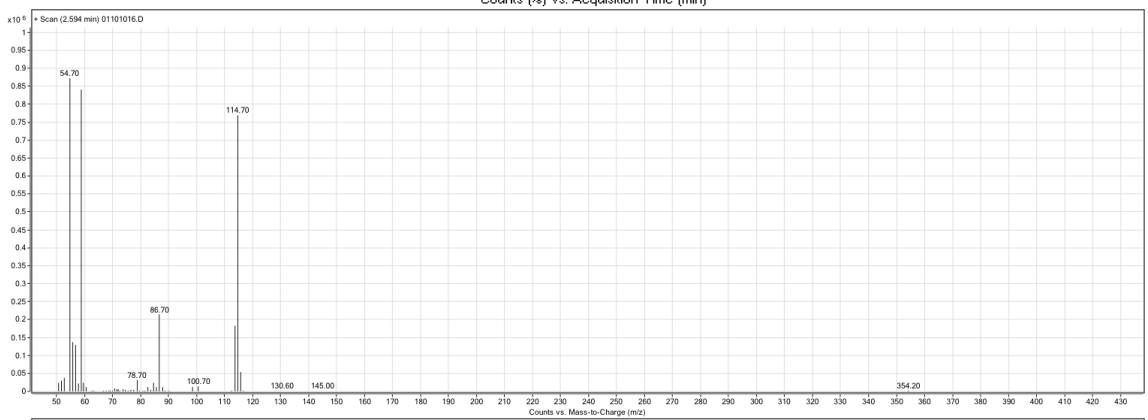
Scan (2.594 min) 01101016.D
54.70
114.70
86.70
78.70
100.70
130.60
145.00
354.20
Counts vs. Mass-to-Charge (m/z)

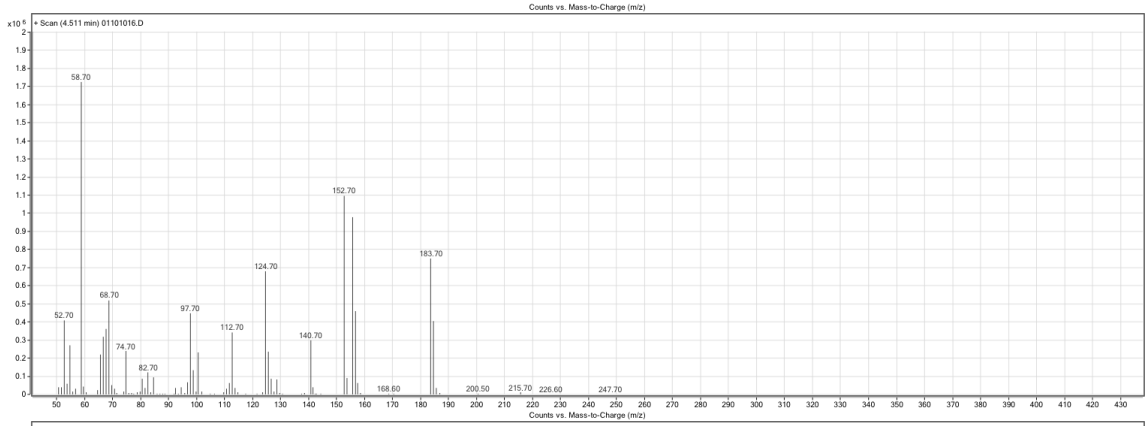
Scan (4.511 min) 01101016.D
58.70
152.70
183.70
124.70
68.70
52.70
97.70
112.70
140.70
74.70
82.70
168.60
200.50
215.70
226.60
247.70
Counts vs. Mass-to-Charge (m/z)

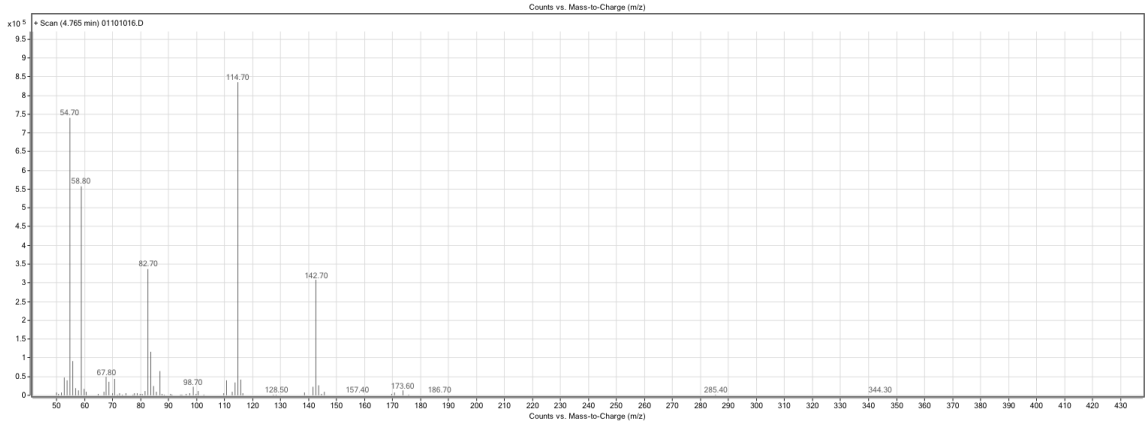
Scan (4.765 min) 01101016.D
114.70
54.70
58.80
82.70
142.70
67.80
98.70
128.50
157.40
173.60
186.70
285.40
344.30
Counts vs. Mass-to-Charge (m/z)

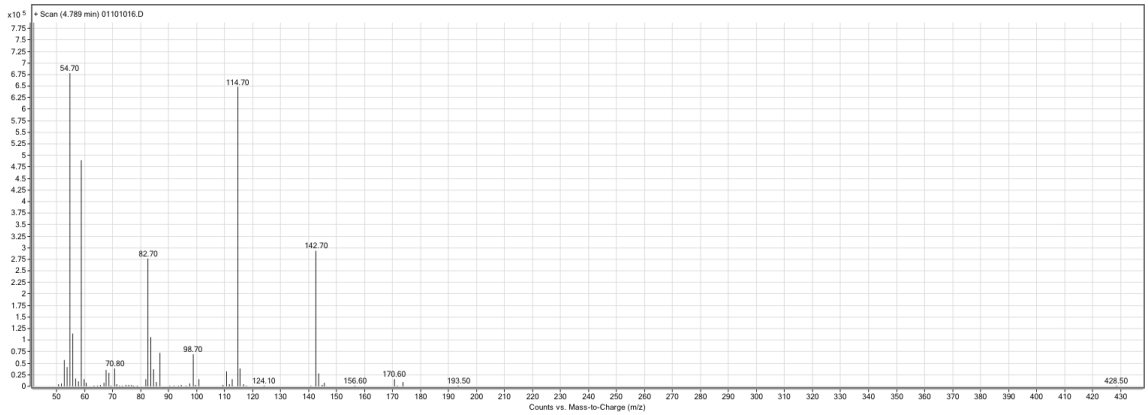

Figure S38 Chromatogram of the reaction mixture corresponding to entry 23, Table S1 (also: entry 13, Table 1), and MS spectra corresponding to analytical GC peaks.

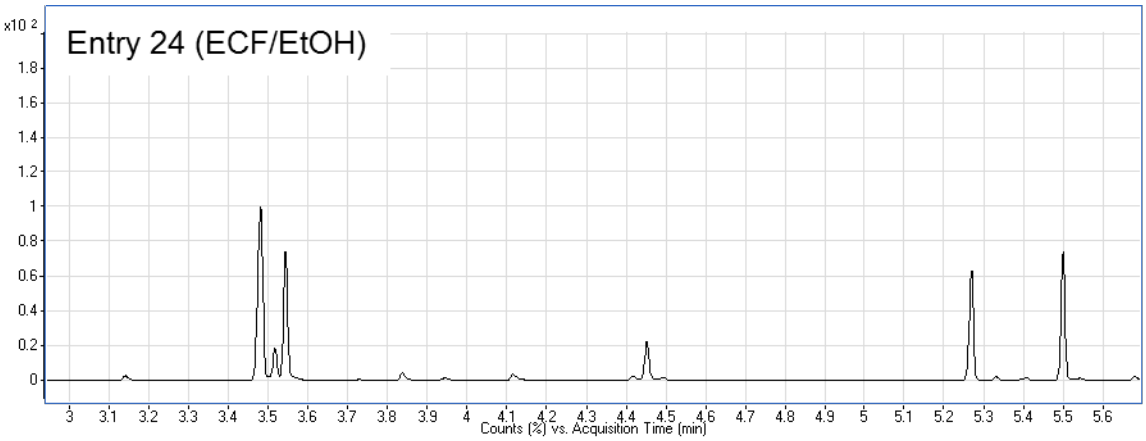

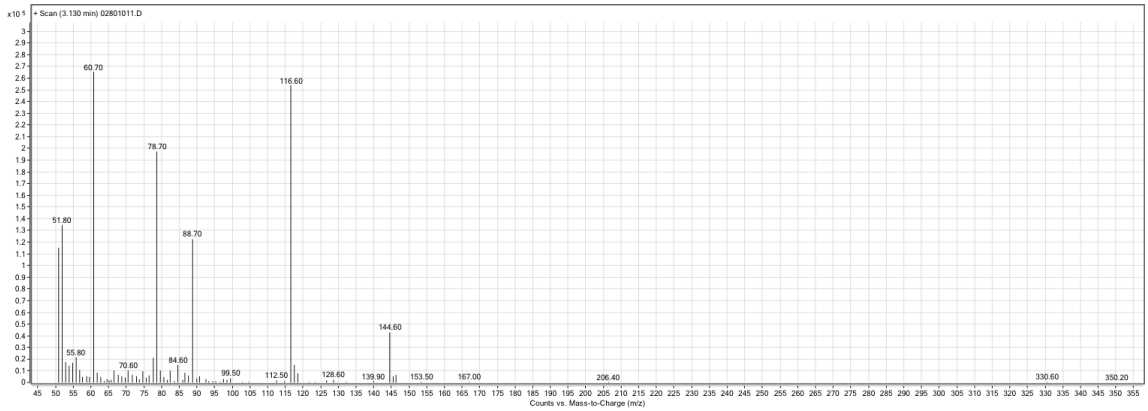

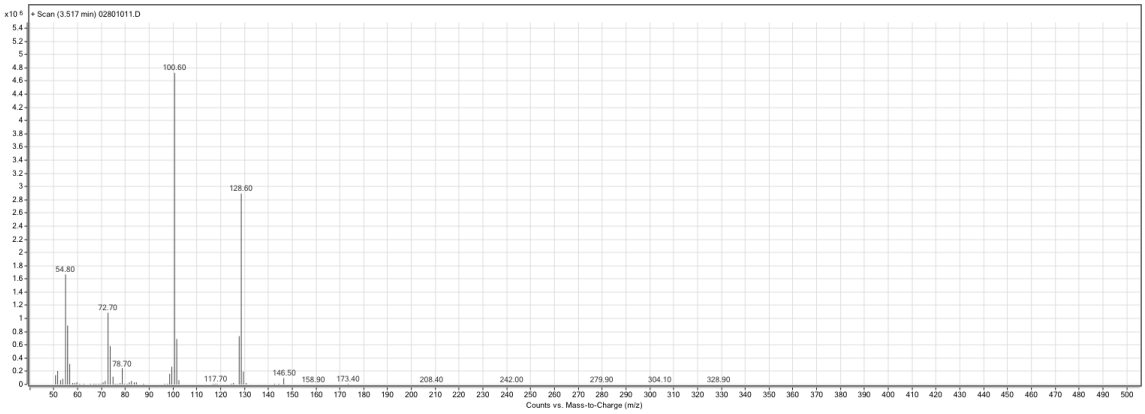
x10 6
+ Scan (3.517 min) 02801011.D
100.60
128.60
54.80
72.70
78.70
117.70
146.50
158.90
173.40
208.40
242.00
279.90
304.10
328.90
Counts vs. Mass-to-Charge (m/z)

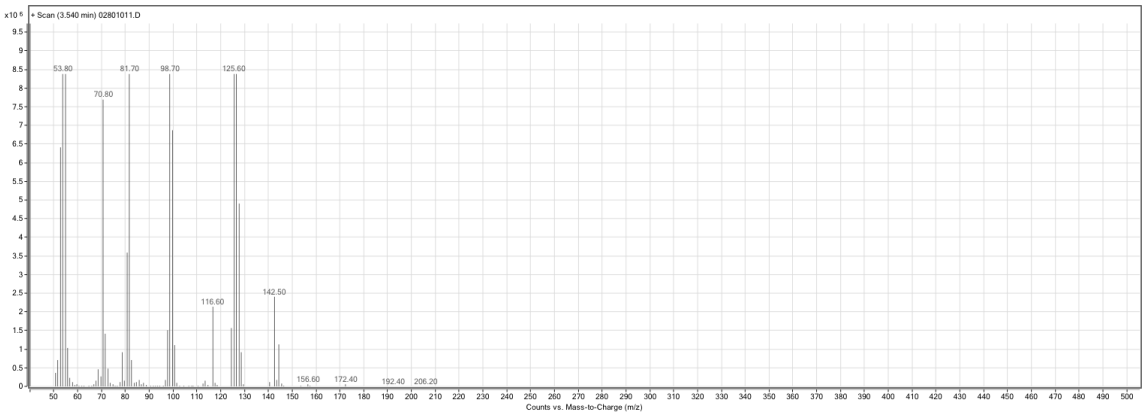
x10 6
+ Scan (3.540 min) 02801011.D
53.80
81.70
98.70
125.60
70.80
116.60
142.50
156.60
172.40
192.40
206.20
Counts vs. Mass-to-Charge (m/z)

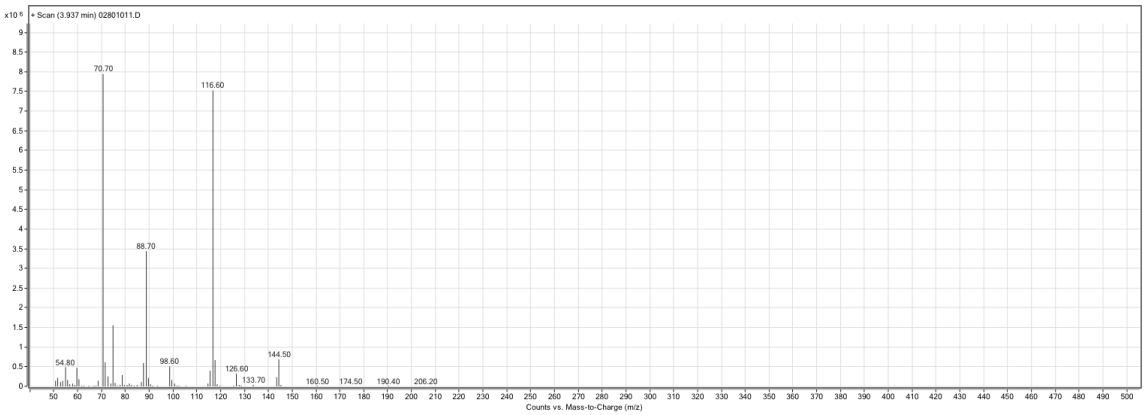
x10 6
+ Scan (3.937 min) 02801011.D
70.70
116.60
88.70
54.80
98.60
126.60
133.70
144.50
160.50
174.50
190.40
206.20
Counts vs. Mass-to-Charge (m/z)

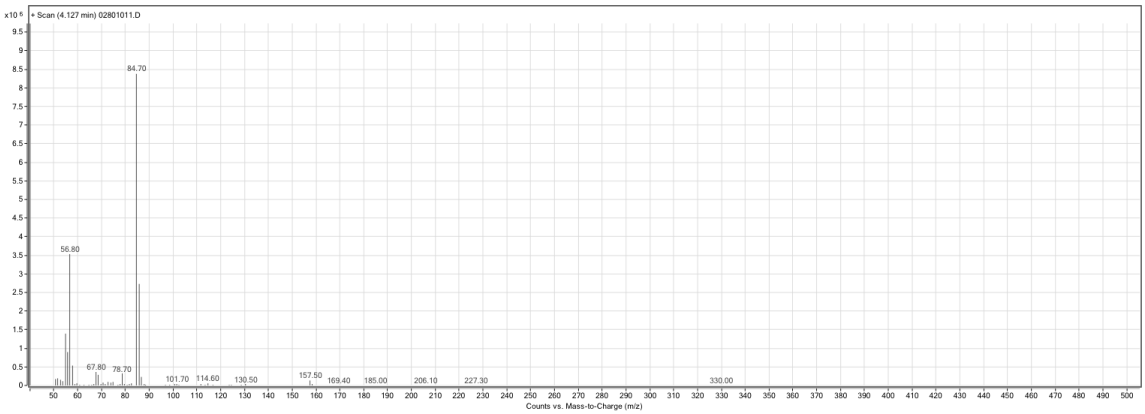
x10 6
+ Scan (4.127 min) 02801011.D
84.70
56.80
67.80
78.70
101.70
114.60
130.50
157.50
169.40
185.00
206.10
227.30
330.00
Counts vs. Mass-to-Charge (m/z)

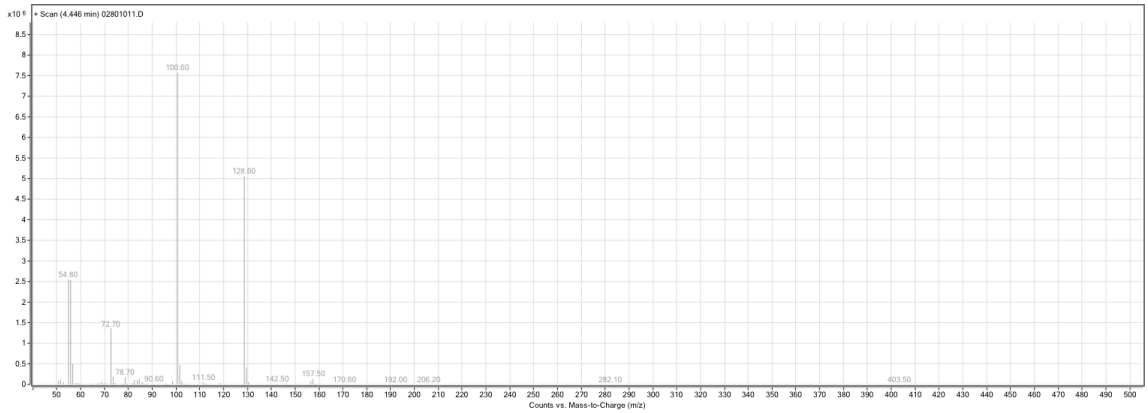
x10 6
+ Scan (4.446 min) 02801011.D
100.60
128.60
54.80
72.70
78.70
90.60
111.50
142.50
157.50
170.60
192.00
206.20
282.10
403.50
Counts vs. Mass-to-Charge (m/z)

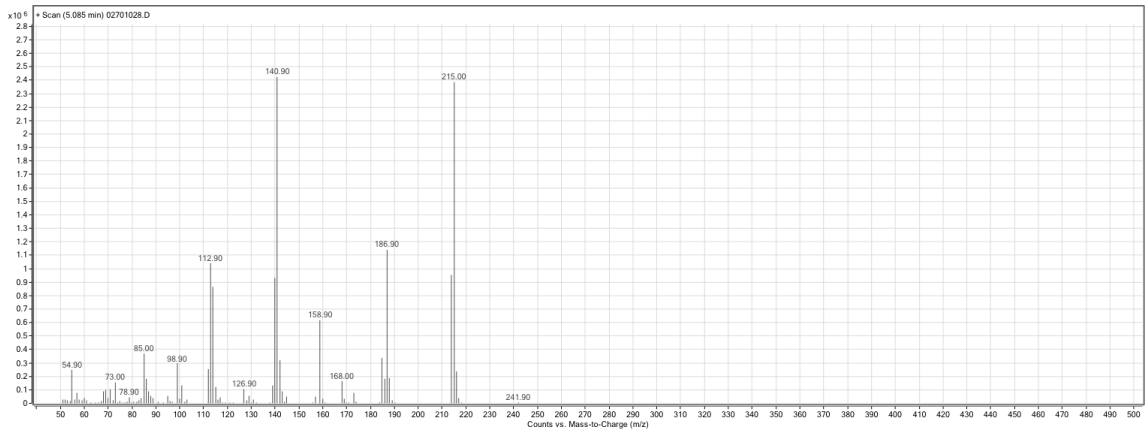
x10 6
+ Scan (5.085 min) 02701028.D
140.90
215.00
186.90
112.90
158.90
85.00
98.90
54.90
73.00
78.90
126.90
168.00
241.90
Counts vs. Mass-to-Charge (m/z)

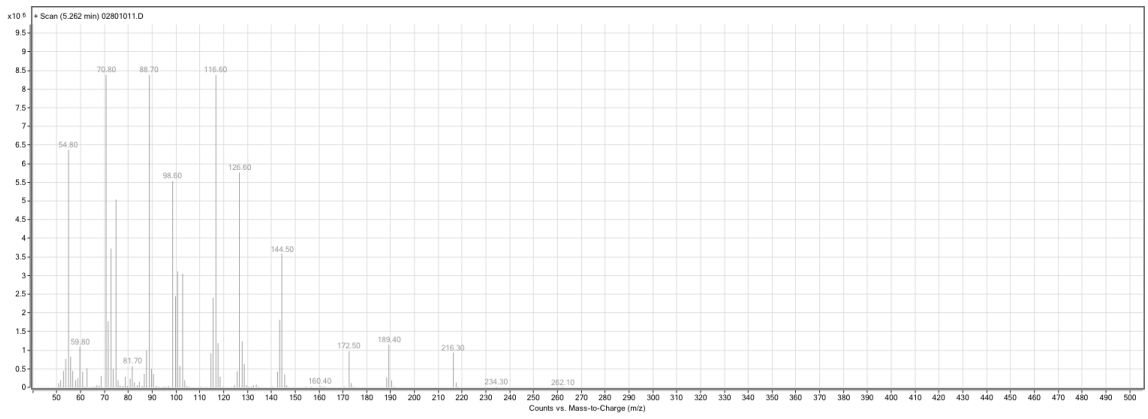
x10 6
+ Scan (5.262 min) 02801011.D
70.80
88.70
116.60
54.80
98.60
126.60
144.50
59.80
81.70
172.50
189.40
216.30
160.40
234.30
262.10
Counts vs. Mass-to-Charge (m/z)

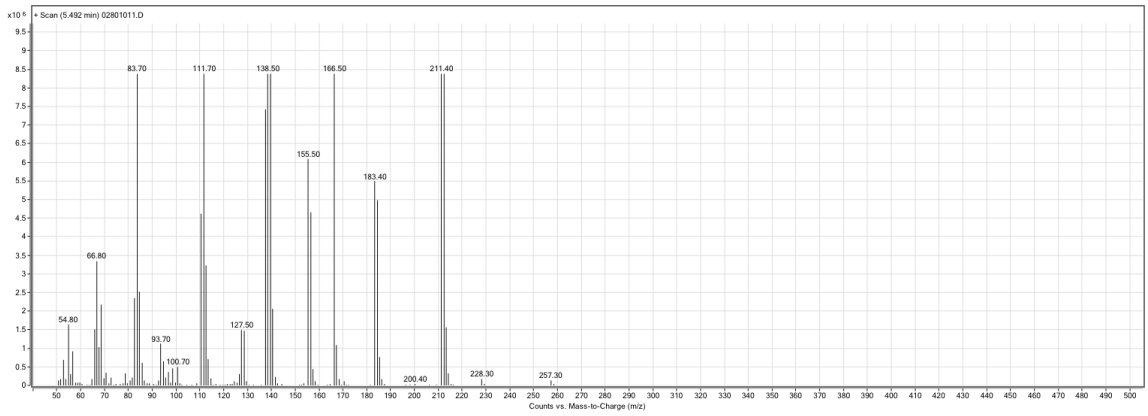
x10 6
+ Scan (5.492 min) 02801011.D
83.70
111.70
138.50
166.50
211.40
155.50
183.40
66.80
54.80
93.70
127.50
100.70
200.40
228.30
257.30
Counts vs. Mass-to-Charge (m/z)

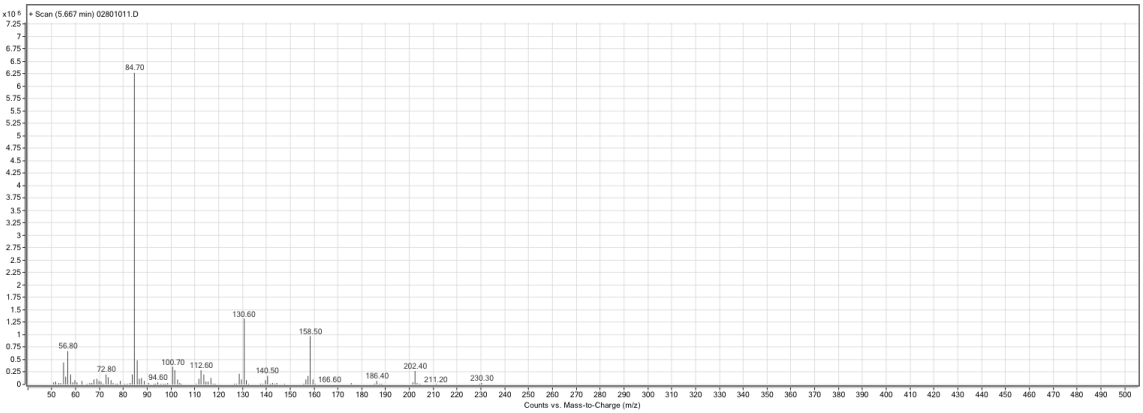

Figure S39 Chromatogram of the reaction mixture corresponding to entry 24, Table S1 (also: entry 14, Table 1), and MS spectra corresponding to analytical GC peaks.

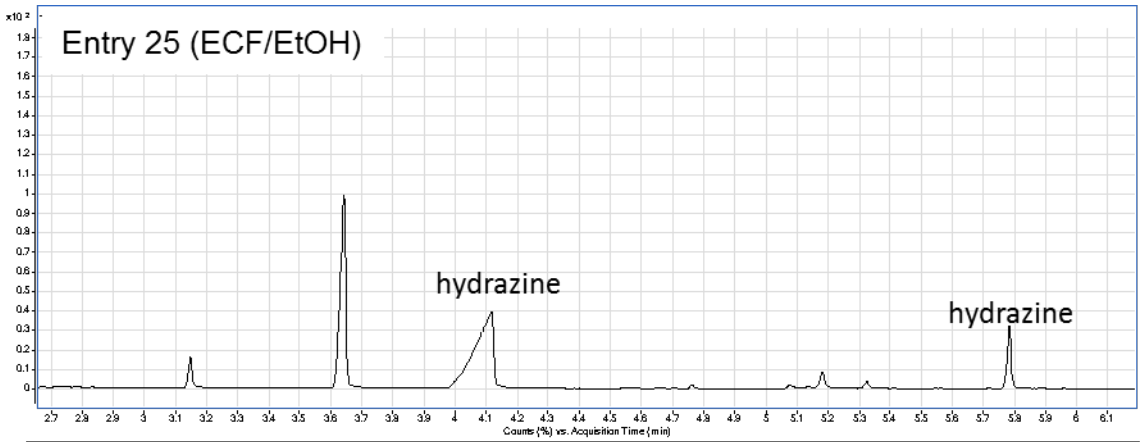

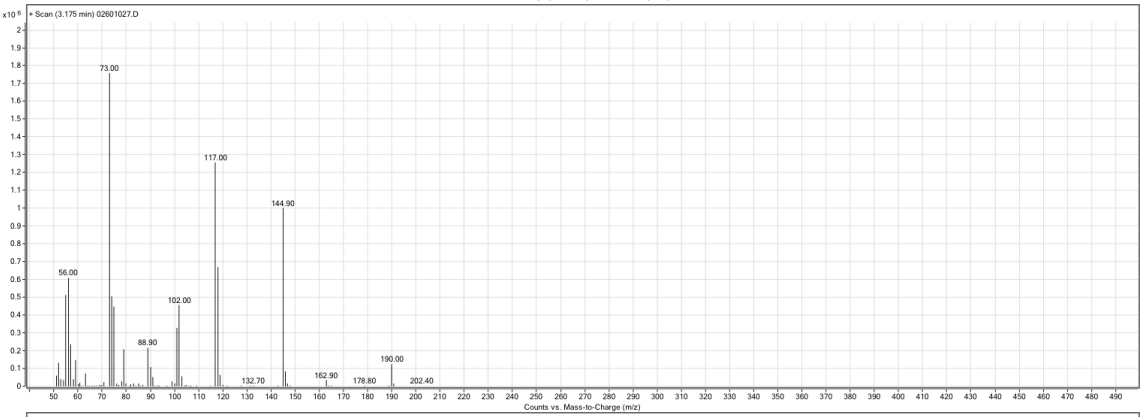

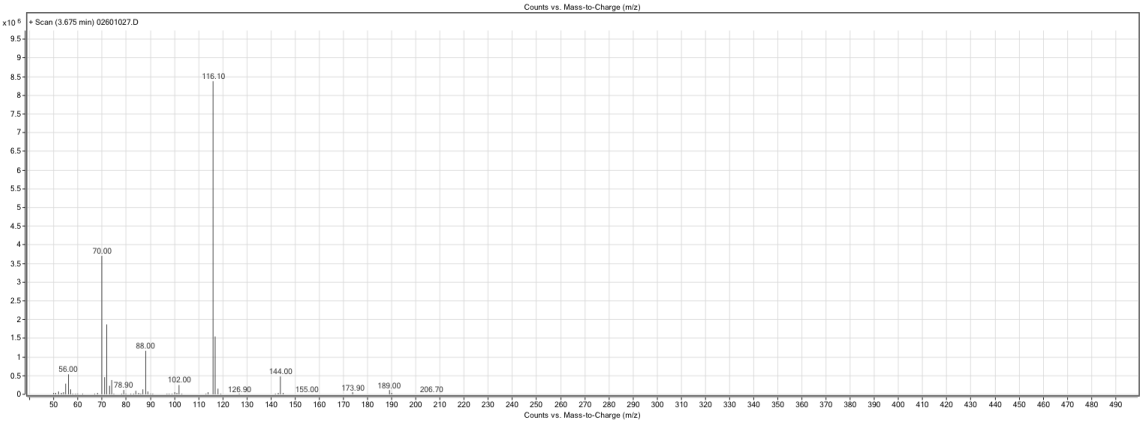

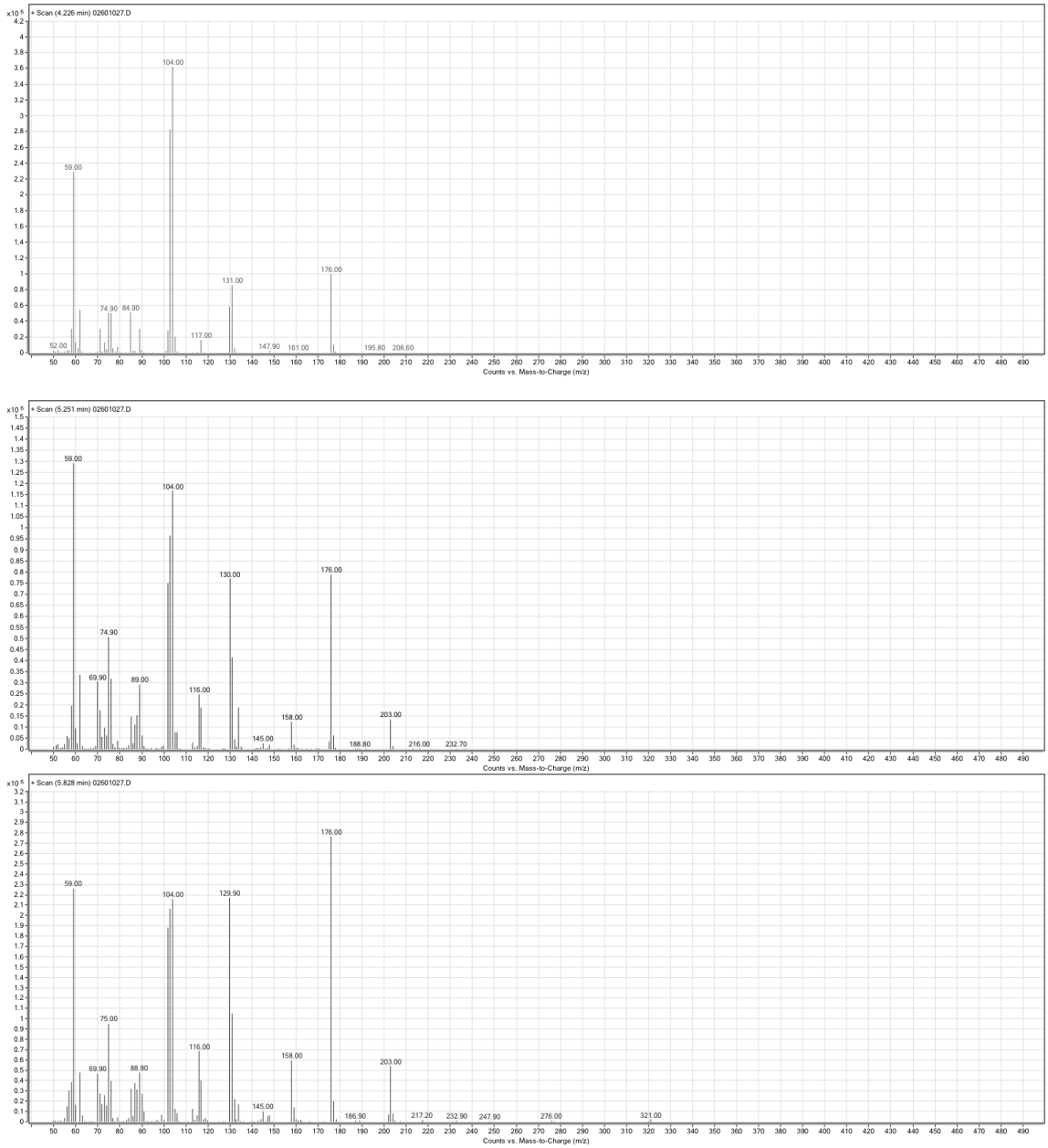

Figure S40 Chromatogram and MS Spectrum of the reaction mixture corresponding to entry 25, Table S1 (also: entry 15, Table 1).

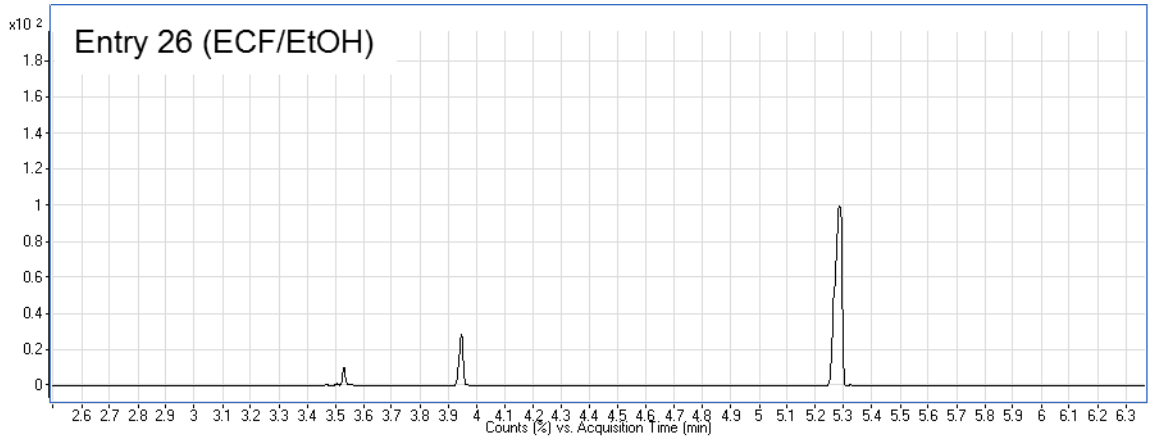

Figure S41 Chromatogram of the reaction mixture corresponding to entry 26 (Table S1).

Sample chromatograms corresponding to entries 1 – 13 in Table S7 can be found below (Fig. S42 – S54).

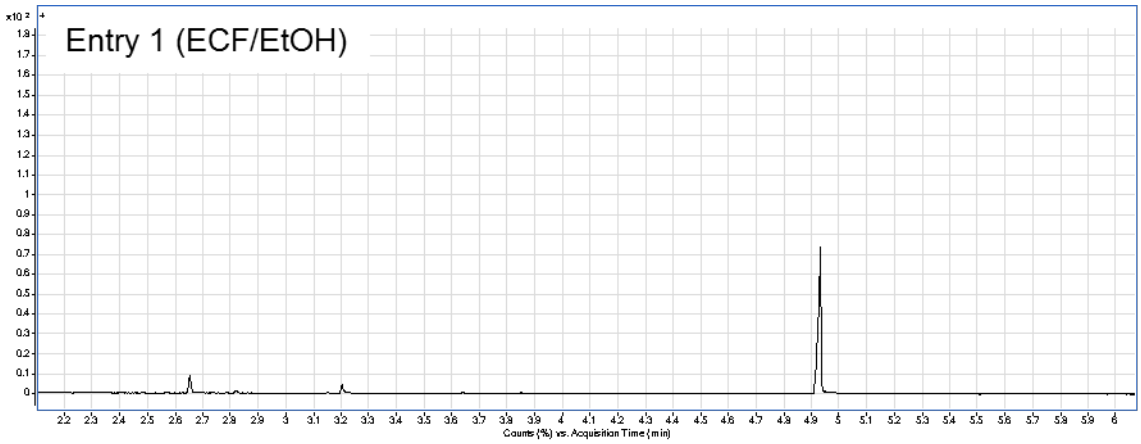

Figure S42 Chromatogram of the reaction mixture corresponding to entry 1 (Table S7).

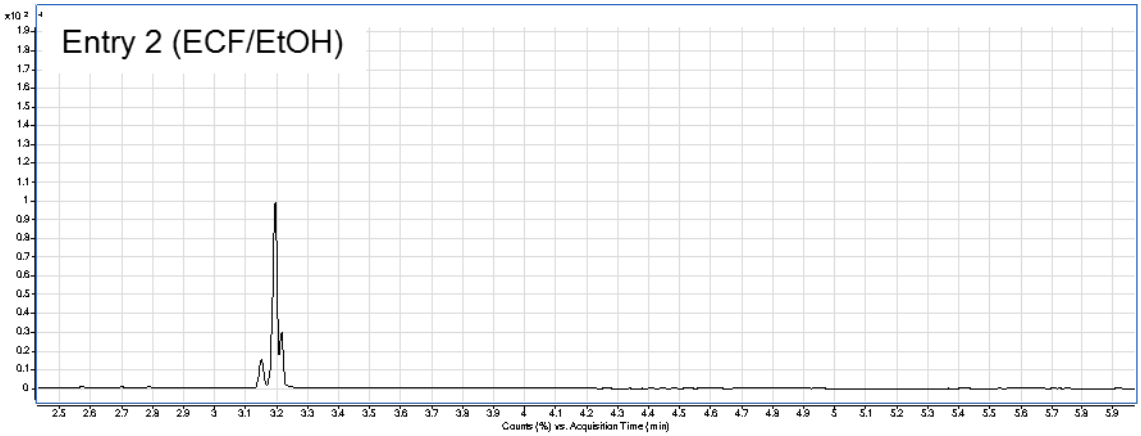

Figure S43 Chromatogram of the reaction mixture corresponding to entry 2 (Table S7).

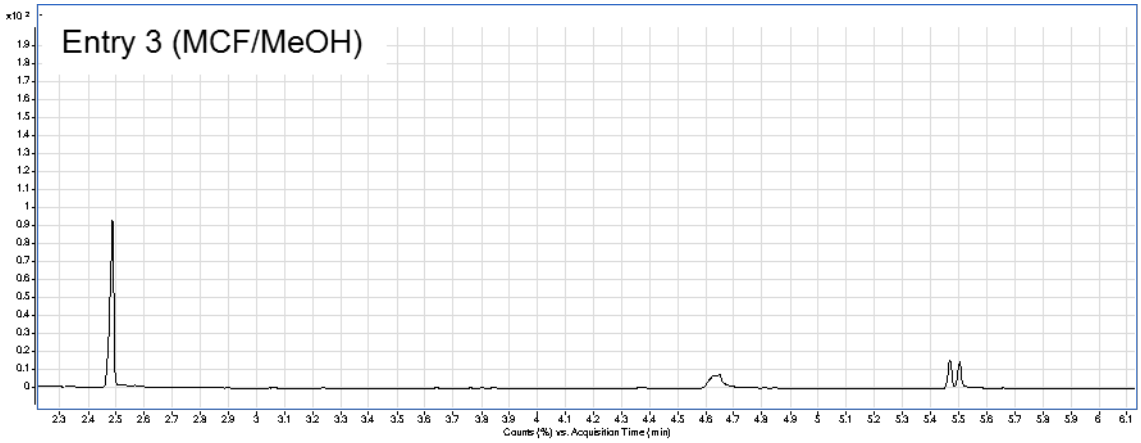

Figure S44 Chromatogram of the reaction mixture corresponding to entry 3 (Table S7).

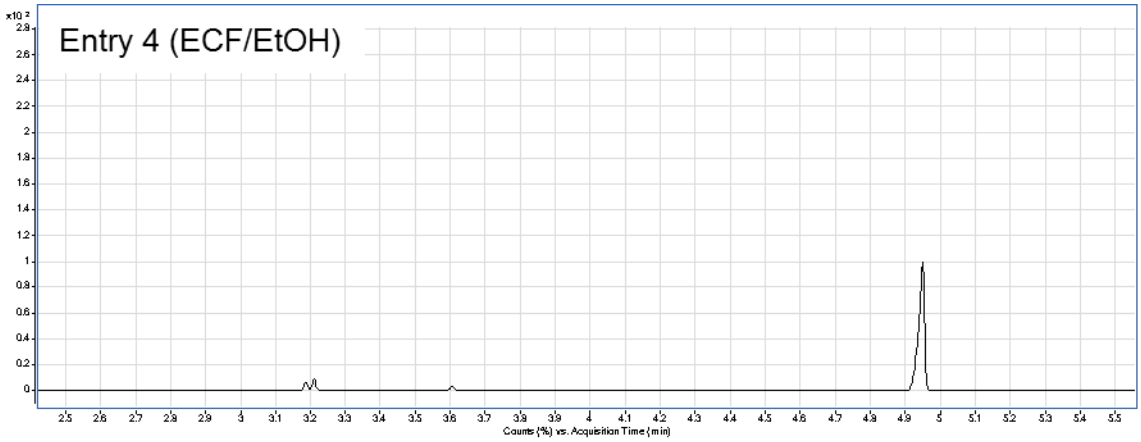

Figure S45 Chromatogram of the reaction mixture corresponding to entry 4 (Table S7).

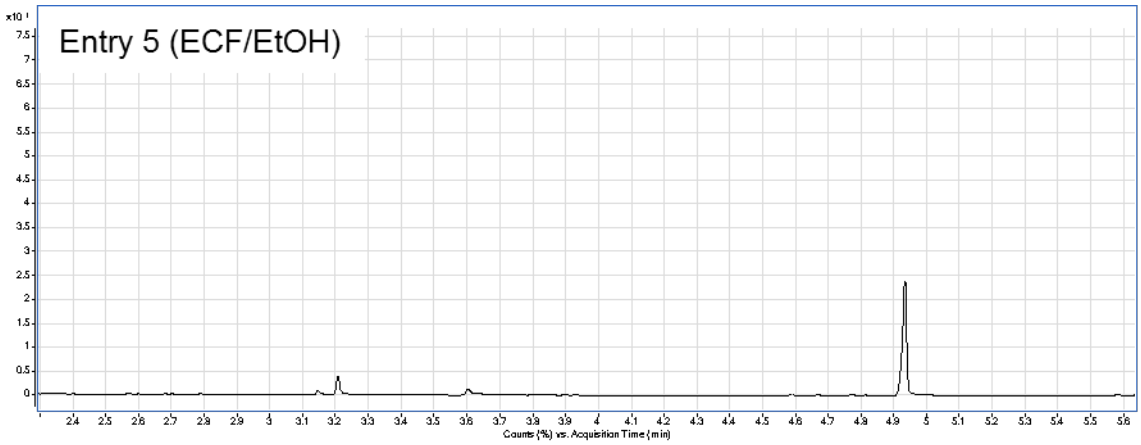

Figure S46 Chromatogram of the reaction mixture corresponding to entry 5 (Table S7).

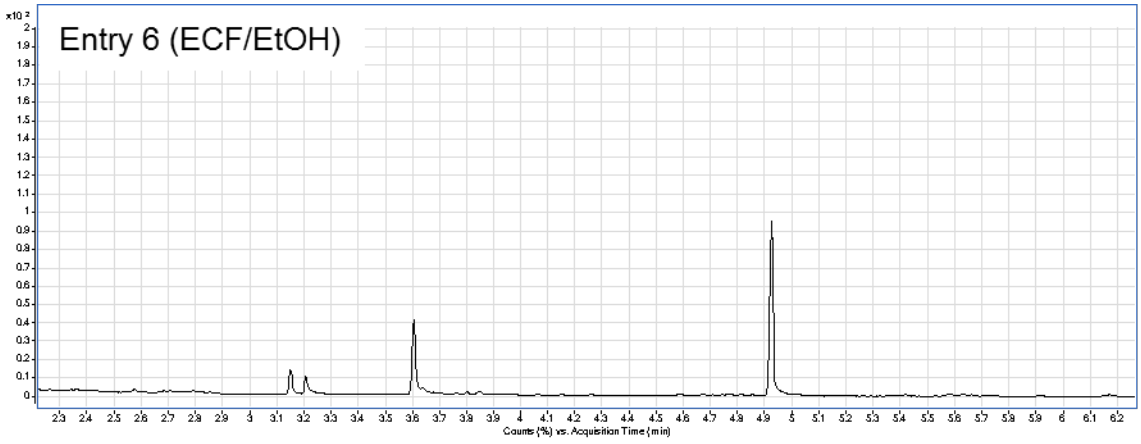

Figure S47 Chromatogram of the reaction mixture corresponding to entry 6 (Table S7).

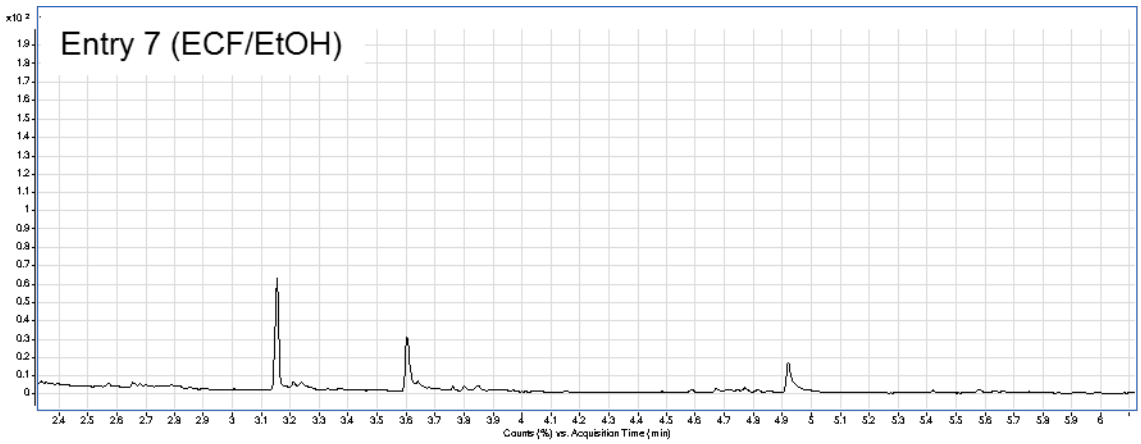

Figure S48 Chromatogram of the reaction mixture corresponding to entry 7 (Table S7).

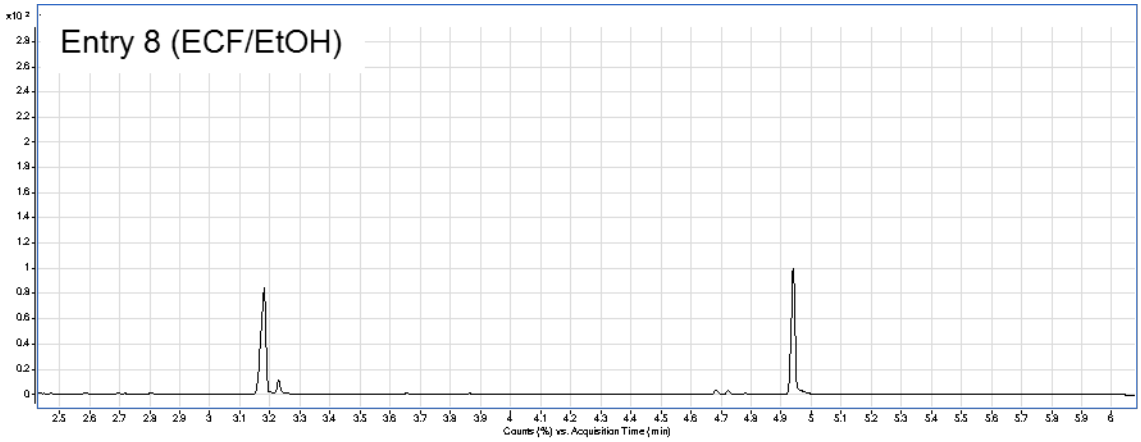

Figure S49 Chromatogram of the reaction mixture corresponding to entry 8 (Table S7).

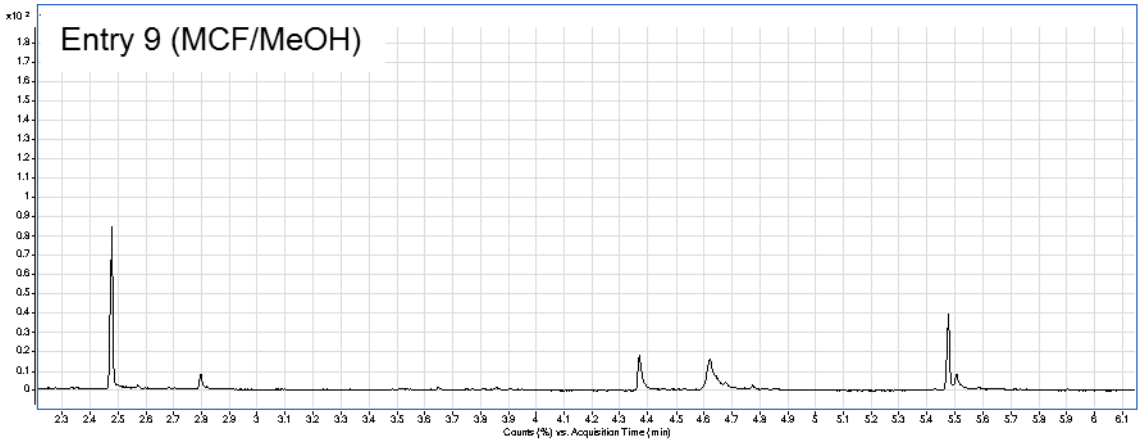

Figure S50 Chromatogram of the reaction mixture corresponding to entry 9 (Table S7).

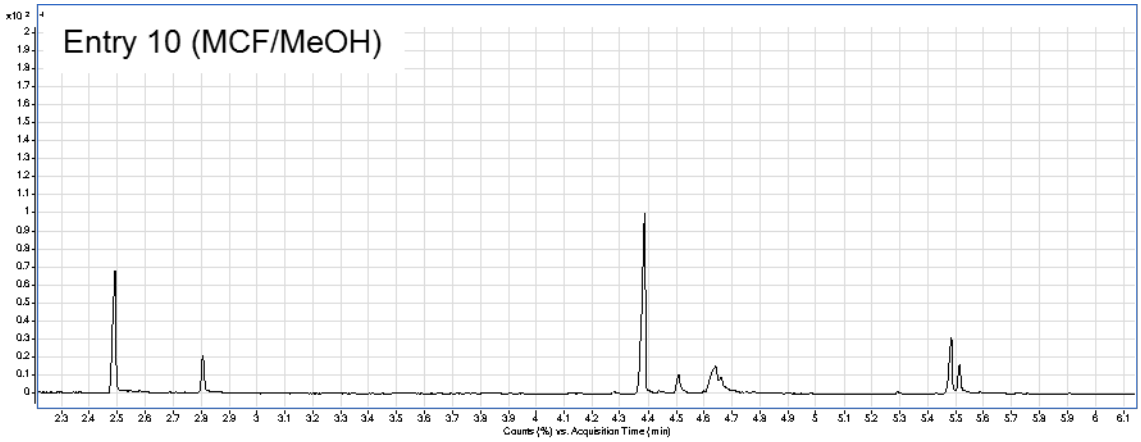

Figure S51 Chromatogram of the reaction mixture corresponding to entry 10 (Table S7).

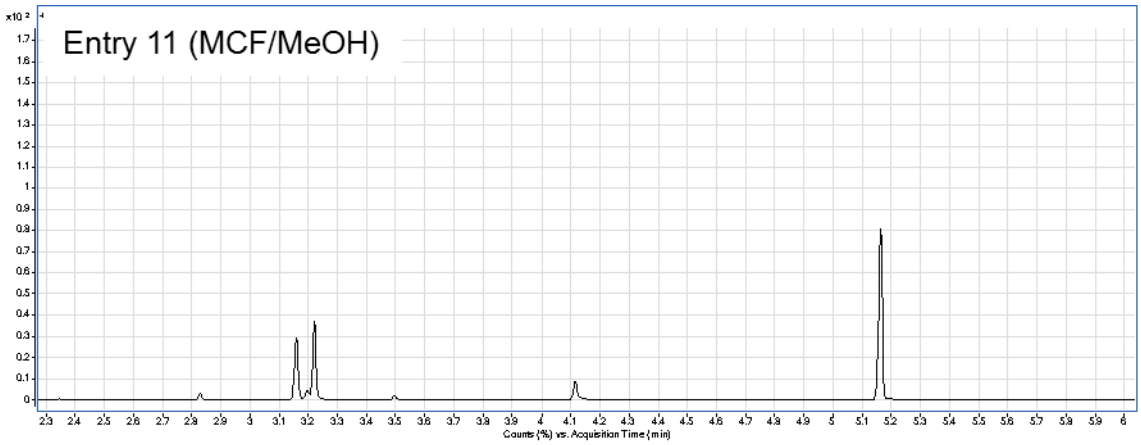

Figure S52 Chromatogram of the reaction mixture corresponding to entry 11 (Table S7).

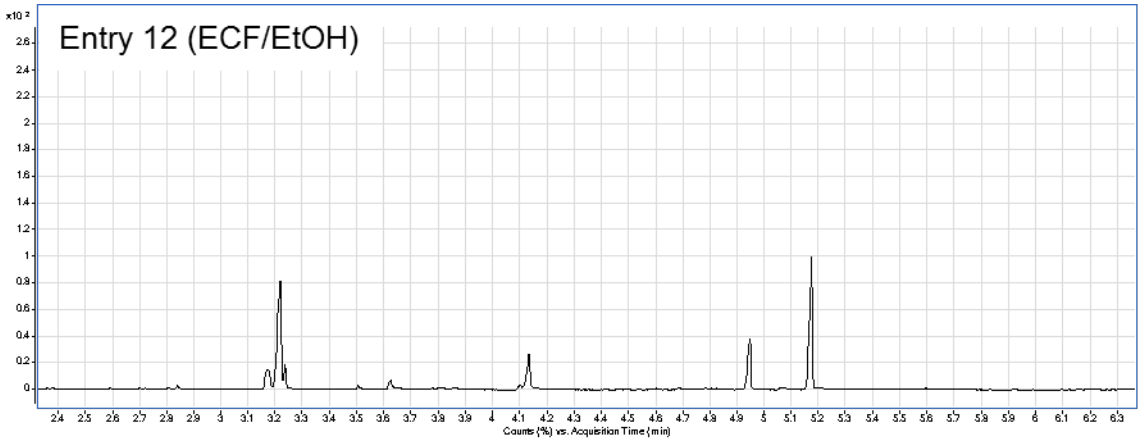

Figure S53 Chromatogram of the reaction mixture corresponding to entry 12 (Table S7).

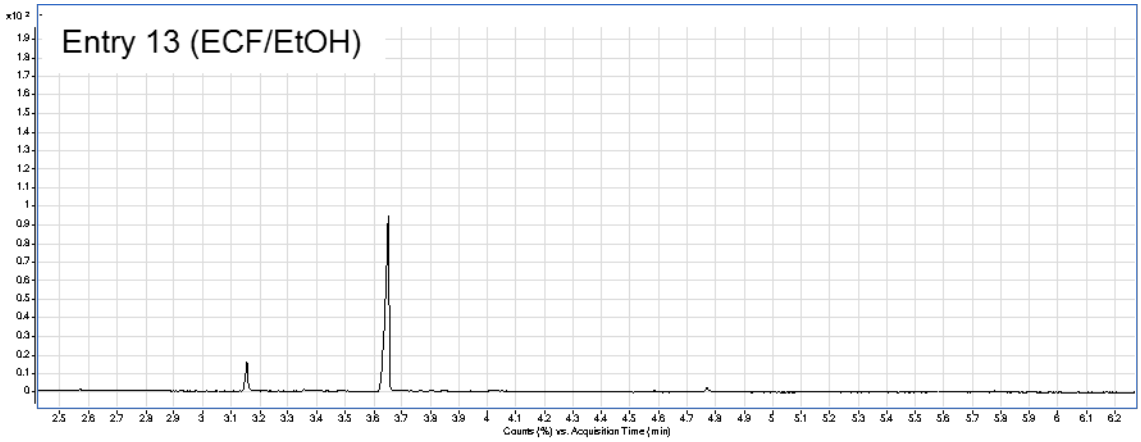

Figure S54 Chromatogram of the reaction mixture corresponding to entry 13 (Table S7).

Yield determination and error analysis

3 mL standard aqueous solutions of rTCA carboxylic acids at different concentrations (0.006 M, 0.013 M, 0.020 M, 0.027 M, 0.033 M and 0.040 M) were prepared by diluting 0.1 – 0.5 M stock solutions of these acids. 100 µL of each standard solution was derivatized using the derivatization procedure described herein (see: Analytical procedures). For each acid, a six-point graph was plotted, correlating the sum of characteristic GC peaks (as integrated automatically by the *Agilent MassHunter Workstation v.B.06.00* software) with substrate concentration (Fig. S55 – S67). Each data point was obtained from three independent measurements (carried out by three different researchers) and the correlation line was obtained from the least-squares fitting (intercept = 0). Error bars on graphs are shown as ± standard deviation for each data point. Overall percentage error of the response factor corresponds to ± standard deviation for each slope value.

The yields of products were calculated by comparing the product peak area with the calibration line. For the purpose of this study, reported are not the absolute percentage yields based on the number of moles of the starting materials, but rather percentage contributions to the total composition of the final reaction mixture. This allows to account for potential concentration changes due to solvent loss (since many reactions were carried out in sealed tubes at temperatures above the boiling point of water), as well as potentially incomplete extraction during the derivatization procedure. Each reaction was performed at least twice to ensure reproducibility, and reported percentage compositions are an average of these two runs, with an error corresponding to ± mean absolute deviation.

Derivatization with ethyl chloroformate (ECF)

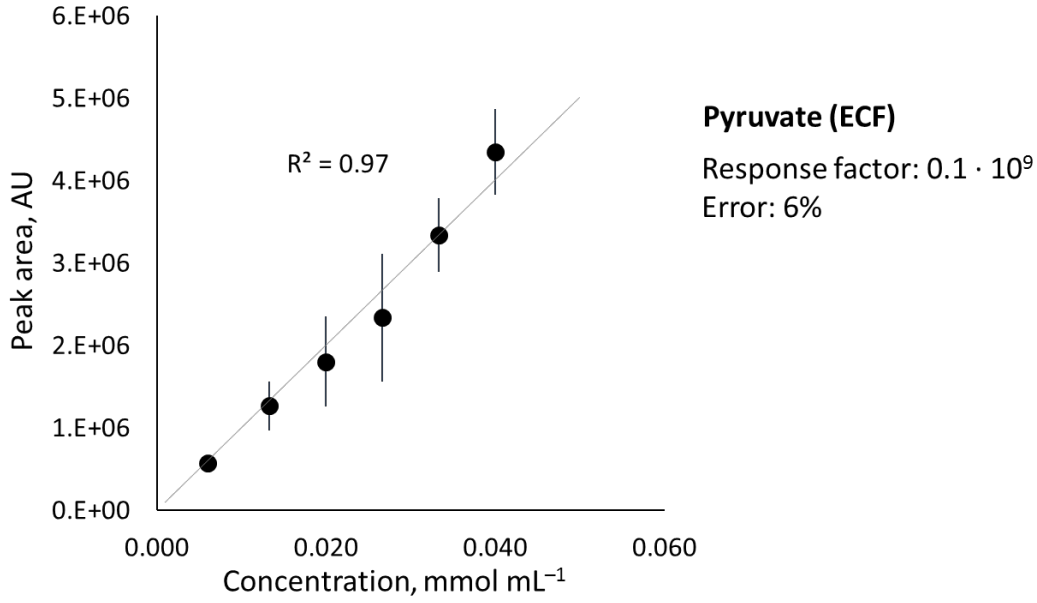

Figure S55 Correlation between the concentration of an aqueous solution of pyruvate and the measured gas chromatography peak area.

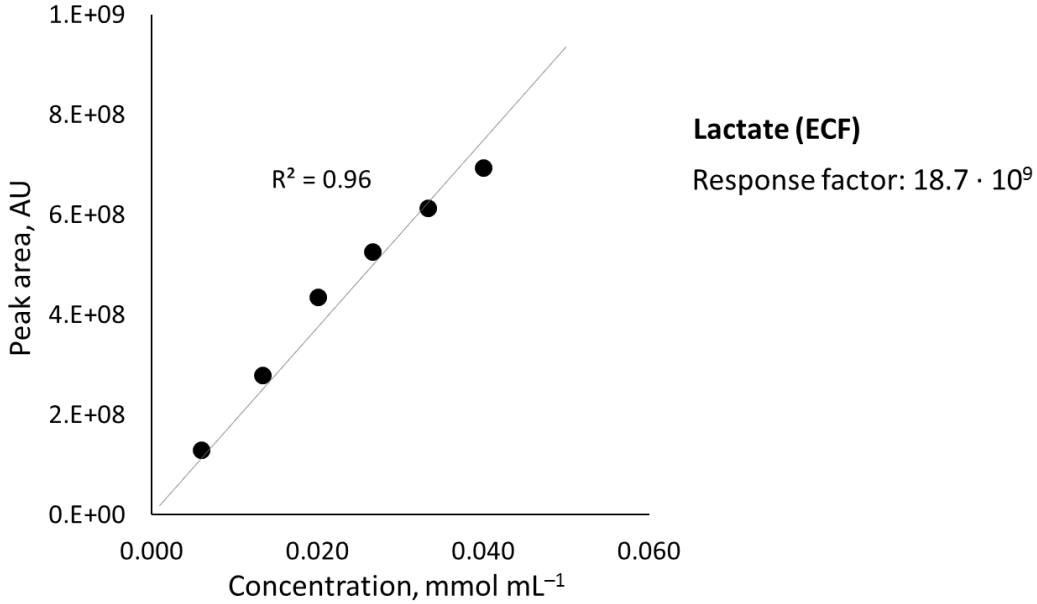

Figure S56 Correlation between the concentration of an aqueous solution of lactate and the measured gas chromatography peak area. Lactate was obtained by a complete reduction of an aqueous solution of sodium pyruvate with $NaBH_4$. The correlation line shown here corresponds to a single run.

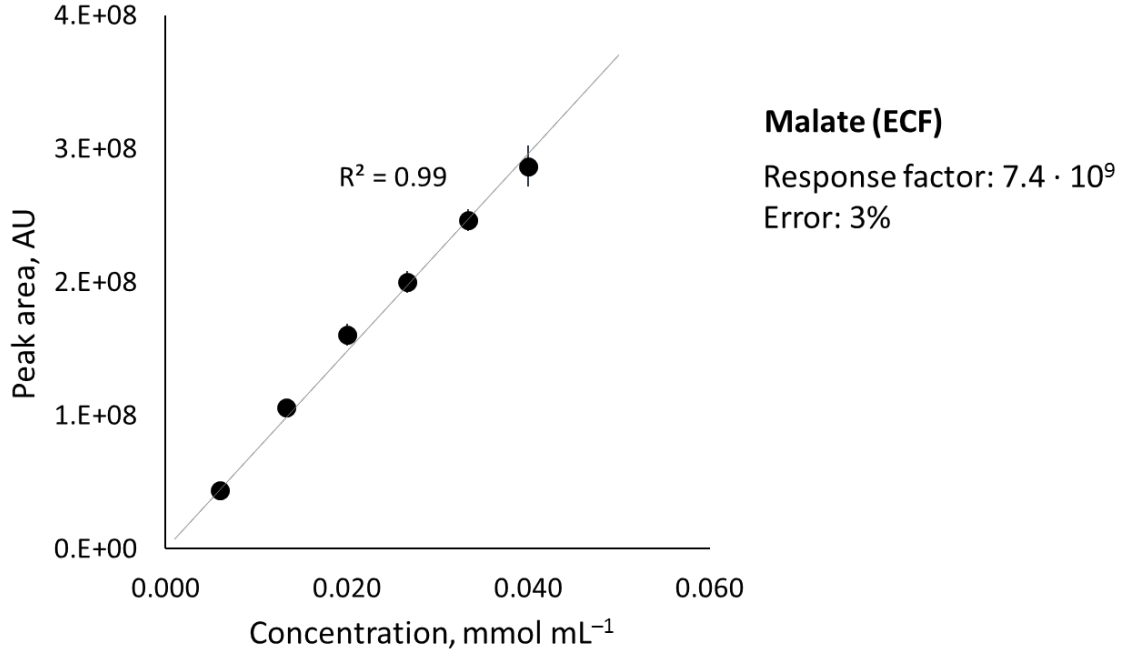

Figure S57 Correlation between the concentration of an aqueous solution of malate and the measured gas chromatography peak area.

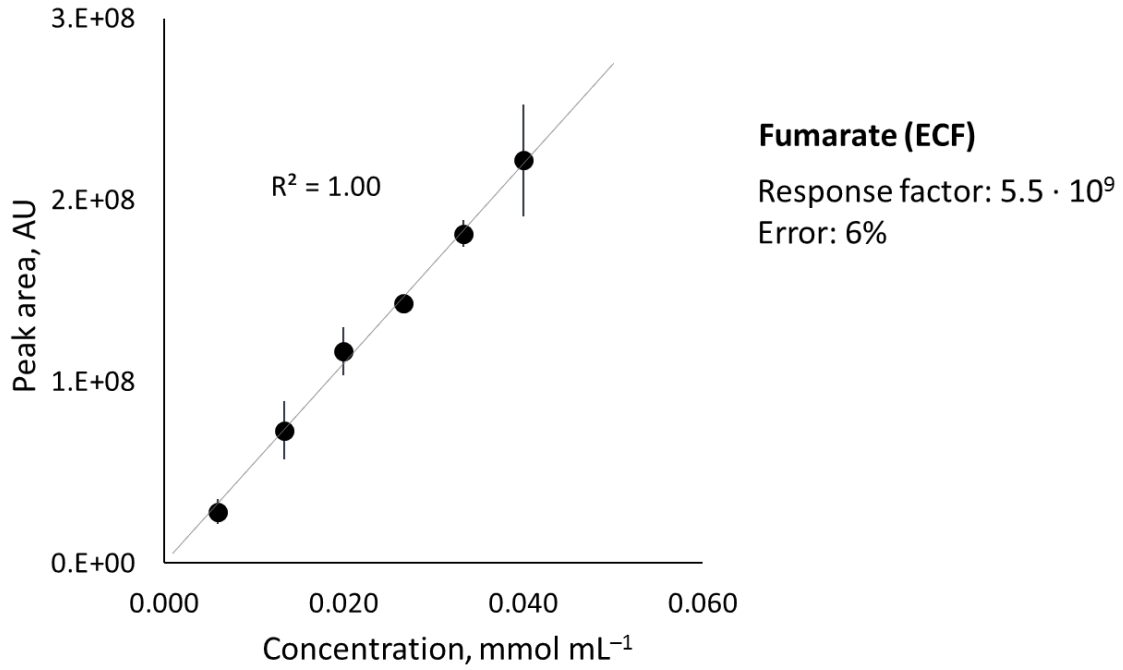

Figure S58 Correlation between the concentration of an aqueous solution of fumarate and the measured gas chromatography peak area.

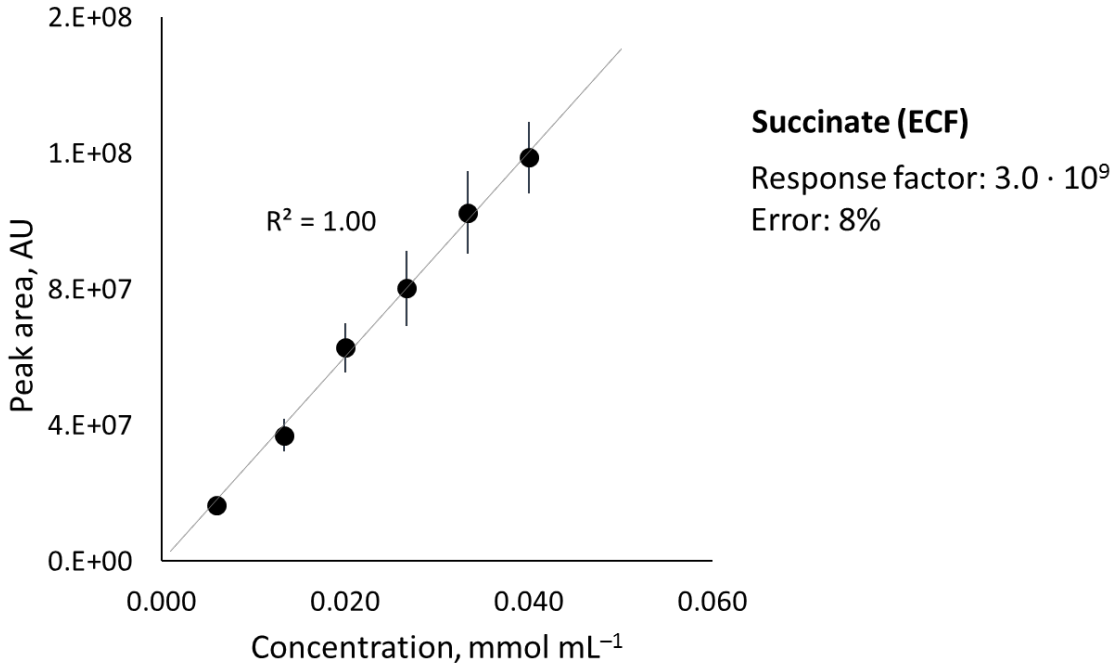

Figure S59 Correlation between the concentration of an aqueous solution of succinate and the measured gas chromatography peak area.

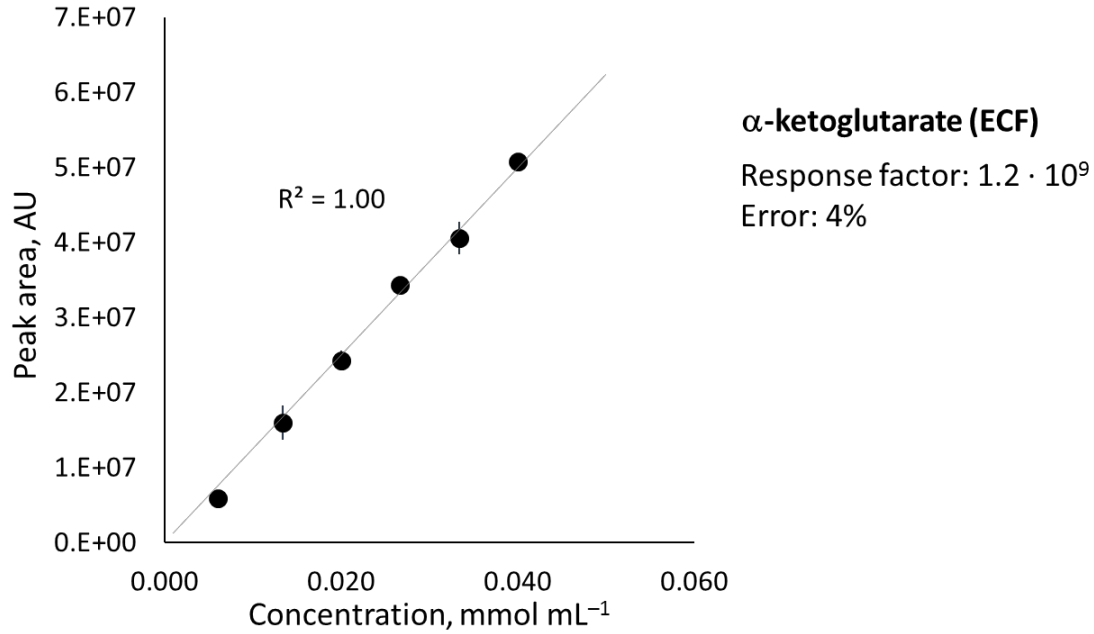

Figure S60 Correlation between the concentration of an aqueous solution of α-ketoglutarate and the measured gas chromatography peak area.

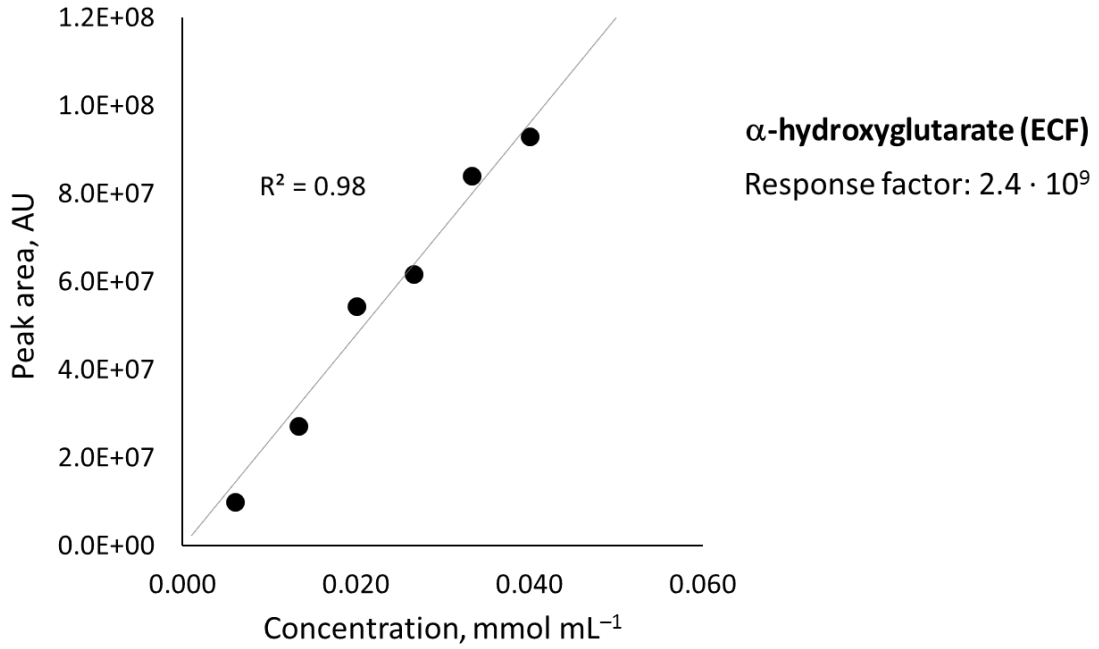

Figure S61 Correlation between the concentration of an aqueous solution of α-hydroxyglutarate and the measured gas chromatography peak area. α-Hydroxyglutarate was obtained by a complete reduction of an aqueous solution of α-ketoglutarate with $NaBH_4$. The correlation line shown here corresponds to a single run.

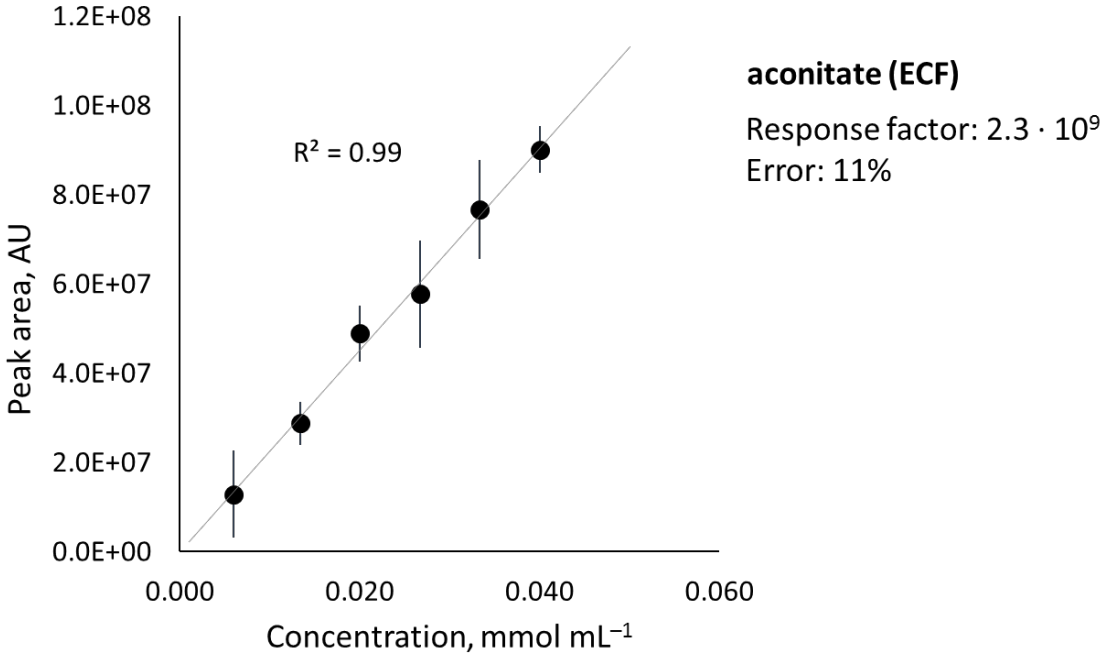

Figure S62 Correlation between the concentration of an aqueous solution of *cis*-aconitate and the measured gas chromatography peak area.

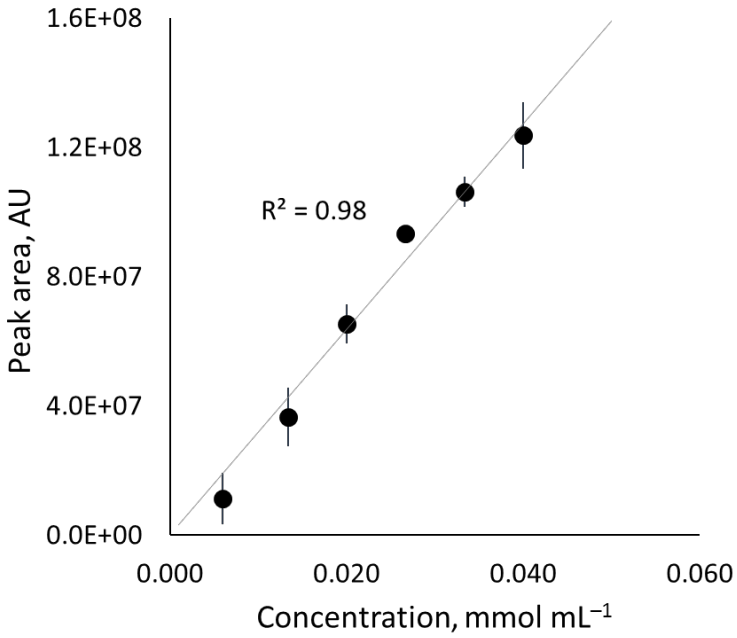

tricarballylate (ECF)

Response factor: $3.2 \cdot 10^9$
Error: 4%

Figure S63 Correlation between the concentration of an aqueous solution of tricarballylate and the measured gas chromatography peak area.

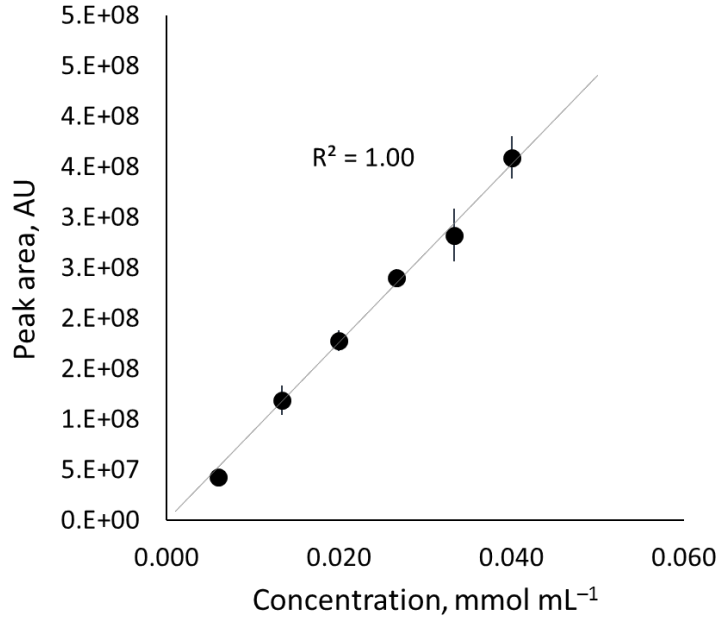

alanine (ECF)

Response factor: $8.8 \cdot 10^9$
Error: 1%

Figure S64 Correlation between the concentration of an aqueous solution of alanine and the measured gas chromatography peak area.

Derivatization with methyl chloroformate (MCF)

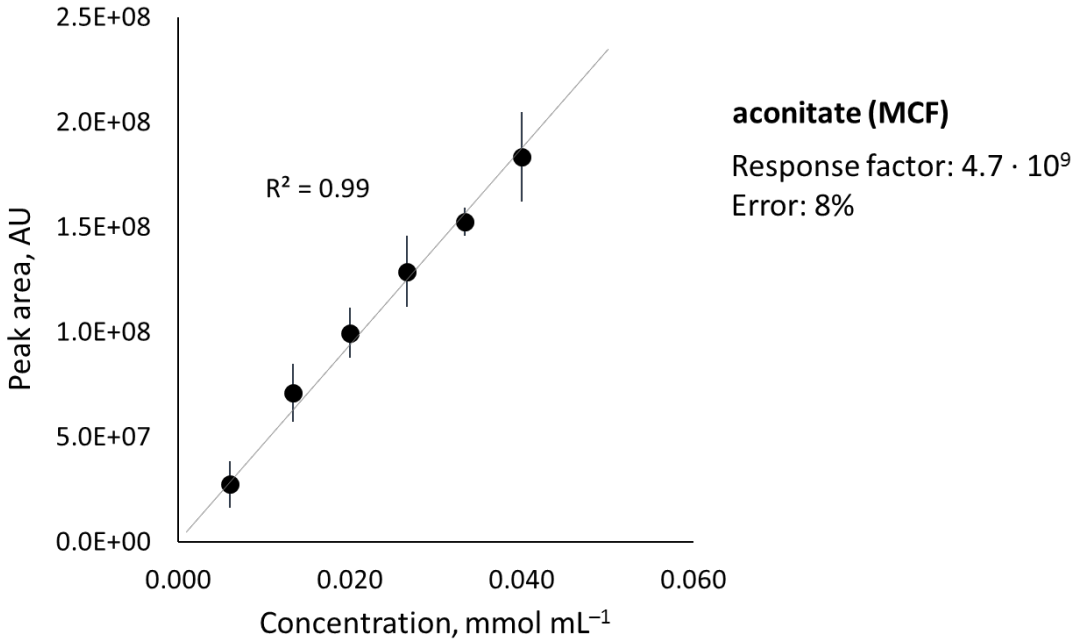

Figure S65 Correlation between the concentration of an aqueous solution of *cis*-aconitate and the measured gas chromatography peak area.

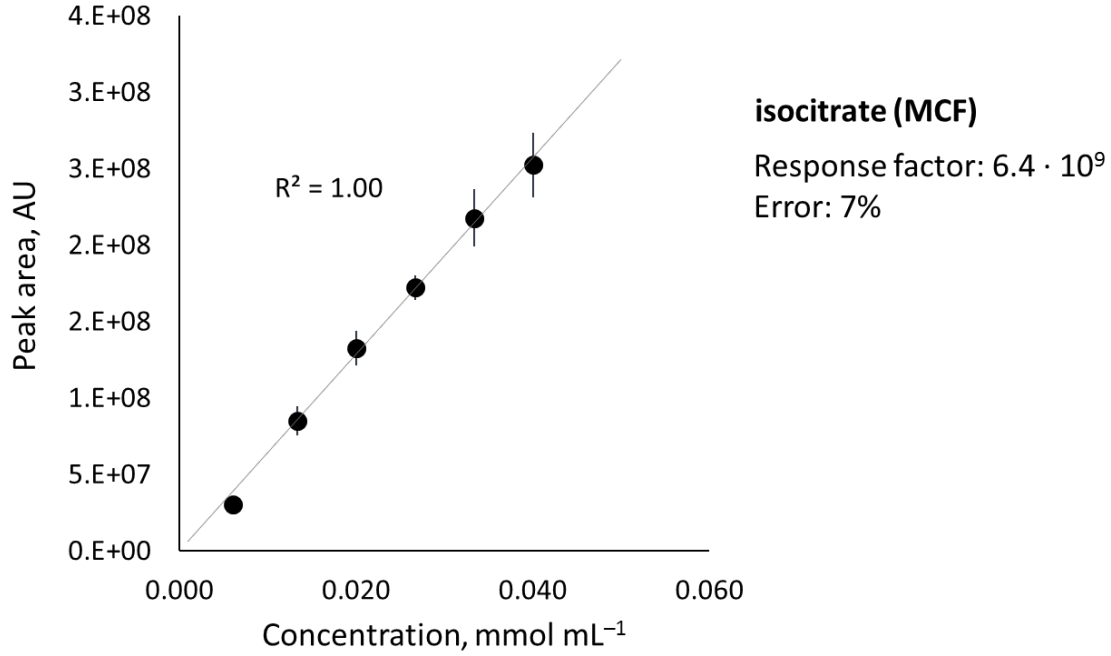

Figure S66 Correlation between the concentration of an aqueous solution of isocitrate and the measured gas chromatography peak area.

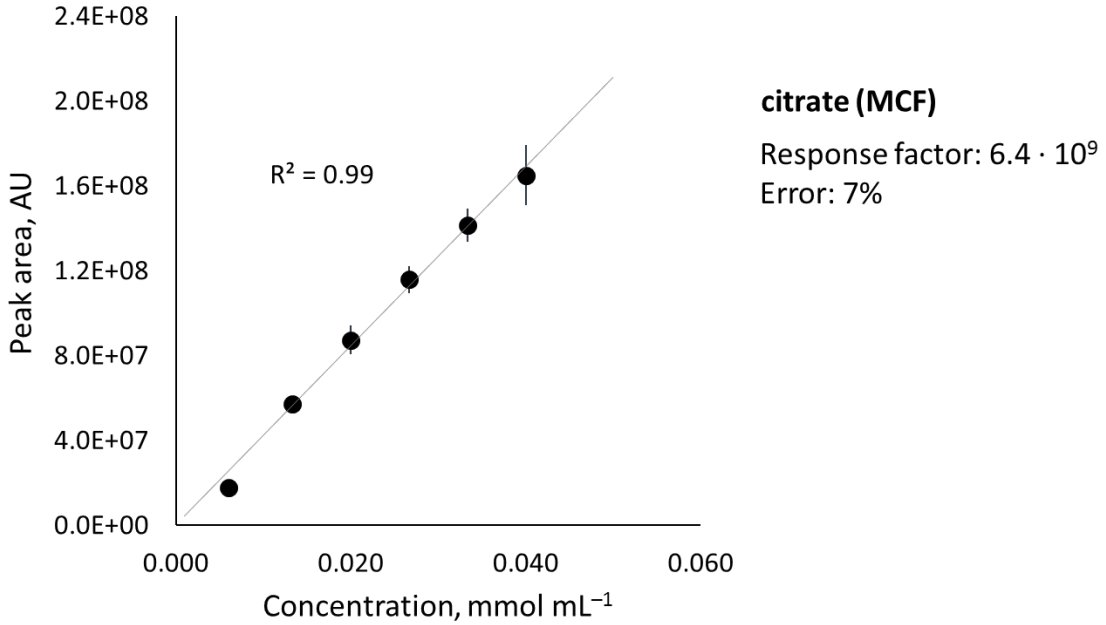

Figure S67 Correlation between the concentration of an aqueous solution of citrate and the measured gas chromatography peak area.

Synthetic procedures

General procedure: Fe^0 / Zn^{2+}/ Cr^{3+} and Ni^0/Zn^{2+}/Cr^{3+} −catalysed reactions (Table S1, Table S7).

To a 10 mL Pyrex pressure tube containing a Teflon-coated magnetic stir bar was added (unless otherwise specified) carboxylic acid substrate(s) (1 equiv, 0.100 mmol of each acid), Fe^0 or Ni^0 powder (10 equiv, 1.0 mmol, 56 mg Fe^0 or 59 mg Ni^0), and/or $ZnCl_2$ (15 equiv, 1.50 mmol, 204 mg), and/or $Cr_2(SO_4)_3 \cdot 12H_2O$ (3 equiv, 0.300 mmol, 183 mg). This was followed by the addition of 3 mL of solvent (unless otherwise specified: 1 M HCl in H_2O). The contents of the tube were flushed with argon for ≈ 30 s. The tube was then quickly sealed and the reaction mixture magnetically stirred for 16 h in a 12-tube metal heating block that was maintained at an internal temperature of 140 °C using an electronic thermocouple. The reaction tube was then removed from the heating block and allowed to cool to room temperature prior to derivatization and GC-MS analysis.

Reductive amination (Table S1, Table S6, Table S7)

A solution of sodium pyruvate (1 equiv, 0.100 mmol, 11.0 mg) and $Cr_2(SO_4)_3 \cdot 12H_2O$ (3 equiv, 0.300 mmol, 183 mg) in 1 M HCl in H_2O (3 mL) was added to a 10 mL Pyrex pressure tube containing a Teflon-coated magnetic stir bar. Hydrazine monohydrate (2 equiv, 0.20 mmol, ~10 μL) was then added, followed by Fe^0 or Ni^0 powder (10 equiv, 1.0 mmol, 56 mg Fe^0 or 59 mg Ni^0). The tube was then quickly sealed and the reaction mixture magnetically stirred for 16 h in a 12-tube metal heating block that was maintained at the specified internal temperature (20-140 °C) using an electronic thermocouple. The reaction tube was then removed from the heating block and allowed to cool to room temperature prior to derivatization and GC-MS analysis.

Metal screens

Malate dehydration – inorganic salts containing the following metals were used in the reaction screen: Zn^{2+}, Cu^{2+}, Ni^{2+}, Co^{2+}, Fe^{2+}, Mn^{2+}, Cr^{2+}, V^{2+}. Zn^{2+} gave the best yields when used together with Fe^0 (2-step reaction) (Table S2).

Isocitrate dehydration – inorganic salts containing the following metals were used in the reaction screen: Zn^{2+}, Cu^{2+}, Ni^{2+}, Co^{2+}, Fe^{2+}, Mn^{2+}, Cr^{2+}, V^{2+}, Pd^{2+}, Cd^{2+}, Fe^{3+}, Mn^{3+}, Cr^{3+}, As^{3+}, Ru^{3+}, Ir^{3+}, Rh^{3+}, Ti^{3+}. Zn^{2+} was selected for further experiments due to high yields and geochemical accessibility, although substantial reactivity was also observed for Cr^{2+}, Pd^{2+}, Fe^{3+}, Mn^{3+}, As^{3+}, Ru^{3+}, Ir^{3+} and Rh^{3+} (Table S3).

Aconitate hydration – inorganic salts containing the following metals were used in the reaction screen: Cu^{+}, Zn^{2+}, Cu^{2+}, Ni^{2+}, Co^{2+}, Fe^{2+}, Mn^{2+}, Cr^{2+}, Cd^{2+}, Hg^{2+}, Fe^{3+}, Co^{3+}, Mn^{3+}, Cr^{3+}, Ti^{3+}, Ru^{3+}, Mo^{4+}, W^{4+}, Mo^{6+}, W^{6+}. Only Cr^{3+} returned a substantial positive result (Table S4).

Reductions – the following metals were used in powder form: Zn, Fe, Ni, Mo. These results were compared against MoO_2 and sodium dithionite. Reducing properties of TPGS-750-M were excluded in a control experiment (Table S5)

Reactions in micellar solutions.

For reactions carried out in micelles, 3 mL of a TPGS-750-M solution (DL-α-tocopherol methoxypolyethylene glycol succinate, 1% w/w) in 1 M HCl was used as the solvent. Stirring was maintained at 1000 rpm. In order to control for the contribution of the surfactant molecule towards succinate detected in the chromatograms, a control reaction was carried out (Reaction 26 in Table S1). A mixture of Fe^0 powder (10 equiv., 1.0 mmol, 56 mg), $ZnCl_2$ (15 equiv. 1.5 mmol, 204 mg), $Cr_2(SO_4)_3 \cdot 12H_2O$ (3 equiv., 0.3 mmol, 183 mg) in TPGS-750-M (3 mL, 1% w/w in 1 M HCl in H_2O) was heated at 140 ^oC for 16 h. After cooling, a 0.1 mmol portion of malic acid was dissolved in the mixture, a 100 μL aliquot of which was immediately derivatised. It was found (two runs) that succinate originating from TPGS-750-M (DL-α-tocopherol methoxypolyethylene glycol succinate) contributes to not more than 1% of the control reaction composition (Table S1). Micelles may play various roles in the oxaloacetate-malate-fumarate-succinate sequence, e.g. bias the malate-fumarate equilibrium towards fumarate by increasing solubilities of fumarate and succinate, or increase the stability of carboxylic acids and thus minimise the mass loss as carbon dioxide.

Portion-wise reagent addition.

For reactions where portion-wise addition of reagents was performed (Reactions 1 and 15 in Table S1): the first half of reagents was added at the start of the reaction; the second portion was added after 24 h to a cooled reaction mixture, after which the reaction vessel was re-sealed and heating resumed.

Reactions with oxalosuccinic acid (Table S1: entries 3 and 19 – 23; Table S7: entries 3 and 9 – 11).

Due to rapid decarboxylation of oxalosuccinic acid and difficulties associated with its storage,[4] it was prepared on demand by *in situ* hydrolysis of triethyl oxalosuccinate ester under typical acidic reaction conditions (1 M HCl).

Triethyl oxalosuccinate

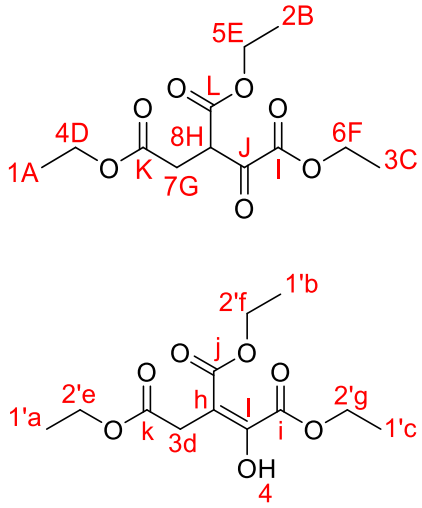

Prepared using the literature procedure[1] from diethyl succinate (5 mmol) and diethyl oxalate (5 mmol), with commercial potassium ethoxide in the place of potassium metal. Triethyl oxalosuccinate was obtained as a light-yellow liquid (1.2 g, 89%).

^{1}H NMR (400 MHz, $CDCl_3$) δ 12.77 (s, enol **4'**), 4.64 (dd, *J* = 8.9, 5.2 Hz, 1H, **8**), 4.34 (q, *J* = 7.1 Hz, 2H, **6**), 4.28 (dd, *J* = 12.1, 7.2 Hz, enol **2'**), 4.17 (dd, *J* = 14.8, 7.7 Hz, 2H, **5**), 4.11 (dd, *J* = 14.3, 7.1 Hz, 2H, **4**), 3.61 (s, enol **3'**), 3.00 (dd, *J* = 17.3, 8.9 Hz, 1H, **7**), 2.88 (dd, *J* = 17.4, 5.1 Hz, 1H, **7**), 1.36 (t, *J* = 7.1 Hz, 3H, **3**), 1.29 (dd, *J* = 13.1, 6.0 Hz, enol **1'**), 1.22 (t, *J* = 7.1 Hz, 3H, **2**), 1.21 (t, *J* = 7.1 Hz, 3H, **1**).

^{13}C NMR (101 MHz, $CDCl_3$) δ 188.30 (**L**), 172.55 (enol **l**), 171.05 (enol **k**), 170.60 (**K**), 167.70 (**J**), 162.32 (enol **j**), 160.21 (**I**), 158.40 (enol **i**), 102.57 (enol **h**), 62.84 (**F**), 62.17 (enol **g**), 62.06 (**E**), 61.99 (enol **f**), 61.21 (**D**), 60.74 (enol **e**), 49.25 (**H**), 31.94 (**G**), 31.27 (enol **d**), 14.15 (enol **c**), 14.00 (**C**), 13.91 (GSD-resolved, enol **a**, **b**) 13.88 (**B**), 13.83 (**A**).

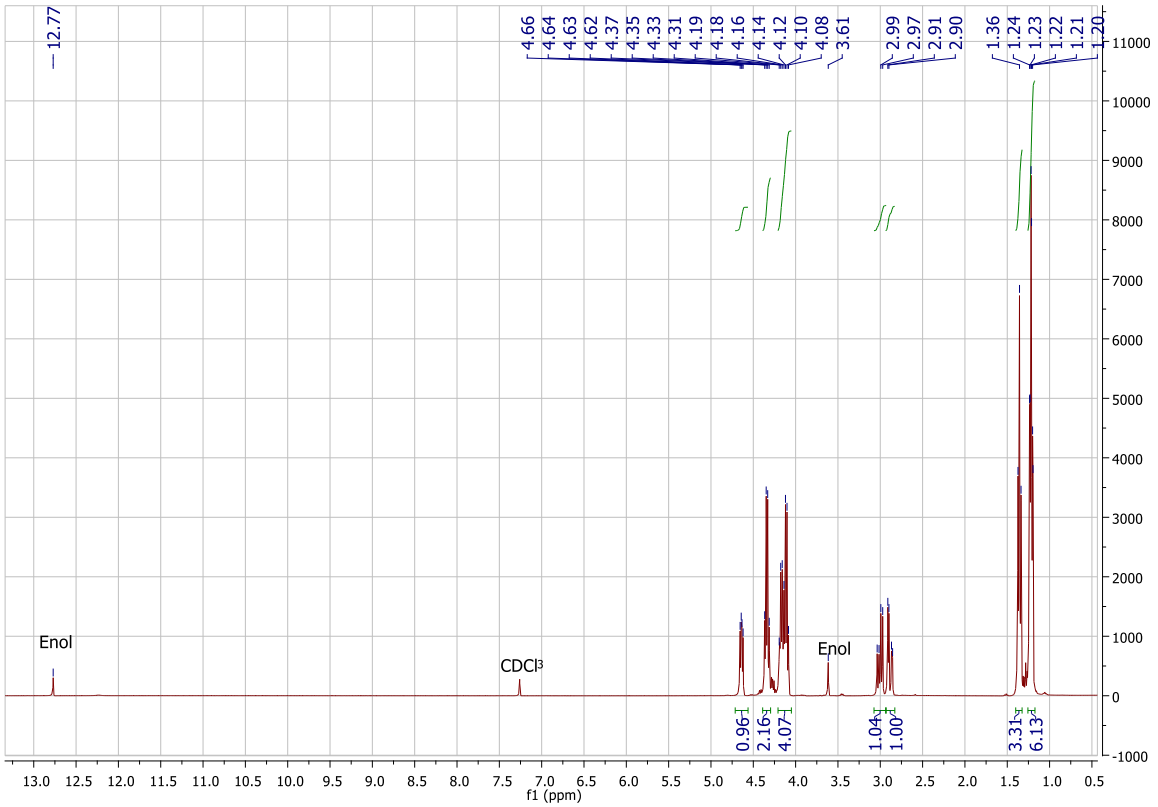

Figure S68 ^{1}H NMR of triethyl oxalosuccinate in $CDCl_3$ at 25 ^{o}C

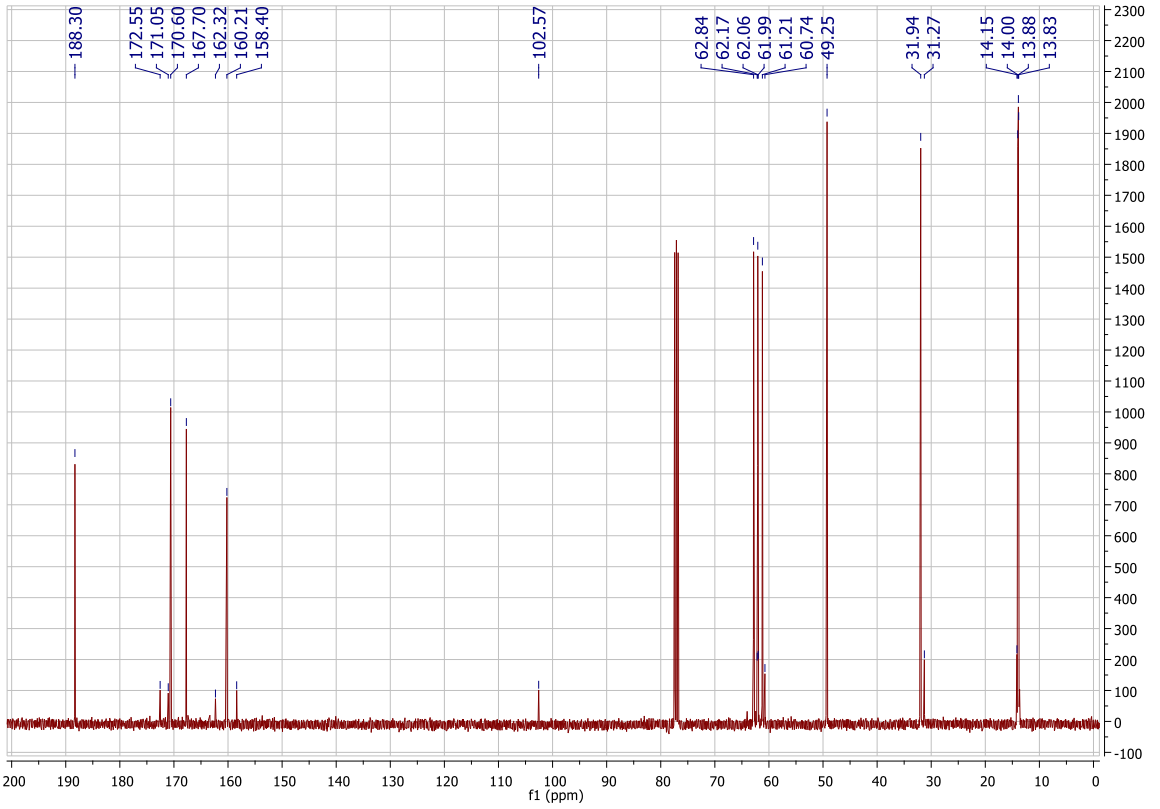

Figure S69 ^{13}C NMR of triethyl oxalosuccinate in $CDCl_3$ at 25 ^{o}C

Cis-aconitic acid

Cis-aconitic acid used in this study was prepared on a gram scale (19.7 g, 45%) from citric acid (48 g, 0.25 mol) using a literature procedure.[2] The identity of the product was confirmed using existing literature data,[5] as well as by comparison of the GC-MS data (chromatogram and MS fragmentation pattern) with an authentic sample.

^{1}H NMR (400 MHz, D_2O) δ 6.91 (s, 1H), 3.74 (s, 2H). 13C NMR (101 MHz, D2O) δ 174.64, 169.32, 168.54, 139.09, 130.48.

Qualitative corroboration of GC-MS data by ^{1}H NMR

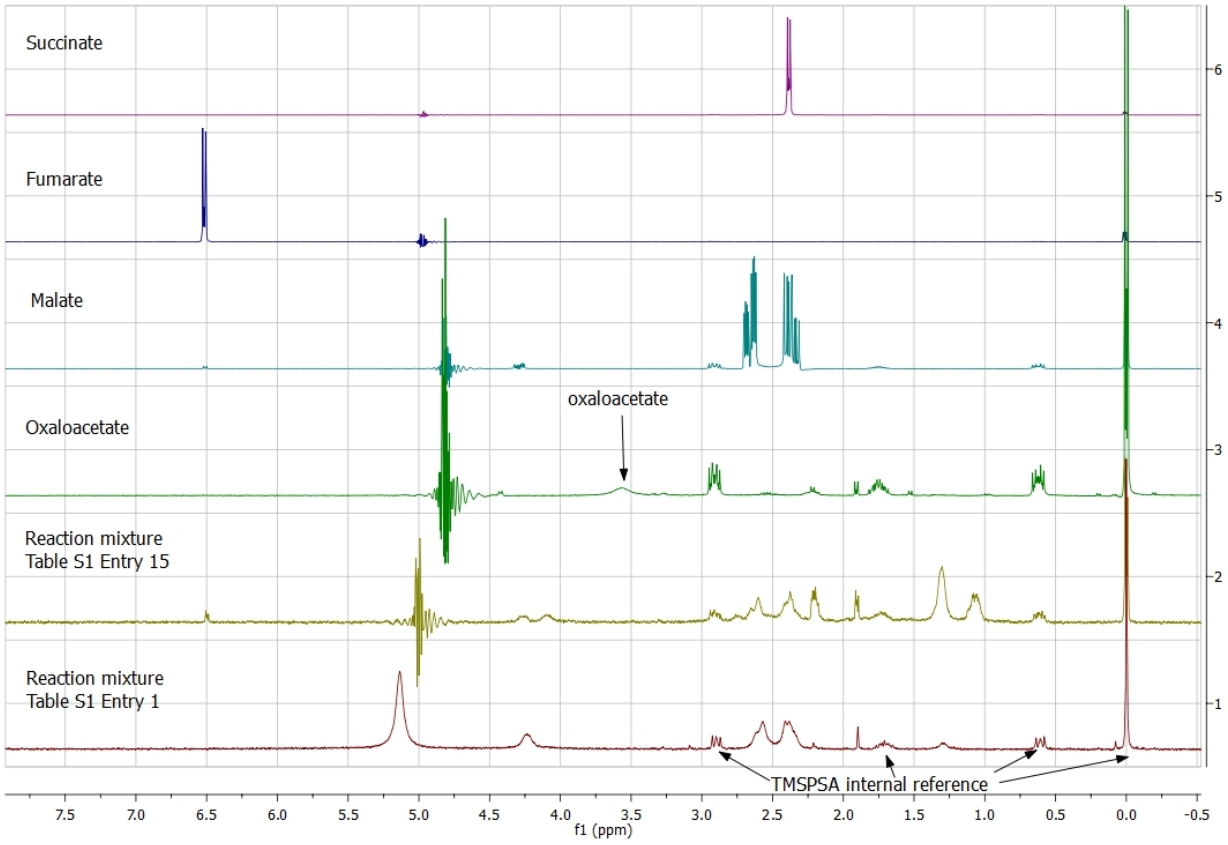

In an attempt to cross-validate the GC-MS analytical method under real reaction conditions, reactions run under conditions corresponding to Table S1, entries 1 and 15 were basified, doped with an internal standard and analysed by ^{1}H NMR. The reaction mixture was basified with solid KOH (pH ~14) to precipitate metal cations. Subsequently, the mixture was centrifuged, and 600 µL of the supernatant was combined in an NMR tube with 75 µL of D_2O and 25 µL of 0.05 M sodium 3-(trimethylsilyl)-1-propanesulfonate (TMSPSA) as the internal reference (CH_3 peak at 0 ppm). Solvent suppression of water in the ^{1}H NMR was achieved using the Bruker ZGESGP 1D sequence for water suppression using excitation sculpting with gradient. Sixteen scans were acquired for each sample. Spectra of the reaction mixtures were compared

against authentic substrate samples prepared using the same procedure. In both cases, resonances corresponding to oxaloacetate had disappeared and the same products detected by GC-MS were indeed confirmed to be present. While ^{1}H NMR under ZGESGP water suppression qualitatively validates the GC-MS data, we hesitate to use it as a quantitative technique for these reactions since 1) the chemical shifts of different di-acids are unresolved (e.g. malate and succinate), and a qualitative deconvolution of the peaks using ^{1}H-^{13}C 2D NMR experiments is not practical at such low concentrations; 2) the water suppression technique affects the magnitude of resonances in proximity to the suppressed water resonance (e.g. the peak of oxaloacetate at 3.5 ppm is not quantifiable); 3) any non-precipitated metal cations might bind the TCA acids, changing the chemical shifts of their typical resonances.

Supporting references

(1) Friedman, L., Kosower, E., *Org. Synth.* **1955**, *3*, 510

(2) Bruce, W. F., *Org. Synth.* **1937**, *17*, 1

(3) Smart, K. F., Aggio, R. B. M., Van Houtte, J. R., Villas-Bôas, S. G., *Nat. Protoc.* **2010**, *5*, 1709-1729

(4) Wiscelinus, W., *Ber. Dtsch. Chem. Ges*. **1889**, *22*, 885

(5) Choi, K. H., Lee, H. J. *et al*, *Anal. Chem.* **2009**, *81*, 4734-4741